FUNCTION OF TWO HEADS OF MYOSIN

IN

MUSCLE CONTRACTION

MAKOTO MIYATA

DEPARTMENT OF BIOLOGY, FACULTY OF SCIENCE, OSAKA UNIVERSITY

February 1988

CONTENTS

ABBREVIATIONS

HMM	heavy meromyosin
S-1	subfragment-1 of myosin
A	monomer in F-actin
M	myosin head
Pyr-FA	F-actin labeled with N-(1-pyrenyl) iodoamide
MLCK	myosin light chain kinase
PK	pyruvate kinase
AMPPNP	adenyl-5'-yl imidodiphosphate
PEP	phosphoenolpyruvate
SDS-PAGE	sodium dodecyl sulfate polyacrylamide gel electrophoresis
DTT	dithiothreitol
TCA	trichloroacetic acid
PEI	polyethyleneimide
Fl	fluorescence intensity
LS	light-scattering intensity

GENERAL INTRODUCTION

Motility is a feature of all forms of life, and muscle contraction is a typical phenomenon of movement in the living organisms. The mechanism of muscle contraction has been studied by many workers in various fields, since muscle has highly ordered structure and the organ is present in animal body in a large amount.

Structure of Muscle

A vertebrate skeletal muscle cell, called muscle fiber is 20 - 100 μm in diameter and several centimeters in length. A muscle fiber has characteristic myofibrils at a large number lying parallel to the main axis of the fiber (Fig. 1). The contractile materials in the myofibrils are organized within a repeating unit called sarcomere having a boundary of Z-lines, and a sarcomere is 2.3 μm in length when muscle is at resting state. The central band of the sarcomere is dark under the phase-contrast microscopy and is called A-band (anisotropic band). On either side of the Z-line are regions which appear light under the microscope; these together are called I-band (isotropic band).

This striated myofibrils are constructed by two kinds of filaments in overlapping arrays; thick filaments with about 11 nm in diameter occupy the A band in the center of a sarcomere while thin filaments with about 5 nm in diameter occupy the I band at the two ends (Fig. 1). Many projections appear on the thick filament bind to the thin filament to form crossbridges.

The chemical compositions of the thick and thin filaments were inferred by Hasselbach (1) and Huxley (2,3). They extracted

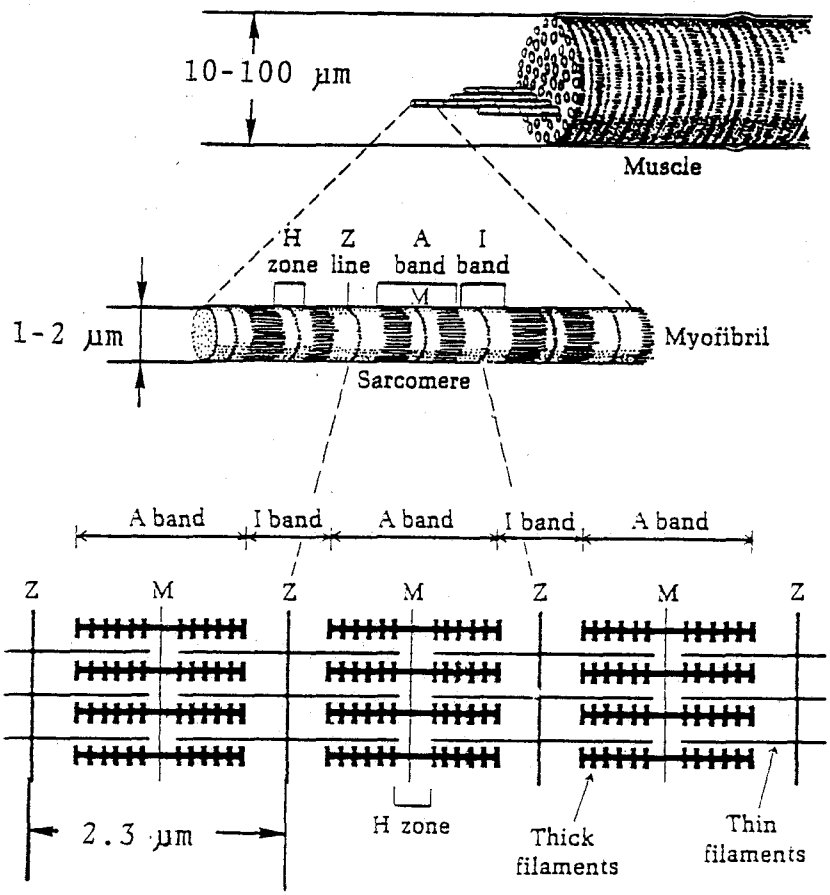

Fig. 1 The structure of striated muscle at two levels of organization. Dimensions shown are for rabbit psoas muscle.

"myosin" specifically in 0.6 M KCl with Mg^{2+}-pyrophosphate, and found that this extraction removes only the thin filament. The remaining nonmyosin material is concentrated in the I band and could be extracted by KI solution which depolymerizes "actin" (4).

Superprecipitation and Sliding theory

Szent-Gyorgyi (5,6) showed that ATPase reaction of myosin is greatly accelerated by actin and that when ATP is added to the complex of actin and myosin (actomyosin) under low ionic strength, actomyosin precipitates very rapidly, and this phenomenon is called superprecipitation.

Huxley and Niederke (7), and Huxley and Hanson (8) found independently that shortening of muscle is brought about by the sliding of thick and thin filaments relative to each other and proposed "sliding theory" for muscle contraction. Therefore, it was concluded that muscle contraction occurs as a result of the sliding of two filaments which is coupled with the interaction of myosin and actin upon reaction with ATP.

Structure of Myosin

Myosin has a molecular weight of about 480,000. It decomposes into peptides (subunits) in denaturing solution. The myosin molecule consists of two heavy chains (HC) with molecular weight of 200,000, and four light chains (LC) with molecular weight between 15,000 to 25,000 each. The size and shape of the myosin

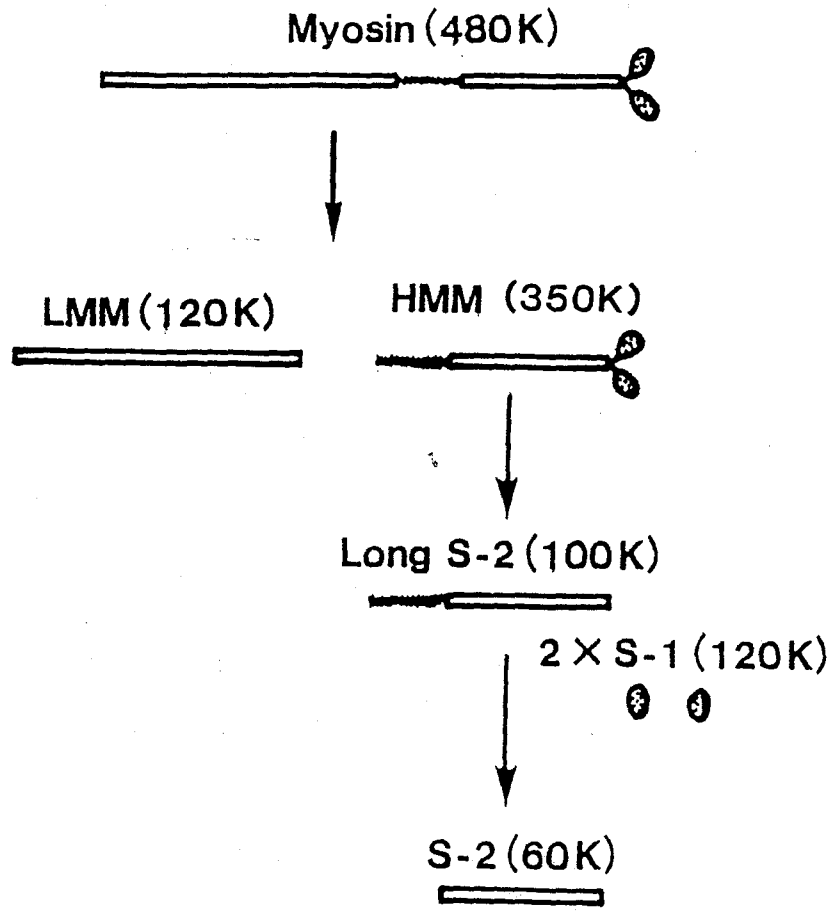

Fig. 2 The formation of subfragments by limited digestion of myosin by proteases.

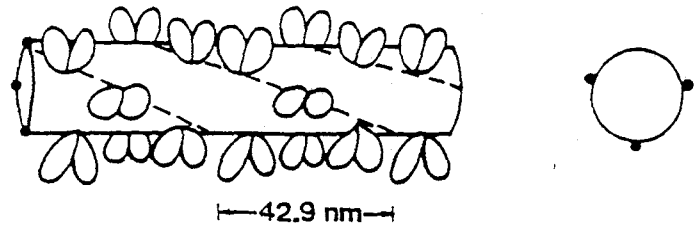

Fig. 3 The radial projection of thick filament in vertebrate skeletal muscle. At each 14.3 nm along the filament there are three myosin molecules. The helix has a pitch of 42.9 nm.

molecule have been studied by electron microscopy (9,10). As shown in Fig. 2, myosin is a rodlike protein with two globular heads. The total length of the myosin molecule is about 160 nm. Two heads about 20 nm in length and 5 nm in diameter are connected to, a tail 150 nm in length and 3 nm in diameter. A bend is often observed around 63 - 73 nm from the end of the tail.

At low ionic strength myosin forms a filament essentially the same as that of the thick filament in myofibrils (11). As shown in Fig. 3, many projections are observed on the surface of the filament except at a bare zone of about 0.15 um in the center of the filament (Fig. 3). The projections bind with the thin filament and form crossbridges as described above.

To study which part of the myosin molecule is responsible for its function, various subfragments were obtained by proteolytic digestion (12). Figure 2 shows schematically the subfragments of myosin obtained after digestion with proteases. Digestion of myosin in the presence of divalent cations yields a heavy meromyosin (HMM) with a molecular weight of about 350,000 and a light meromyosin (LMM) with a molecular weight of about 120,000 and a length of 70 nm. HMM is soluble even at low ionic strength and retained the ATPase activity and actin binding ability. On the other hand, LMM has neither ATPase activity nor actin-binding ability, but assembles into filaments at low ionic strength. When HMM is further digested in the absence of divalent cations, 1 mol of HMM yields 2 mol of subfragment-1 (S-1) and 1 mol of subfragment-2 (S-2). S-1 has a molecular weight of 12,000 and a length of 20 nm, while S-2 has a molecular weight of 60,000 and a

length of 50 nm. ATPase activity and actin-binding ability are retained in S-1. These investigations showed that LMM part of myosin forms the backbone of the thick filament and that the two heads which react with ATP and bind to actin form the projection of the thick filament.

Reaction of Two Heads of Myosin with ATP

Myosin has two separate heads which react with ATP and interact with actin. To solve the mechanism of muscle contraction we have to elucidate how these two heads interact with actin coupled with ATP hydrolysis and what is the function of each head.

It has been reported that the two heads of skeletal muscle myosin are not functionally and structurally identical (13). When ATP is added to myosin in the presence of Mg ion, one of the two heads (head B) rapidly forms M_P^{ADP} complex (Fig. 4). Since the decomposition of this complex is much slower than its formation, the formation of M_P^{ADP} can be detected as the initial rapid liberation of Pi when ATPase reaction is terminated by adding TCA (Fig. 4). The other head (head A) forms MATP complex as a reaction reaction intermediate. The formation of this complex can be detected as the bound ATP which is not in the equilibrium with the M_P^{ADP} complex.

Several differences between the chemical structure of two heads of myosin have been reported. Both heads have one specific lysine residue which rapidly reacts with trinitrobenzensulfonate (TNBS), but the lysine residue only in head B is reactive in the presence of pyrophosphate (14). Based on this finding it was

HEAD A

HEAD B

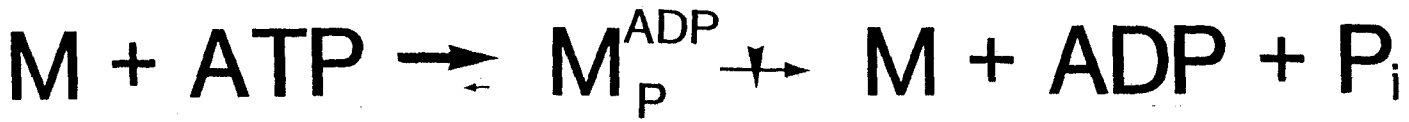

Fig. 4 Mechanism of myosin ATPase reaction catalyzed by head A and B.

shown that amino acid sequence around the reactive lysine residues of two heads are different (15). Furthermore, the specific thiol residue (SHr) which binds strongly with p-chloromercuribenzoate (pCMB) was shown to locate only on head A of myosin (16).

Function of Two heads of myosin

The function of head B in muscle contraction gradually became clear by the studies on the mechanism of ATPase in the presence of actin. As shown in Fig. 5, in the presence of actin, head B catalyzes the actomyosin ATPase reaction, which is directly coupled to muscle contraction. In the actomyosin ATPase reaction, ATP is hydrolyzed *via* two routes (17,18) one with dissociation of actomyosin *via* A + M_P^{ADP} (outer cycle) and the other *via* direct decomposition of A M_P^{ADP} into A M + ADP + Pi (inner cycle), where M and A represent head B of myosin and actin, respectively. It was suggested that muscle contraction occurs by a cyclic interaction of myosin head B with F-actin: (1) formation of crossbridge by binding of myosin head B with F-actin (2) development of tension by the conformational change of the crossbridge, and (3) dissociation of myosin head B from the actin filament. These contraction steps correspond to those of the actomyosin ATPase reaction, as shown in Fig. 5.

On contrary to head B, little is known about the role of head A. Two hypotheses have been proposed for the function of head A. The first is concerned to the regulation of muscle contraction. Contraction of skeletal muscle is regulated by the concentration

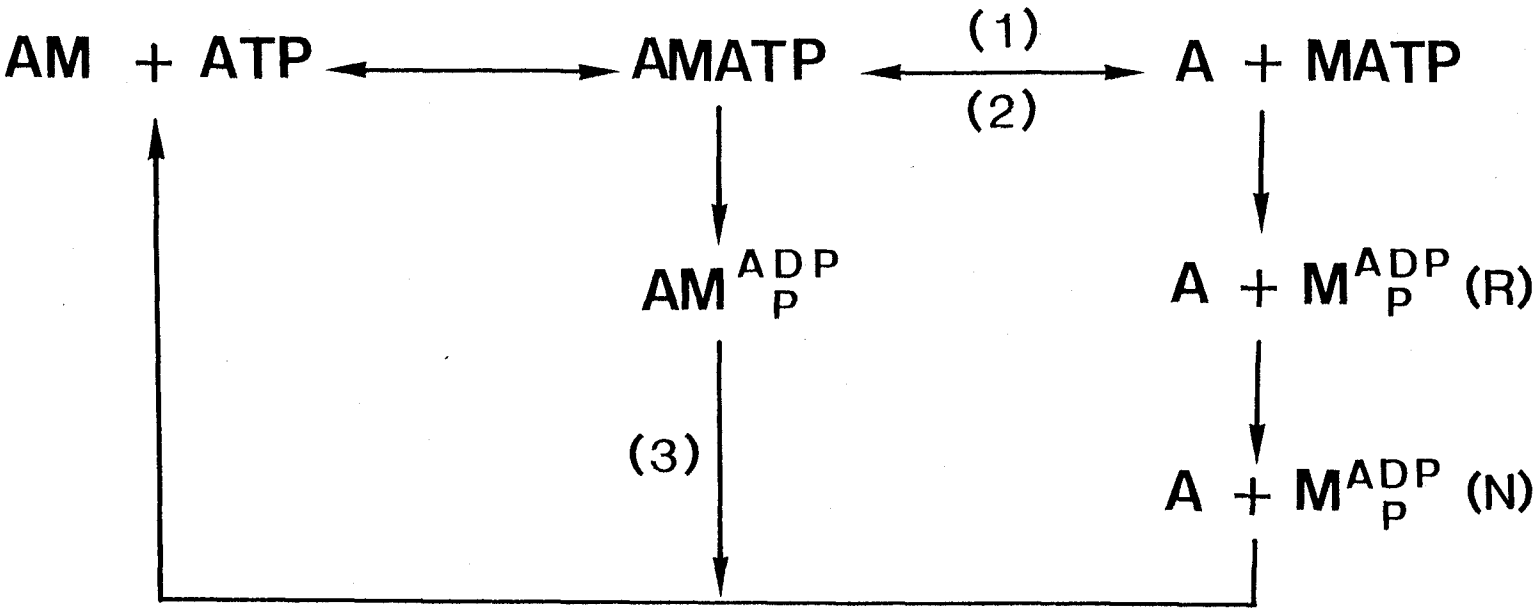

Fig. 5 The mechnism of actomyosin ATPase reaction performed by head B.

of Ca^{2+} in muscle cell through the conformational change in thin filaments. When Ca binds to troponin C in the thin filament, the thin filament is converted from the inactive to active form. Therefore it was proposed that the binding of head A with thin filament convert the conformation of actin filament rapidly to the active state, when the Ca^{2+} concentration sifts from low to high (19).

On the other hand, the regulation of smooth muscle contraction differs from that of skeletal muscle (20). The contraction of smooth muscle is regulated mainly through the phosphorylation of myosin light chains (21). Furthermore, it was shown (22) that the binding of smooth muscle myosin heads do not induce the conversion of the thin filament into active state. Ikebe et al. (23), reported that there is no heterogeneity in smooth muscle myosin heads.

Other hypothesis is that head A plays the role of preventing the slippage of crossbridges (13), i.e. head A binds with F-actin when head B dissociates from F-actin and dissociates from F-actin when head B is in the state of M_P^{ADP} (Fig. 6). This hypothesis is based on the observation of the fast release of ATP from the reaction intermediate formed by head A. For examining the validity of this hypothesis, it is very important to know how the existence of head A influences in the association to and the dissociation of head B from F-actin.

Keeping in view the vast amount of literatures in the field of muscle research, I have undertaken the present study to elucidate the heterogeneity and the functional aspects of myosin heads and the molecular mechanism of interactions involved in two

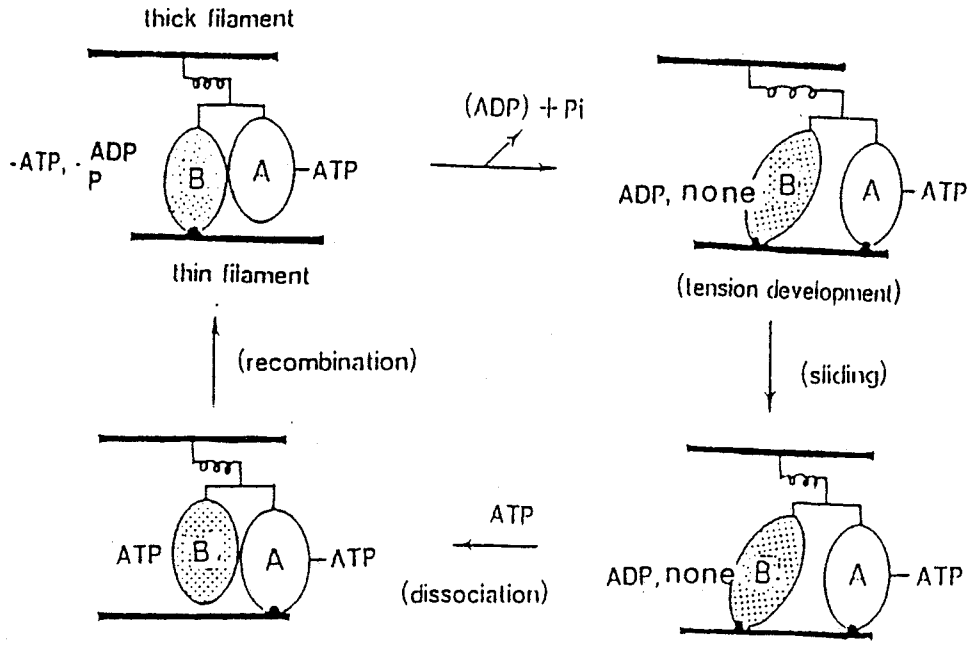

Fig. 6 The second hypothesis about the function of myosin head A.

myosin heads, actin and nucleotides. The findings of the investigations have been presented in following 5 parts:

Part 1 & 2 — Describes the studies using chicken gizzard smooth muscle showing the heterogeneity of myosin heads.

Part 3 — Deals with the studies on rabbit skeletal muscle myofibrils particularly the formation of myosin-nucleotide complexes.

Part 4 & 5 — Presents the cooperativity of myosin two heads in the binding to F-actin using rabbit skeletal muscle.

REFERENCES

1. Hasselbach, W. (1953) Z. Naturforsch. 8b, 449
2. Huxley, H. E. (1953) Biochim. Biophys. Acta 12, 387
3. Huxley, H. E. & Hanson, H. E. (1954) Nature 173, 973
4. Hanson, J. & Huxley, H. E. (1955) Symp. Soc. Exptl. Biol. 9, 228
5. Szent-György, A. (1942) Stud. Inst. Med. Chem. Univ. Szeged. 1,17
6. Szent-György, A. (1942) Chemistry of muscle Contraction 2nd ed. Academic Press, New York
7. Huxley, A. E. & Niedergerke, R. (1954) Nature 173, 971
8. Huxley, H. E. & Hanson, J. (1954) Nature 173, 973
9. Slayter, H. & Lowey, S. (1967) Proc. Natl. Acad. Sci. (USA), 58, 1611-1618
10. Elliott, A. & Offer, G. (1978) J. Mol. Biol. 123, 505-519
11. Huxley, H. E. (1963) J. Mol. Biol. 7, 281-308
12. Lowey, S. (1971) Myosin: molecule and filament in subunits in Biological Systems, part A, ed. S. N. Timasheff & G. C. Fasman, pp. 201-259
13. Inoue, A., Takenaka, H., Arata, T., & Tonomura, Y. (1979) Adv. Biophys. 13, 1-194
14. Miyanishi, T., Inoue, A., & Tonomura, Y. (1979) J. Biochem. 85, 747-753
15. Miyanishi, T., Maita, T., Matsuda, G., & Tonomura, Y. (1982) J. Biochem. 91, 1845-1853
16. Shibata-Sekiya, K. & Tonomura, Y. (1975) J. Biochem. 77, 543-557
17. Inoue, A., Ikebe M., &Tonomura, Y. (1980) J. Biochem. 88,

1663-1677

18. Inoue, A., Shigekawa, M., & Tonomura, Y. (1979) J. Biochem. 74, 923-934
19. Inoue, A. & Tonomura, Y. (1975) J. Biochem. 78, 83-92
20. Stephens, N. L. (1977) The Biochemistry of Smooth Muscle Baltimore: University Park Press
21. Bremel. R. D. (1974) Nature 252, 399-400
22. Filo, R. S., Bohr, D. F., & Ruegg, J. C. (1965) Science 147, 1582-1582
23. Ikebe, M., Onishi, H., & Tonomura, Y. (1982) J. Biochem. 88, 1629-1641
24. Arata, T., Inoue, A., & Tonomura, Y. (1975) J. Biochem. 77, 895-900
25. Furukawa, K., Ikebe, M., Inoue, A., & Tonomura, Y. (1980) J. Biochem. 88, 1629-1641

I

Reaction of Two Heads of Gizzard Myosin with ATP

SUMMARY

The reaction intermediates formed by two heads of smooth muscle myosin were studied. The amount of myosin-phosphate-ADP complex, M_P^{ADP}, formed was measured from the Pi-burst size over a wide range of ATP concentrations. At low concentrations of ATP, the Pi-burst size was 0.5 mol/mol myosin head, and the apparent K_d value was about 0.15 μM. However, at high ATP concentrations, the Pi burst size increased from 0.5 to 0.75 mol/mol myosin head with an observed K_d value of 15 μM. The binding of nucleotides to gizzard myosin during ATPase reaction was directly measured by a centrifugation method. Myosin bound 0.5 mol of nucleotides (ATP and ADP) with high affinity ($K_d \simeq 1$ μM) and 0.35 mol of nucleotides with low affinity (K_d = 24 μM) for ATP. These results indicate that gizzard myosin has two kinds of nucleotide binding sites, one forms M_P^{ADP} with high affinity for ATP and the other forms M_P^{ADP} and MATP with low affinity for ATP.

We studied the correlation between the formation of M_P^{ADP} and the dissociation of actomyosin. The amount of Pi-burst size was not affected by the existence of F-actin, and when 0.5 mol of ATP per mol of myosin head was added to actomyosin (1 mg/ml F-actin, 5 uM myosin at 0°C) most (93%) of added ATP was hydrolyzed in the Pi-burst phase. All gizzard actomyosin dissociated when 1 mol of ATP per mol myosin head was added to actomyosin. However, the extent of actomyosin dissociation at 0.5 mol of ATP per mol myosin head depended on the experimental conditions. In 0.35 mg/ml F-actin and at 0°C, where myosin binds weakly to F-actin, more than half of the myosin molecule dissociated from F-actin.

Under the condition where myosin binds tightly to F-actin (1 mg/ml F-actin and at 20°C), only less than 1/4 of myosin dissociated from F-actin. These results indicate that smooth muscle myosin forms M_P^{ADP} with a high affinity for ATP in one of the two heads of the myosin molecule and that the formation of M_P^{ADP} in the high affinity site results in the remarkable weakening of the binding of other head to F-actin.

INTRODUCTION

Muscle contraction occurs as a result of interaction between myosin and actin coupled to ATP hydrolysis. The myosin molecule has two heads which interact with F-actin and react with ATP, but why it has two heads is not yet known. In skeletal muscle myosin we (1,2) showed that the two heads of myosin form different ATPase intermediates. One head (head B) forms the myosin-phosphate-ADP complex (M_P^{ADP}) with high affinity for ATP and the other head (head A) forms the myosin-ATP complex (MATP) with low affinity for ATP. Also, the amino acid sequence around the specific lysine residue in head B differs from that in head A (3,4). On the other hand, Ikebe et al. (5) reported that MATP and M_P^{ADP} were formed with the same affinity for ATP, in gizzard myosin. They (5) claimed that the two heads of smooth muscle myosin are identical, both forming M_P^{ADP} which is in rapid equilibrium with MATP. However, their results were obtained only under limited conditions and can be explained by a mechanism in which MATP and M_P^{ADP} are formed by the different heads but with the same affinity for ATP. In this study, we measured the formation of reaction intermediates under a wide range of conditions and compared the results with the dissociation of actomyosin. The results obtained clearly indicate that gizzard myosin also has two nonidentical heads.

EXPERIMENTAL PROCEDURE

Chicken gizzard myosin (dephosphorylated) was prepared by the method of Ebashi(6). Skeletal muscle myosin was prepared from rabbit white skeletal muscle by the method of Perry (7). Skeletal muscle F-actin was prepared from acetone powder of rabbit skeletal muscle by the method of Spudich and Watt (8). ATP remaining in the F-actin solution was removed by ultracentrifugation at 100,000 x g for 3 h. The values of 48 and 4.2×10^4 were used as the molecular weights of myosin and actin monomer, respectively. Pyruvate kinase (PK) was prepared according to the method of Tietz and Ochoa (9). Chicken gizzard native tropomyosin was prepared by the method of Ebashi (10). The protein concentrations were determined by means of the biuret reaction calibrated by nitrogen determination.

ATP and staurosporin were purchased from Kohjin Co.,Ltd,Tokyo and Kyowa Medex Co.,Ltd, respectively. Phosphoenolpyruvate (PEP) and phalloidin were purchased from Boehringer Mannheim GmbH. Sodium Vanadate (NaVi) was prepared by the method of Goodno (11). (γ-^{32}P)ATP was synthesized enzymatically by the method of Johnson and Walseth (12). (α-^{32}P)ADP was obtained by enzymatic hydrolysis of (α-^{32}P)ATP (Radiochemical Center Amersham, England) and was purified by formation of stable myosin-Vi-ADP complex (11). (α-^{32}P)ATP (5 μM) was incubated with 5 uM skeletal muscle myosin in 0.5 M KCl, 10 mM $MgCl_2$, 1 mM NaVi , 0.1 mM EDTA, and 10 mM imidazole-HCl at pH 7.0 and 20°C for 4 h. The myosin-Vi- (α-^{32}P)ADP complex was collected by ammonium sulfate fractionation (45-60%) after dissolving the precipitate

in the same buffer. (α-^{32}P)ADP was released from myosin by raising the temperature to 90°C for 30 s. The denatured myosin was removed by centrifugation at 100,000 x g for 1 h. This cycle was repeated.

The ATPase reaction of myosin was measured from the time course of ^{32}Pi liberation using (γ-^{32}P)ATP as substrate (12). The reaction medium usually contained 0.5 M KCl, 10 mM $MgCl_2$, 0.1 mM EDTA, 50 mM imidazole-HCl at pH 7.0 and 0°C. Myosin (3 μM) was mixed with various concentrations of (γ-^{32}P)ATP and the reaction was quenched with 5% TCA and 0.1 mM cold Pi + 0.1 mM cold ATP as carrier. The amount of ^{32}Pi was determined as described previously (13). The size of the Pi burst was estimated by extrapolating the time course of Pi liberation in the steady state to time zero. The rate of Pi burst was determined in 0.2 -0.8 μM (γ-^{32}P)ATP and 0.1 μM myosin in the same buffer. The extent of phosphorylation of myosin light chain by MLCK was determined according to the method of Adelstain and Klee (14).

To determine the amount of tightly bound ATP the reaction was quenched with the same volume of 10 mM cold ATP, and after 10 min the reaction was stopped with 5% TCA and 0.1 mM Pi + 0.1 mM cold ATP as carrier, and then the amount of ^{32}Pi was determined.

The binding of nucleotide to myosin during the ATPase reaction was measured using a centrifugation method employing low ionic strength in which myosin forms a thick filament. Myosin (10 μM) was mixed with 5-100 μM (α-^{32}P)ADP in the presence of ATP-regenerating system (1 mg/ml PK and 5 mM PEP) in 50 mM KCl, 10 mM $MgCl_2$, 0.1 mM EDTA, and 50 mM imidazole-HCl at pH 7.0 and

0°C. The reaction mixture (1 ml) was applied to 25 µl of 60% sucrose in a centrifuge tube, and after centrifugation in a swing rotor at 150,000 x g for 30 min the radioactivity of the supernatant was measured.

The extent of ATP-induced dissociation of actomyosin was estimated from the change in light-scattering intensity (15) at 400 nm using a stopped-flow apparatus combined with a Hitachi-Perkin Elmer MPF-2A fluorescent spectrophotometer (16). The time course of change in fluorescence intensity at 340 nm with 288 nm excitation was measured using the same apparatus.

The binding ability of myosin to F-actin was examined by the centrifugation method. The solution (0.5 ml) containing 2 µM (0.96 mg/ml) myosin and 0.5 mg/ml F-actin in the presence or absence of 2 mM ATP in the reaction medium was centrifuged at 100,000 x g for 8-60 min and the amounts of myosin and F-actin in the supernatant were determined by the Bradford method (17) and SDS-PAGE using the buffer system of Laemmli (18).

RESULTS

Pi-Burst Size at Various ATP Concentrations—The amount of myosin-phosphate-ADP complex, M_P^{ADP}, was measured from the Pi-burst size at wide range of ATP concentrations. Figure 1 shows the time-courses of Pi liberation when the reactions were started by adding 2 or 100 μM (γ-^{32}P)ATP to 0.5 or 10 μM myosin, respectively. The reactions were quenched by TCA or unlabelled ATP. The sizes of Pi burst estimated by extrapolating the steady state rate of Pi liberation to time zero were 0.50 and 0.71 mol/mol myosin head, respectively, at 2 and 100 μM (γ-^{32}P)ATP. When the ATPase reactions were quenched with 5 mM unlabelled ATP, they were 0.54 and 0.78 mol/mol myosin, respectively, at 2 and 100 μM labelled ATP. The concentration of unlabelled ATP used for quenching was so high that when myosin was allowed to react with the mixture of labelled and unlabelled ATP for 10 min, less than 1% of labelled ATP was inverted to ADP and Pi.

Figure 2 shows the dependence of the size of the Pi burst on ATP concentration added. The dependence appeared to resolve into two phases. The Pi-burst size increased to 0.5 mol/mol myosin head at ATP concentration below 1 μM. The observed dissociation constant for ATP was about 0.15 μM. When the concentration of ATP was increased further to 100 μM, the Pi-burst size increased from 0.50 to 0.73 mol/mol myosin head. The observed dissociation constant of ATP for the increase in Pi-burst size was 15 μM. To examine the possibility that Pi burst with low affinity for ATP is due to the phosphorylation and dephosphorylation of myosin light chain, we studied the effect of MLCK inhibitor and EGTA

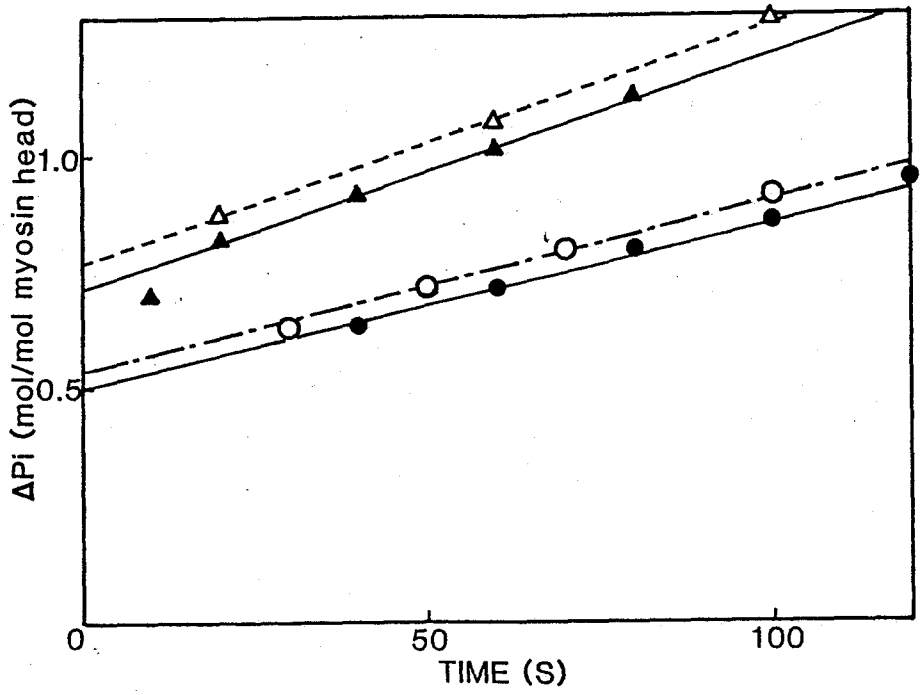

Fig. 1. Time course of ^{32}Pi liberation in the initial phase of gizzard myosin Mg^{2+}-ATPase reaction at low and high ATP concentrations, and the effect of quenching the gizzard myosin ATPase reaction by addition of excess unlabelled ATP. The reaction was started by mixing (γ-^{32}P)ATP with gizzard myosin and quenched with 5% TCA (●, ▲). The reaction was also quenched with 5 mM unlabelled ATP (O, △) and finally stopped with 5% TCA. 0.5 M KCl, 10 mM $MgCl_2$, 0.1 mM EDTA, 50 mM imidazole-HCl at pH 7.0, and 0°C. ● , O , 0.5 μM gizzard myosin and 2 μM (γ-^{32}P)ATP; ▲, △ , 10 μM gizzard myosin and 100 μM (γ-^{32}P)ATP.

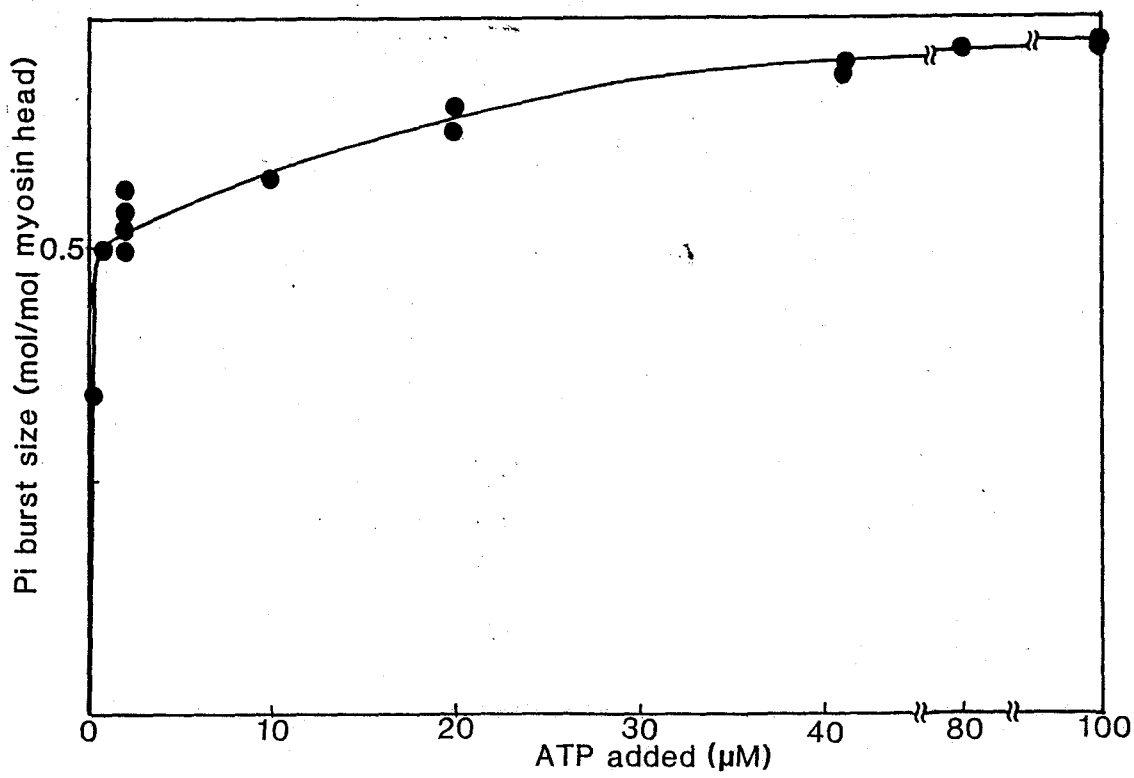

Fig. 2. Dependence on ATP concentration of the Pi-burst size in the gizzard myosin Mg^{2+}-ATPase reaction. 2-100 μM ATP. Myosin concentration was 1/4 - 1/10 that of ATP. Other conditions were the same as those for Fig. 1. The size of the Pi burst was estimated by extrapolating the time course of ^{32}Pi liberation in the steady state to time zero.

on the Pi-burst size in 50 μM ATP and 3 μM myosin. The phosphoryla tion of myosin light chain by 0.5 mg/ml of smooth muscle native tropomyosin was inhibited by 40 nM staurosporin or 1 mM EGTA. However, 40 nM staurosporin or 1 mM EGTA did not affect the Pi-burst size and steady-state rate of the ATPase reaction measured under the same conditions except that smooth muscle native tropomyosin was absent.

The affinity of ATP for formation of M_P^{ADP} at low ATP concentration was estimated from the rate constants for formation and decomposition of M_P^{ADP}. When myosin forms M_P^{ADP}, the tryptophan fluorescence of myosin increases (19). The rate of M_P^{ADP} decomposition was measured from the decrease in fluorescence intensity after adding ATP to myosin. Figure 3 A shows the time course of change in fluorescence intensity after adding 2 μM ATP to 2 μM gizzard myosin at the time shown by the arrow. The tryptophan fluorescence increased rapidly and then decreased gradually. The magnitude of fluorescense change of smooth muscle myosin induced by ATP was 6.5%. The half time of decrease was 91 s and the rate of decomposition of M_P^{ADP} was 7.6×10^{-3} s^{-1}. Figure 3 B shows the dependence on ATP concentration of the rate of Pi burst by gizzard myosin. The rate of Pi burst was estimated from the initial velocity of the Pi burst regarding as the amount of the Pi-burst site was 0.5 mol/mol myosin head. The rate increased linearly as the concentration of ATP added increased from 0.2 to 1 μM. The second order rate constant of M_P^{ADP} formation, k_f, was estimated to be 6.3×10^4 $s^{-1}M^{-1}$. The Michaelis constant, K_m, for formation of M_P^{ADP} was estimated as k_d/k_f to be 1.2×10^{-7} M.

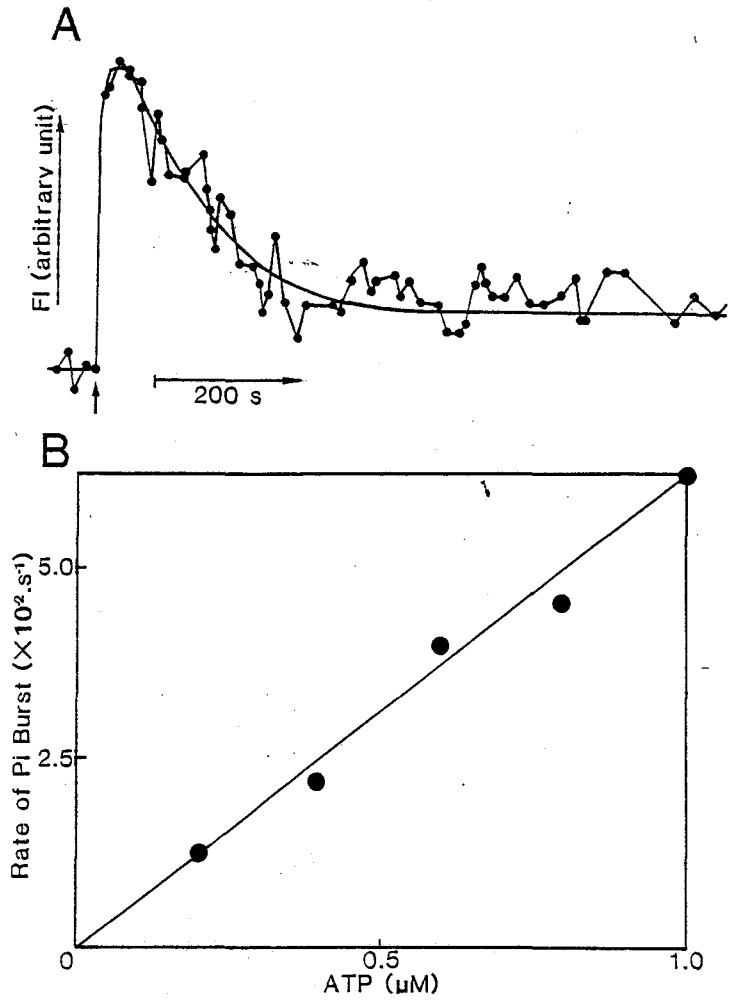

Fig. 3. A) Time course of recovery in the ATP-induced increase in tryptophan fluorescence. ATP (2 μM) was mixed with 2 μM gizzard myosin at the time shown by the arrow, and the fluorescence intensity at 340 nm excited at 288 nm was recorded. Other conditions were the same as those for Fig. 1.
B) Dependence on ATP concentration of the rate of Pi burst. The ATPase reaction was started by mixing 0.2-1.0 μM (γ-^{32}P)ATP with 0.1 μM gizzard myosin and stopped with 5% TCA. The rate of initial rapid liberation of Pi was plotted against ATP concentrations added. The rate was calculated from the initial velocity of Pi liberation regarding as the amount of burst was 0.5 mol/mol myosin head. Other conditions were the same as those for Fig. 1.

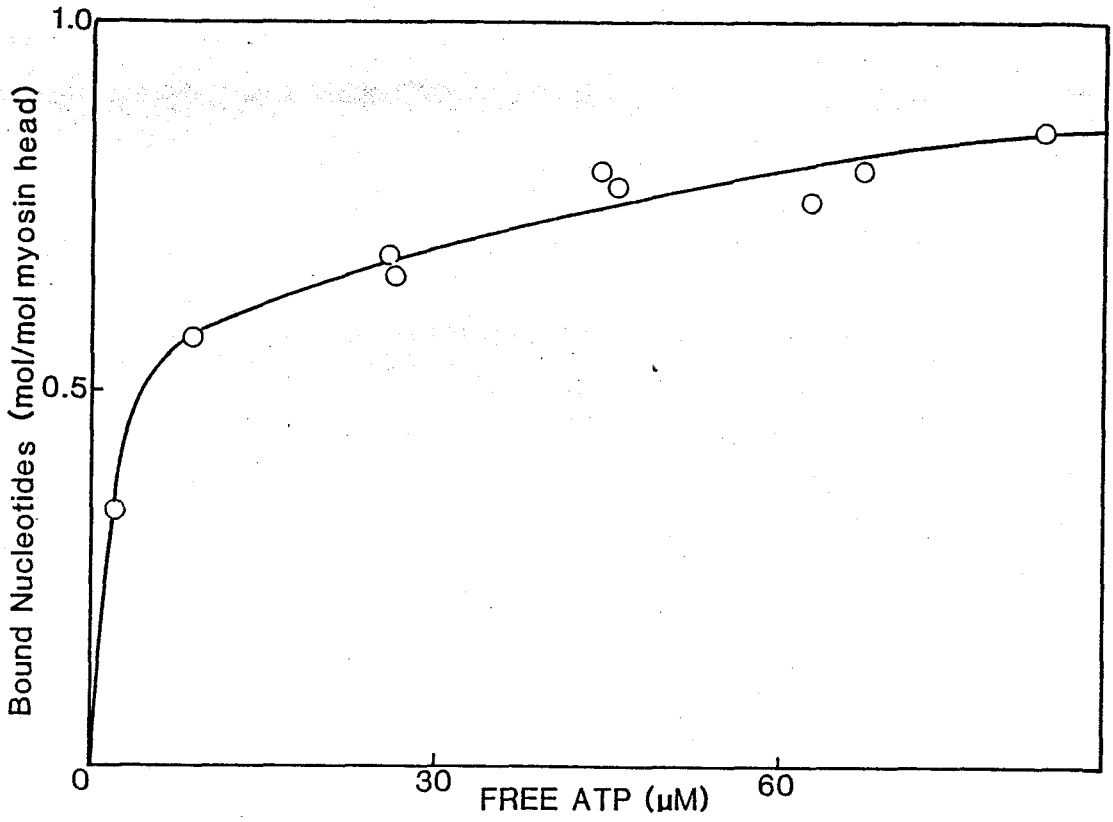

Fig. 4. Dependence on ATP concentration of the amount of nucleotide bound to myosin during the ATPase reaction. Various concentrations (5-200 μM) of (α-^{32}P)ATP were mixed with 10 μM gizzard myosin at low ionic strength in the presence of the ATP-regenerating system (1 mg/ml PK and 5 mM PEP). After 5 min the mixture was centrifuged at 150,000 x g for 30 min, and the radioactivity in the supernatant was measured. 50 mM KCl, 10 mM $MgCl_2$, 0.1 mM EDTA, 50 mM imidazole-HCl at pH 7.0, 0°C.

Binding of Nucleotide to Gizzard Myosin during the ATPase Reaction at Low Ionic Strength—Using a centrifugation method, we measured the amount of nucleotide bound to myosin under the conditions where myosin forms a thick filament and hydrolyzes ATP. As shown in Fig. 4, the amount of total bound nucleotides (ATP and ADP) also increased by two phases with an increase in ATP concentration. The nucleotide (0.5 mol per myosin head) bound to myosin with high affinity ($K_d \simeq 1$ μM), and 0.31 mol of nucleotides per mol of myosin head bound with low affinity (K_d = 24 μM).

Formation of Myosin-P-ADP Complex in the Presence of F-Actin—To correlate M_P^{ADP} formation with actomyosin dissociation, we examined the effects of F-actin on the Pi-burst size. Figure 5 shows the time course of ^{32}Pi liberation after adding 2 or 40 μM (γ-^{32}P)ATP to gizzard myosin in the presence (○, △) or absence (●, ▲) of 0.5 mg/ml F-actin. When 40 μM ATP was mixed with 5 uM gizzard myosin, the Pi-burst size was 0.68 mol/mol myosin head both in the presence and absence of F-actin. The ATPase activity in the steady state increased from 0.0082 s^{-1} to 0.0116 s^{-1} by the presence of F-actin. When 2 μM ATP was mixed with 0.5 μM gizzard myosin, the Pi burst size was 0.5 mol per mol myosin head both in the presence and absence of 0.5 mg/ml F-actin. The ATPase activity increased from 0.0076 s^{-1} to 0.0094 s^{-1} by the presence of 0.5 mg/ml F-actin. Figure 6 shows the single turnover hydrolysis of ATP by gizzard myosin in the presence (○) or absence (●) of F-actin. When 5 uM ATP was mixed with 5 uM myosin in the absence of F-actin, ATP was hydrolyzed rapidly into ADP + Pi. The amount of ATP hydrolyzed in the Pi-burst phase,

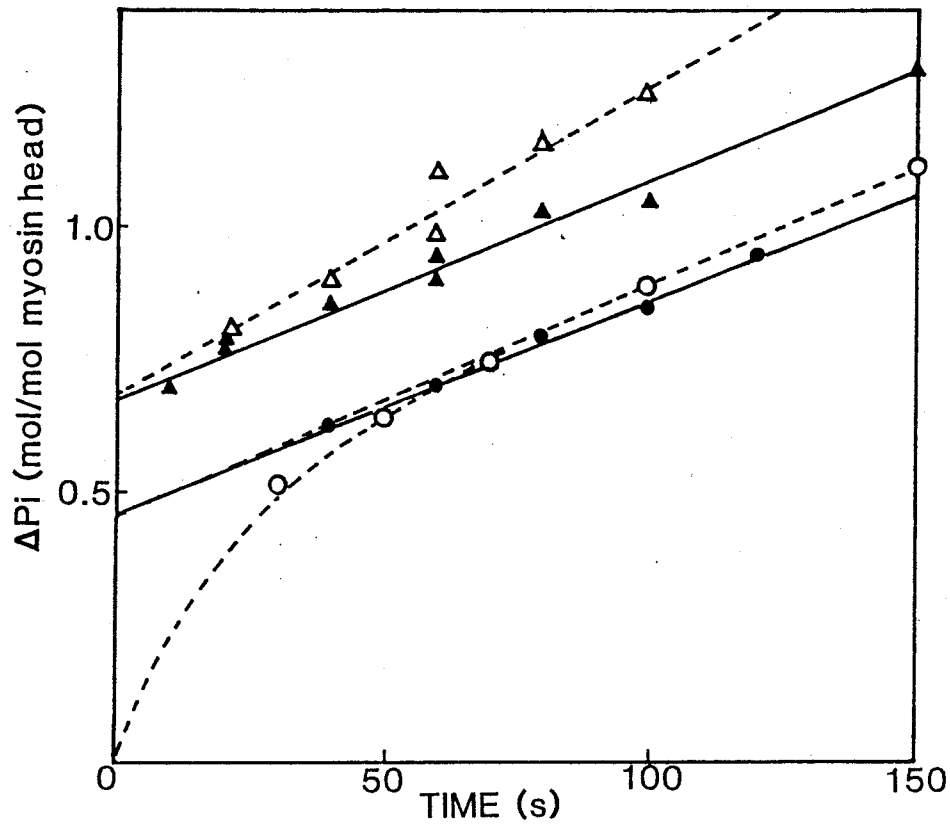

Fig. 5. Effect of F-actin on the initial Pi-burst of gizzard myosin Mg^{2+}-ATPase. Time course of Pi liberation in the initial phase of gizzard myosin Mg^{2+}-ATPase was measured in the absence (●, ▲) or presence of 0.5 (○) or 1 mg/ml (△) skeletal muscle F-actin. ●, ○, 0.5 μM myosin and 2 μM (γ-^{32}P)ATP; ▲, △, 5 μM myosin and 40 μM ATP. Other conditions were the same as those for Fig. 1.

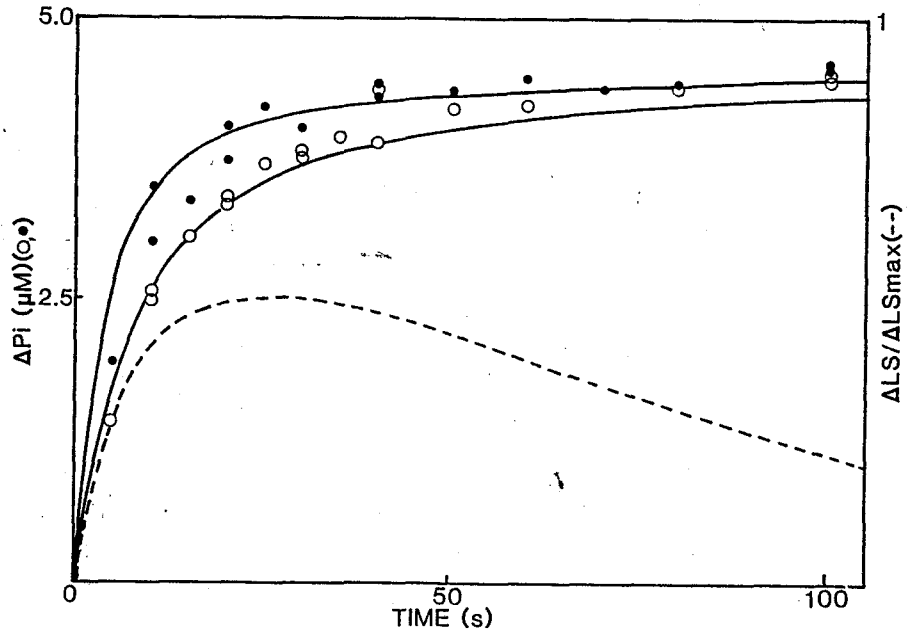

Fig. 6. Single-turnover hydrolysis of ATP by gizzard actomyosin and the time course of dissociation and recombination of actomyosin after ATP addition. The time course of Pi liberation was measured after starting the reaction by mixing 5 μM (γ-^{32}P)ATP with 5 μM gizzard myosin in the absence (●) or presence (○) of 1 mg/ml skeletal muscle F-actin. Upper and middle curves indicate the time courses of hydrolysis which were calculated using 6.3×10^4 $s^{-1}M^{-1}$ and 2.9×10^4 $s^{-1}M^{-1}$ as the second order rate constant, respectively. The time course of dissociation and recombination of actomyosin was measured from the decrease and recovery of light-scattering intensity at 400 nm (ΔLS) after mixing 5 μM ATP with the complex of 5 μM gizzard myosin and 1 mg/ml skeletal muscle F-actin and is represented as $\Delta LS / \Delta LS_{max}$ (----). ΔLS_{max} was estimated from the extent of light-scattering change when 2 mM ATP was added to the actomyosin complex. Other conditions except for the protein concentrations, were the same as those for Fig. 1.

Δ Pi_{max}, was 93% of ATP added. The solid line indicates the time course of Pi liberation calculated from the second order rate constant of 6.3×10^4 $s^{-1}M^{-1}$, which was obtained in Fig. 3 B. The time course of Pi burst in the presence of 1 mg/ml F-actin was in good agreement with the line calculated from the second order rate constant 2.9×10^4 $s^{-1}M^{-1}$. Thus, F-actin reduced the Pi-burst rate. Similar results were obtained even at 20 C. When 2 μM gizzard myosin was mixed with 4 or 8 μM ATP in the presence of 0.5 mg/ml F-actin, the Pi-burst size was 0.57 or 0.59 mol per mol of myosin head, respectively, and the second order rate constant of Pi burst was found to be 2.9×10^5 $s^{-1}M^{-1}$. When 2 μM ATP was mixed with 2 μM myosin under the same conditions, 80% of ATP was converted to ADP and Pi at the rate constant of 2.9×10^5 $s^{-1}M^{-1}$ (data not shown).

Dissociation of Acto-Gizzard Myosin by Mg^{2+}-ATP—Before we estimated the extent of actomyosin dissociation from the change in light-scattering intensity after the addition of ATP, the binding ability of gizzard myosin to F-actin was checked by the centrifugation method (Table I). In a control experiment, myosin or actin alone was centrifuged at 100,000 x g for 8.5-60 min. Actin was precipitated almost completely (96%) by the centrifugation for 28.5 min. However, myosin was precipitated very slowly (4.5, 5.7, 8 and 21%, respectively at 8.5, 19, 28.5 and 60 min). On the other hand, when actomyosin was centrifuged in the absence of ATP, 93.3% and 99.3% of the proteins were precipitated at 28.5 min and 60 min, respectively. When actomyosin was centrifugeed in the presence of 2 mM ATP for 28.5 min and 60 min, 91% and 78%, respectively of myosin remained in

TABLE I. Binding ability of myosin to F-actin. The reaction mixture containing 2 μM gizzard myosin and/or 0.5 mg/ml F-actin in 15 uM phalloidin, 0.5 M KCl, 10 mM $MgCl_2$, 0.1 mM EDTA, and 50 mM imidazole-HCl at pH 7.0 and 0°C was centrifuged at 100,000 x g for 8.5, 19, 28.5 and 60 min, and the amounts in the supernatant were determined by the Bradford method. The amounts of proteins were shown taking the value before the centrifugation (time 0) as 100%.

	Supernatant after centrifugation (%)				
Time for centrifugation (min)	0	8.5	19	28.5	60
Myosin	100	96	94	92	79
Actin	100	54	7.3	4.1	0.2
Actomyosin (-ATP)	100	8.5	1.3	2.7	0.7
Actomyosin (+ATP)	100	87	69	60	49
	(100)			(91)	(78)

The values in the parenthesises show the amounts of myosin in the supernatant determinded by SDS-PAGE.

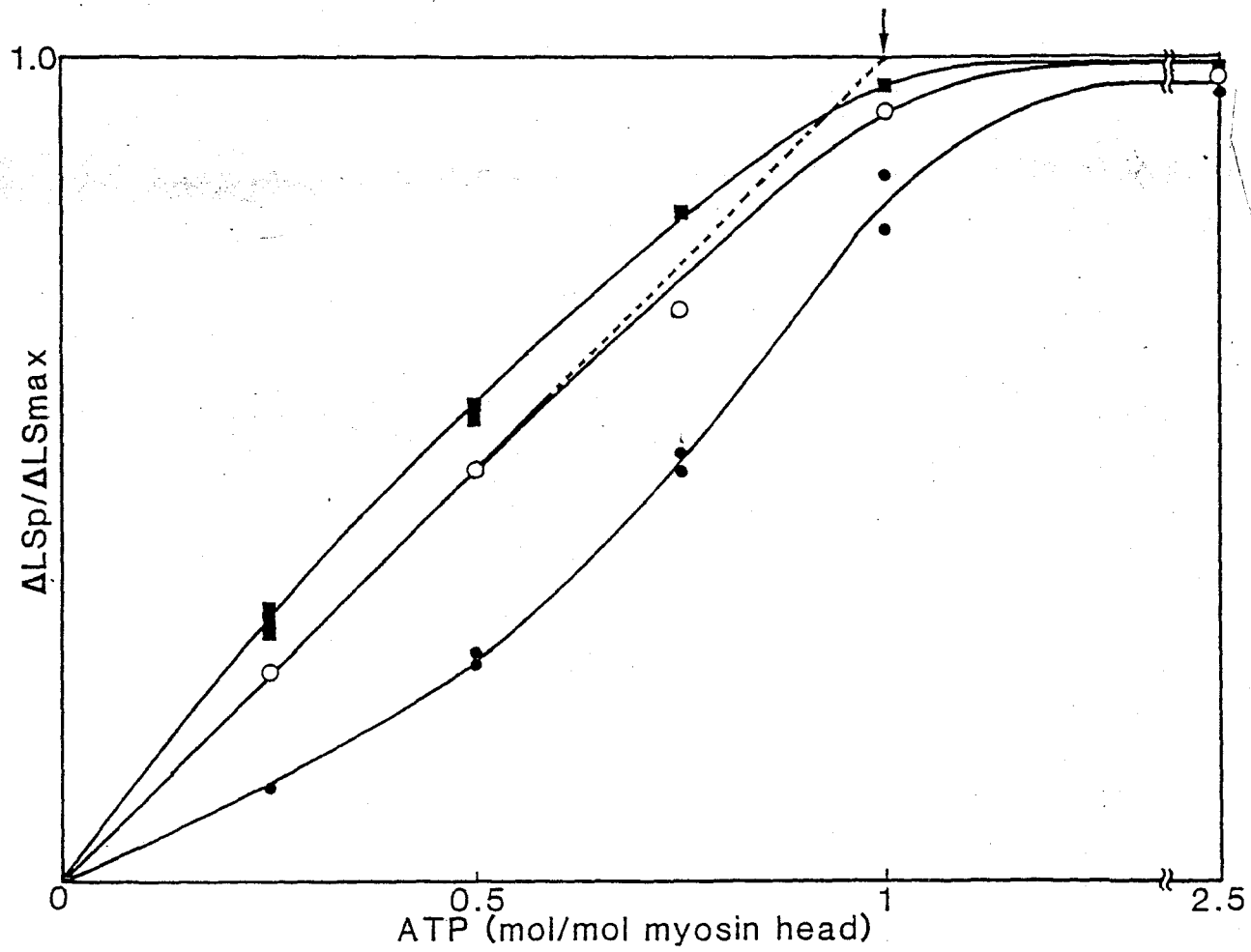

Fig. 7. Dependence on ATP concentration of the extent of dissociation of acto-gizzard myosin. The extent of dissociation of actomyosin is represented as $\Delta LS_p/\Delta LS_{max}$ at given ATP concentrations. $\Delta LS_p/\Delta LS_{max}$ was obtained as the amplitude at the plateau in the time course of light-scattering intensity $\Delta LS/\Delta LSmax$ (see Fig. 6). ●, ○, 5 μM gizzard myosin, 1 mg/ml F-actin at 0 (○) or 20°C (●). ■, 3 μM gizzard myosin, 0.35 mg/ml F-actin at 0°C. Other conditions were the same as those for Fig. 1.

the supernatant. These values were the same as those when myosin alone was centrifuged for 28.5 and 60 min (92 and 79%, respectively). Therefore, myosin does not bind to F-actin in the presence of 2 mM ATP.

The extent of dissociation of actomyosin induced by ATP was measured from the change in light-scattering (ΔLS). The maximum change in light-scattering intensity by the complete dissociation of actomyosin (ΔLS_{max}) was estimated by the addition of 0.1-2 mM ATP which causes actomyosin to dissociate completely as shown by the results from the centrifugation method (see above). The broken line in Fig. 6 represents the time course of the change in light-scattering intensity of actomyosin. The extent of decrease in light-scattering followed the amount of Pi liberation until 15 s. The ratio of $\Delta LS/\Delta LS_{max}$ to $\Delta Pi/\Delta Pi_{max}$ was 0.77-0.85. The value of $\Delta LS/\Delta LS_{max}$ reached a maximal level of 0.5 at 25 s, and then recovered at the rate of 1.3×10^{-2} s^{-1}.

Figure 7 shows the extent of actomyosin dissociation at a given ATP concentration. The extent was represented as $\Delta LS_p/\Delta LS_{max}$ where ΔLS_p is the intensity change at the plateau phase as shown by the broken line in Fig. 6, and it was plotted against the amount of ATP added. Almost all myosin dissociated from F-actin when 1 mol of ATP per mol myosin head was added to actomyosin, while the extent of dissociation induced by less than 1 mol/mol myosin of ATP varied with the experimental conditions. When ATP was added to the mixture of 5 uM myosin and 1 mg/ml F-actin at 20°C, where myosin binds tightly to F-actin, about 1/4 of the myosin was dissociated by 0.5 mol of ATP per mol myosin head. On the other hand, in the presence of 3 μM myosin and 0.35

mg/ml F-actin at 0°C, where myosin binds weakly with F-actin, more than half of the myosin (56%) was dissociated by 0.5 mol of ATP per mol of myosin head. The extent of dissociation increased linearly with an increase in the concentration of ATP added when ATP was added to 5 μM myosin and 1 mg/ml F-actin at 0°C. The amount of M_P^{ADP} formed was less than that of ATP added when the light-scattering change was in the plateau phase, since the rate of M_P^{ADP} formation was not sufficiently high compared to that of M_P^{ADP} decomposition. We attempted to estimate the correlation between M_P^{ADP} formation and actomyosin dissociation from Fig. 6. When 0.25, 0.31 and 0.34 mol of M_P^{ADP} per mol myosin were formed, the extent of dissociation of actomyosin were 0.43, 0.49 and 0.51, respectively.

DISCUSSION

Myosin has two heads, each of which can bind to actin and react with nucleotide. The functions of the two heads have been studied mainly with skeletal muscle myosin. We (1,2) have shown that each head of skeletal muscle myosin forms a different intermediate during ATPase reaction. One head (head B) forms M_P^{ADP} with high affinity for ATP, while the other (head A) forms MATP with low affinity for ATP. However, Ikebe et al. (20) reported that smooth muscle myosin of chicken gizzard muscle has two identical heads which form MATP and M_P^{ADP} in rapid equilibrium.

In the present study, we examined the intermediates formed by gizzard myosin. The formation of M_P^{ADP} can be easily detected by the rapid Pi liberation in the initial phase of the reaction. We measured the Pi burst size under various ATP concentrations (Fig. 2). The Pi burst of 0.5 mol per myosin head was observed at low ATP concentrations. The observed dissociation constant was about 0.15 μM. At a high ATP concentration, the Pi burst size increased from 0.5 to 0.73 mol per myosin head. The affinity of ATP for the increase in Pi-burst size was 15 μM. We considered that the Pi burst with high affinity for ATP was due to the formation of M_P^{ADP} which has been characterized in skeletal muscle myosin, since the dissociation constant of ATP for M_P^{ADP} formation calculated from the rates of formation and decomposition of M_P^{ADP} (0.12 μM) (Fig. 3) agreed with that of the high affinity Pi-burst site.

We directly measured the amount of nucleotides bound to

myosin by a centrifugation method under the conditions in which myosin forms thick filament (Fig. 4). Nucleotide binding under these conditions also could be resolved into two phases with different affinities for ATP. The amount of the high affinity site was 0.5 mol/mol myosin head and the dissociation constant was of the same order of magnitude as that of Pi burst and that calculated from the rates of formation and decomposition of M_P^{ADP}. On the other hand, the amount of the low affinity site was 0.31 mol/mol head which was slightly larger than that of the Pi burst (0.23 mol/mol). The present results suggested that head A of gizzard myosin forms M_P^{ADP}, with low affinity for ATP. However, since the amount of M_P^{ADP} formed in this site is smaller than the stoichiometric value, and since the dissociation constant of the low affinity Pi burst is higher (15 μM) than that for the actomyosin dissociation by ATP (1-2 μM), the possibility remained that the low affinity Pi-burst occurs at a site other than the head which is like head A of skeletal muscle myosin.

Furukawa et al. (21) reported that in the case of skeletal muscle myosin the Pi-burst size increased to more than 0.5 mol per myosin head. They showed that so called "extra burst" is due to the formation of free Pi in the initial phase of myosin ATPase reaction. However, in the case of gizzard myosin we could not detect the formation of free Pi in the initial phase even in high concentration of ATP (data not shown). Therefore, the Pi burst of gizzard myosin with low affinity for ATP is not caused by the mechanism of the extra burst.

We considered that the Pi burst with low affinity for ATP is not due to the phosphorylation of light chain, since the

phosphate incorporated into light chain is stable in TCA (22) and all the experiments were performed in the absence of Ca^{2+}, where the phosphorylation does not take place. The Pi burst with low affinity for ATP is also not due to the rapid phosphorylation and dephosphorylation of myosin light chain, because we could not detect free Pi formation in the initial phase. Furthermore, staurosporin or EGTA, which inhibited the phosphorylation of myosin light chain with MLCK, did not affect the Pi-burst size (see "RESULTS").

We could not find the increase in the Pi-burst size of the ATPase reaction of skeletal muscle myosin when a high concentration of ATP was added to myosin (data not shown). This result agrees with those observed previously by Kanazawa and Tonomura (23) and Inoue et al. (24). In skeletal muscle myosin, head A forms the myosin-ATP complex (MATP) with low affinity for ATP (2,25).

Ikebe and his coworkers (20) reported that both heads of myosin form M_P^{ADP} and MATP and that the complexes are in equilibrium. We searched for tightly bound ATP (MATP) by quenching the ATPase reaction with unlabelled ATP. When the ATPase reaction of gizzard myosin was quenched with unlabelled ATP, only a small amount of labelled Pi was formed (Figs. 1 and 5). This result suggests that M_P^{ADP} was in rapid equilibrium with only a small amount of MATP.

The next question was whether or not the two kinds of sites exist in a single myosin molecule. To answer it, we compared the extent of actomyosin dissociation with formation of reaction intermediates. We studied the intermediates formed by gizzard

myosin in the presence of skeletal F-actin at high ionic strength. F-actin slightly accelerated the steady state rate of ATP hydrolysis even in 0.5 M KCl and inhibited the rate of phosphate burst. However, the size of the Pi burst was not affected by the presence of F-actin. When 0.5 mol ATP per mol myosin head was added to myosin, 0.47 mol M_P^{ADP} per mol myosin head was formed whether or not F-actin was present (Fig. 6). We measured the actomyosin dissociation induced by ATP with the light-scattering method. Under the conditions in which myosin binds loosely to F-actin, i.e. 0.35 mg/ml F-actin at 0°C, 0.5 mol of ATP per mol myosin induced the dissociation of more than half of the myosin from F-actin. Since all the ATP added was not converted into M_P^{ADP} when light-scattering change was at the plateau phase (Fig. 6), the extent of dissociation of actomyosin by formation of 0.5 mol of M_P^{ADP} per mol myosin head should be much higher than 0.5. It is emphasized that the extent of actomyosin dissociation is about 1.5 fold that of formation of M_P^{ADP} per myosin head (Fig. 6). Furthermore, if actomyosin dissociates only when both heads of myosin react with ATP, dissociation of actomyosin by ATP should occur after a lag phase. But we could not observed such a lag phase. The present results suggested that M_P^{ADP} is formed in one of the two heads of myosin and that formation of M_P^{ADP} in one (head B) of the two heads induces the dissociation of actomyosin. The present results on the dissociation of smooth muscle myosin by ATP was similar to that of skeletal muscle myosin. Onishi et al. (26) reported that all skeletal muscle myosin dissociates from F-actin with 0.5 mol of ATP per mol myosin head under restricted conditions.

On the other hand, under the condition where myosin binds tightly to F-actin, 1/4 of myosin dissociated from F-actin when 0.5 mol of ATP per mol myosin was added (Fig. 7). Therefore, under this condition dissociation of actomyosin requires not only the formation of M_P^{ADP} in head B but also the reaction of ATP to the other head. This result also showed that high affinity sites are not located on the both heads of one myosin molecule, since if half of the myosin molecule reacts with all the ATP added, half of myosin would dissociate from F-actin with 0.5 mol of ATP per mol of myosin head.

Actomyosin dissociated almost completely by addition of 1 mol of ATP per mol myosin head. The observed K_d value for ATP in actomyosin dissociation was 1-2 μM which was less than those of low affinity nucleotide binding (Fig. 4) and low affinity Pi-burst (Fig. 2 and 5). It is not clear why the affinity of actomyosin for ATP is so high. One possibility is that affinity of head A for ATP is strengthened by the existence of F-actin.

Inoue et al. (27) reported that relaxation of actomyosin in the presence of troponin and tropomyosin by removal of Ca^{2+} requires the binding of ATP to head A. The mechanism of Ca^{2+} control of smooth muscle is quite different from that of skeletal muscle (28). In skeletal muscle, Ca^{2+} binds to troponin C on the thin filament, while the contraction of smooth muscle is regulated by the Ca^{2+}-dependent phosphorylation of the myosin light chain. Furthermore, relaxation of skeletal muscle requires a high concentration of ATP, while that of smooth muscle does not (29). Ikebe and his coworkers (5) claimed that the nonidentical two-headed structure of myosin was necessary for thin filament-

linked regulation, and that myosin from smooth muscle, which has its contraction regulated by phosphorylation of the myosin light chain, has two identical heads. However, in the present study, we found that smooth muscle myosin also has a nonidentical two-headed structure. Therefore, we suggest that this nonidentical two-headed structure of myosin is required not only for the regulation of muscle contraction but also for the contraction itself such as in smooth movement of myosin head along the thin filament.

REFERENCES

1. Inoue, A., Takenaka, H., Arata, T. & Tonomura, Y. (1979) Adv. Biophys. 13, 1-194
2. Inoue, A. & Tonomura, Y. (1974) J. Biochem. 76, 755-764
3. Miyanishi, T., Inoue, A,. & Tonomura, Y. (1979) J. Biochem. 85, 747-753
4. Miyanishi, T., Maita, T., Matsuda, G. & Tonomura, Y. (1982) J. Biochem. 91, 1845-1853
5. Ikebe, M., Onishi, H., & Tonomura, Y. (1982) J. Biochem. 91, 1855-1873
6. Ebashi, S. (1976) J. Biochem. 79, 229-231
7. Perry, S.V. (1955) in Methods in Enzymology (Colowich, S.T. & Kaplan, N.O., eds) Vol. 2, pp. 582-588, Academic Press, New York
8. Spudich, J.A. & Watt, S. (1971) J. Biol. Chem. 246, 4866-4871
9. Tietz, A. & Ochoa, S. (1962) in Methods in Enzymology (Colowick, S.P. & Kaplan, N.O., eds.) Vol. 5, pp. 365-369, Academic Press, New York
10. Ebashi, S. (1976) J. Biochem. 79, 229-231
11. Goodno, C.C. (1979) Proc. Natl. Acad. Sci. U.S.A. 76, 2620-2624
12. Johnson, R.A. & Walseth, T.F. (1979) Adv. Cyclic Nucleotide Res. 10, 137-167
13. Nakamura, H. & Tonomura, Y. (1968) J. Biochem. 63, 279-294
14. Adelstein, R.S., & Klee, C.B. (1982) in Methods in Enzymology (Colowich, S.P. & Kaplan, N.O., eds.) Vol. 85, pp. 298-231 Academic Press, New York

15. Inoue, A. & Tonomura, Y. (1980) J. Biochem. 88, 1643-1651
16. Takemori, S., Nakamura, M., Suzuki, K., Katagiri, M., & Nakamura, T. (1972) Biochem. Biophys. Acta 284, 382-393
17. Bradford, M. (1976) Anal.Biochem. 72, 248-254
18. Laemmli, V.K. (1970) Nature 277, 680-685
19. Werber, M.M., Szent-Gyorgyi, A.G., & Fasman, G.D. (1972) Biochemistry 11, 2872-2883
20. Furukawa, K., Inoue, A., & Tonomura, Y. (1981) J. Biochem. 89, 1283-1292
21. Sobieszek, A. (1977) Eur. J. Biochem. 73, 477-483
22. Kanazawa, T., & Tonomura, Y. (1965) J. Biochem. 57, 604-615
23. Inoue, A., Shibata-Sekiya, K., & Tonomura, Y. (1972) J. Biochem. 71, 115-124
24. Furukawa, K., Ikebe, M., Inoue, A., & Tonomura, Y. (1980) J. Biochem. 88, 1629-1641
25. Onishi, H., Nakamura, H., & Tonomura, Y. (1968) J. Biochem. 64, 769-784
26. Inoue, A. & Tonomura, Y.(1975) J. Biochem. 78, 83-92
27. Bremel, R.D. (1974) Nature 252, 399-400
28. Filo, R.S., Bohr, D.F,. & Ruegg, J.C. (1965) Science 147, 1582-1583

II

Heterogeneity in the Reaction of Chicken Gizzard Myosin Subfragment-1 with Magnesium Adenosine Triphosphate

SUMMARY

We studied whether smooth muscle myosin has identical or non-identical heads by analyzing the reactions of chicken gizzard myosin subfragment-1 with Mg^{2+}-ATP in the presence and absence of F-actin at high ionic strength. Gizzard S-1 bound tightly with F-actin, and dissociated from F-actin by one mol of ATP per mol of S-1, indicating that each S-1 has one active site for interaction with ATP. We estimated the amount of the myosin-phosphate-ADP complex (M_p^{ADP}) from the initial rapid liberation of Pi after stopping the ATPase reaction with TCA (Pi-burst). At ATP concentrations below 5 μM the Pi-burst size was 0.5 mol/mol S-1 with dissociation constant of 0.3 μM. The Pi-burst size increased slightly to 0.65 mol/mol S-1 with further increase in ATP concentration. The amount of MATP estimated as the difference between the amount of S-1 dissociated from F-actin and that of Pi-burst size was 0.4 mol/mol of S-1. The observed affinity of MATP formation for ATP was almost the same as that of Pi-burst size. However, MATP was not decomposed into ADP and Pi after chasing the MATP formation by cold ATP suggesting that MATP is rapidly replaced to M + ATP. A rapid release of ATP from MATP was observed directly by adding excess skeletal S-1 which hydrolyzes free ATP very rapidly. On the other hand M_p^{ADP} decomposed slowly to M + ADP + Pi, although we concluded that MATP and M_p^{ADP} are formed in the different heads of gizzard myosin.

INTRODUCTION

Myosin has two separated heads and each of them can bind with F-actin and reacts with ATP. The function of two heads has mainly been studied on rabbit skeletal muscle myosin, and it was shown (1-3) that the myosin-phosphate-ADP complex (M_P^{ADP}) is formed in one head (head B), while the myosin-ATP complex (MATP) is formed in the other head (head A) of the myosin molecule. F-actin greatly accelerates the decomposition of M_P^{ADP} and actomyosin ATP ase reaction which is coupled with muscle contraction occurs only in head B (1,4-6). We (7) showed that relaxation of contraction requires the binding of ATP to head A, however, the function of this head in the contraction has not been clarified.

To understand the function of head A, it is important to know whether all the myosin have non-identical head or not. The reaction intermediates of the ATPase of smooth muscle myosin have been studied by several workers. Formation of M_P^{ADP} was studied from the initial rapid liberation of TCA-labile Pi. Takeuchi and Tonomura (8-10) showed that arterial myosin showed 1 mole of Pi-burst per mol of myosin. Srivastava et al. (11) and Ikebe et al. (12) reported that gizzard myosin showed 1 mol of Pi-burst per mol of myosin. However, Ikebe et al. (13) reported that Pi-burst size of gizzard myosin was higher than 1 mol per mol of myosin and that the affinity of ATP for formation of MATP was equal to that of M_P^{ADP}. Then, they (13) proposed that the two heads of smooth muscle myosin are identical, and that both heads form M_P^{ADP} which is in rapid equilibrium with MATP. However, it

is not evident whether two heads of smooth muscle are identical only from their results.

In this study, We examined the detailed kinetic properties of MATP and M_P^{ADP} in the ATPase reaction of chicken gizzard myosin subfragment-1. We found that amount of M_P^{ADP} with high affinity for ATP was 0.5 mol per mol of myosin head, but that the Pi-burst size increased considerably with increase in ATP concentration. Furtheremore, the amount of MATP was also 0.5 mol/mol myosin head and ATP is liberated very fast from MATP, while M_P^{ADP} decomposed slowly into M + ADP + Pi. Therefore, we concluded that MATP and M_P^{ADP} are formed in the different heads of smooth muscle myosin as in the case of skeletal muscle myosin.

EXPERIMENTAL PROCEDURE

Chicken gizzard myosin subfragment-1 (S-1) was prepared by two methods. One is to digest gizzard myosin with papain. Gizzard myosin was prepared by the method of Ebashi (14), and myosin (15 mg/ml) in 0.12 M NaCl, 20 mM KPi, at pH 7.0 and 0°C was digested with 0.15 mg/ml papain. After 20 mi the reaction was quenched with 0.2 mM tosyl-L-lysine chloromethylketon (TLCK). S-1 was purified by ammoniun sulfate fractionation (45-60%) and the chromatography on DEAE-cellulose column as described by Weeds and Taylor (15). The other method is to treat myofibrils with papain as described by Cooke (16). Chicken gizzard myofibrils were prepared by the method of Sobieszek and Bremel (17), and gizzard S-1 was prepared by treatment of myofibrils with papain as described by Marston and Taylor (18). The Pi-burst size and the steady-state rate of the S-1 Mg^{2+}-ATPase reaction were the same for both S-1 preparations, then the S-1 prepared by the latter method was mainly used.

Skeletal muscle myosin was prepared from rabbit white muscle as described by Perry (19). Skeletal muscle S-1 was prepared by chymotryptic digestion of myosin as described by Weeds and Taylor (15). F-actin was prepared from an acetone powder of rabbit skeletal muscle by the method of Spudich and Watt (20). ATP remaining in the F-actin solution was removed by ultracentrifugation at 100,000 x g for 3 h. Papain and chymotrypsin were purchased from Sigma Chemical. Co. Pyruvate kinase was prepared by the method of Tiez and Ochoa (21). The protein concentrations were determined by means of the biuret reaction calibrated by

nitrogen determination. The value of 12 and 4.2×10^4 were used as molecular weights of S-1 and actin monomer, respectively (22).

ATP was purchard from Kohjin Co. Ltd, Tokyo. PEP was purchased from Sigma Chemical. Co. (γ-^{32})ATP was synthesized enzymatically by the method of Johnson and Walseth (23).

The ATPase reactions by myosin and S-1 were measured from the time course of ^{32}Pi-liberation using (γ-^{32}P)ATP as substrate (24). The reaction buffer usually contained 0.5 M KCl, 10 mM $MgCl_2$, 0.1 mM EDTA, and 40 mM Tris-HCl at pH 7.8 and 20°C. The reaction was started by mixing various concentrations of (γ-^{32}P)ATP with 3 μM gizzard S-1 in the presence or absence of 0.45 mg/ml skeletal muscle F-actin, and the reaction was quenched by adding 5% TCA with 0.1 mM Pi and ATP as carriers. The amount of radio labelled Pi was determined as described previously (24). The size of the Pi burst was estimated by extrapolating the steady state rate of Pi liberation to time zero. The rate of Pi burst was determined from the initial rate of the ATPase reaction. The reaction was started by adding 0.2 or 0.4 μM (γ-^{32}P)ATP to 0.1 μM S-1 in the presence or absence of 0.45 mg/ml F-actin in the reaction buffer.

To determine the amount of tightly bound ATP the reaction was quenched with the same volume of 10 mM cold ATP (final 5 mM), and after 5 min the reaction was stopped with 5% TCA conyaining 0.1 mM Pi and ATP, and the amount of ^{32}Pi was determined as described above.

The rate of release of ATP from gizzard S-1-ATP complex was measured from the decrease in the amount of ATP in the reaction buffer when free ATP was removed by adding exess skeletal S-1 to

the reaction mixture. S-1 ATPase reaction was started by adding 4 or 7.5 μM (γ-^{32}P)ATP to 3 μM S-1 and 0.45 mg/ml F-actin. At 20 s after starting the reaction the equol volume of the solution containing 50 μM (final 25 μM) skeletal muscle S-1, and then the reaction was stopped at various time with 5% TCA + 0.1 mM Pi as carrier. The amount of (γ-^{32}P)ATP remaining was determined after extracting Pi using Martin-Doty method (25).

The binding ability of S-1 to F-actin was tested by the ultracentrifugation method. One ml of the solution containing 4 μM S-1 and 1 mg/ml F-actin in the presence or absence of 2 mM ATP in the reaction buffer was centrifuged at 100,000 x g for 1.5 hr and the amounts of S-1 and F-actin in the supernatant and the precipitate were determined by SDS-gel electrophoresis (26) using the buffer system of Laemmli (27).

The extent of ATP-induced dissociation of acto-S-1 was estimated from the change in light-scattering intensity at 400 nm (28,29) using a stopped-flow apparatus combined with Hitachi-Perkin Elmer MFP-2A fluorescent spectrophotometer (30). We (28,31) have shown that the increment in the light-scattering intendity on adding S-1 to F-actin in the absence of ATP increased proportionally to the amount of S-1 added and was unaffected by the concentration of F-actin. Furtheremore, we (28) showed that the extent of binding of S-1 with F-actin measured by the light-scattering change was equal to that measured by the ultracentrifugation methods.

The time course of change in fluorescence intensity at 340 nm with 296 nm exitation was measured using the the stopped-flow apparatus as described above in 3 μM S-1, 1.5-7.5 μM ATP in the

presence or absence of 0.45 mg/ml F-actin in the reaction buffer.

RESULTS

Size of Initial Burst of Pi-Liberation by Smooth Muscle Myosin Subfragment-1—Size of initial burst of Pi-liberation was measured at various concentrations of ATP in 0.5 M KCl, 5 mM $MgCl_2$, 0.1 mM EDTA, 50 mM imidazole-HCl at pH 7.0 and 20°C. To compare the Pi-burst size with the extent of dissociation of acto-S-1, the experiment were performed in the presence of F-actin. Figure 1 shows the effect of F-actin (0.45 mg/ml) on the time course of TCA-labile Pi formation when 7.5 μM (γ-^{32}P)ATP was added to 3 μM S-1. Pi was rapidly formed in the initial phase of the reaction. The size of Pi-burst was estimated by extrapolating the steady state rate of Pi-liberation to time zero. The Pi-burst size was 0.62 mol/mol S-1 in the absence of F-actin, and it decreased to 0.52 mol/mol of S-1 by the presence of 0.45 mg/ml F-actin. On the other hand, the steady-state rate of ATPase reaction (0.017 s^{-1}) was unaffected by the presence of F-actin.

Closed circle in Fig. 2 shows the dependence on ATP concentration of the size of Pi-burst. Vaious concentrations (1.5-15 μM) of (γ-^{32}P)ATP was added to 3 μM gizzard S-1 and 0.45 mg/ml skeletal muscle F-actin in the reaction buffer, and the size of Pi-burst was estimated as described above. When the concentration of (γ-^{32}P)ATP added was less than that of S-1 (1.5 and 3 μM) the burst size was about one third that of (γ-^{32}P)ATP added (0.54 and 1.0 μM, respectively). The burst size increased to 0.5 mol/mol S-1 (1.5 μM) at 6 μM (γ-^{32}P)ATP added. Pi-burst size increased gradually with further increase in (γ-^{32}P)ATP and

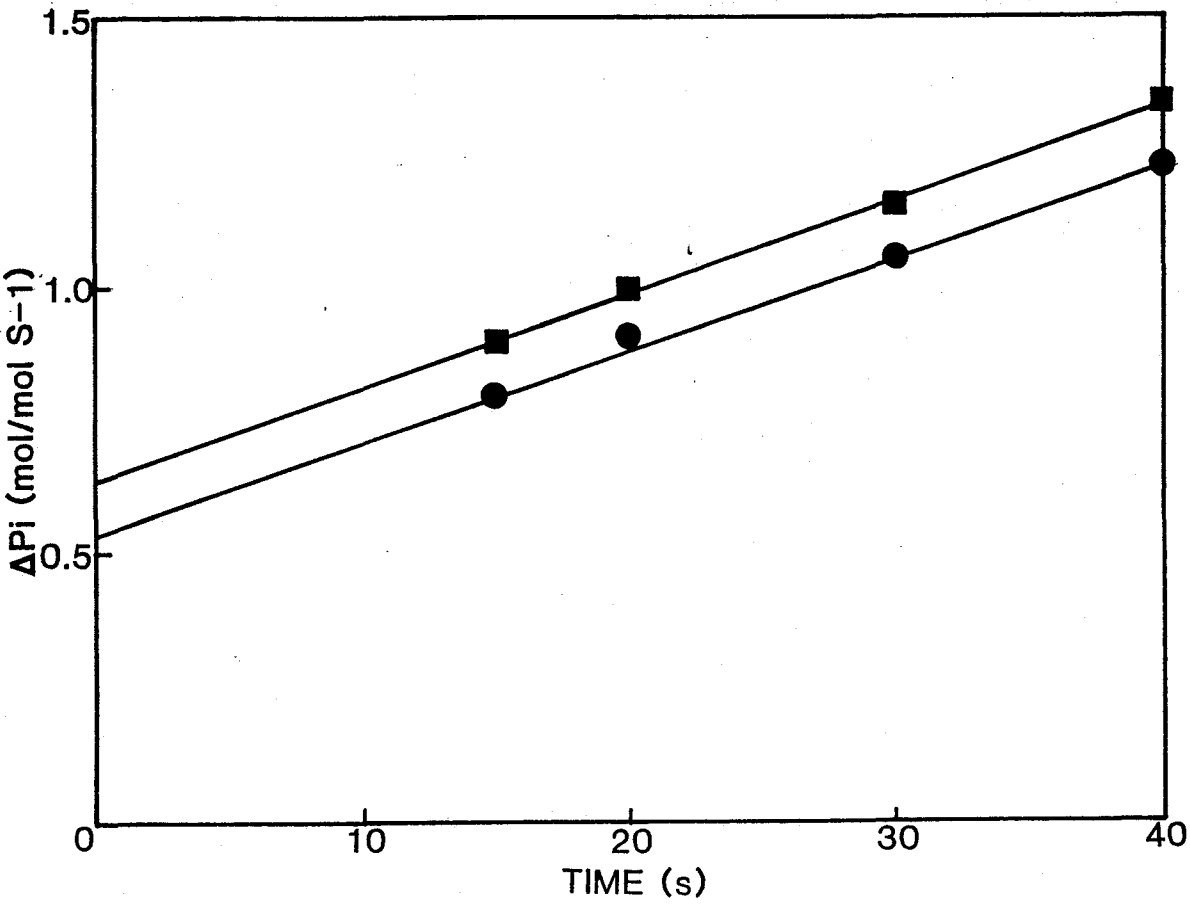

Fig. 1 Time course of ^{32}Pi liberation in the initial phase of gizzard S-1 Mg^{2+}-ATPase reaction in the presence and absence of skeletal muscle F-actin. The reaction was started by mixing 7.5 uM (γ-^{32}P)ATP with 3 μM gizzard S-1 in 0.5 M KCl, 10 mM $MgCl_2$, 0.1 mM EDTA, and 40 mM Tris-HCl at pH 7.8 and 20°C, and was quenched by adding 5% TCA with 0.1 mM Pi as carrier. ■ , - F-actin; ● , + 0.45 mg/ml skeletal muscle F-actin.

reached to 0.63 mol/mol S-1 (1.9 μM) at 15 μM (γ-^{32}P)ATP.

Dissociation of Acto-S-1 Induced by ATP—To estimate the amount of nucleotide bound to S-1 we measured the extent of dissociation of acto-S-1 induced by ATP. It was shown (29) that at high ionic strength acto-S-1 dissociates almost completely by high concentration of ATP and that acto-S-1 dissociates by 1 mol of ATP per mol of S-1. We first examined whether S-1 preparation can bind with F-actin. As shown in table I, when acto-S-1 was centrifuged in the absence of ATP, S-1 was completely bound with F-actin. When ATP was added to acto-S-1 more than 90 % of S-1 dissociated from F-actin.

The extent of ATP-induced acto-S-1 dissociation was measured from the decrease in light-scattering intensity. We (28) have shown that in the absence of nucleotide light-scattering intensity of F-actin increased linearly with increase in S-1 concentration and reached a saturated value at a molar ratio of S-1 : actin monomer of 1 : 1 and that the extent of binding of S-1 measured by a light-scattering method was equal to that measured by an ultracentrifugal separation method (28).

The time course of change in light-scattering intensity at 400 nm after adding ATP to acto-S-1 was recorded using a stopped-flow method. The light-scattering intensity decreased very rapidly and then recovered slowly to the original level. The rate of the recovery phase (0.018-0.020 s^{-1}) was independent on the concentration of ATP. Then, the extent of dissociation of acto-S-1 was estimated from the maximal decrease in light-scattering intensity. Open circle in Fig. 2 shows the dependence

TABLE I. Binding ability of S-1 to F-actin. ATP (2 mM) was added to 4 μM S-1 and 1 mg/ml F-actin in the reaction buffer and the mixture was centrifuged at 100,000 x g for 2 hr. The amounts of S-1 and F-actin in the supernatant were determined by SDS-PAGE.

		S-1	F-actin
Before centrifugation		4.0 uM (100 %)	1.0 mg/ml (100 %)
Supernatant after centrifugation	- ATP	0 uM (0 %)	0.15 mg/ml (15 %)
	+ ATP	3.7 uM (93 %)	0.05 mg/ml (5 %)

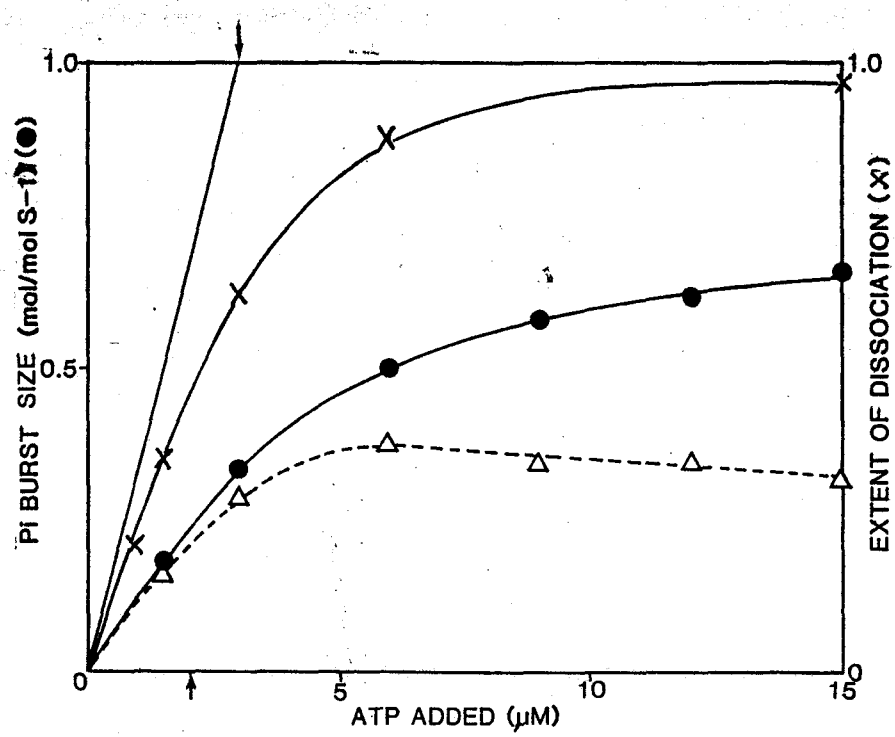

Fig. 2. Dependence on ATP concentration of the extent of dissociation of acto-gizzard S-1, the size of Pi-burst and the amount of S-1-ATP complex. The extent of dissociation of acto-S-1 by ATP (×) was measured from the time course of change in the light-scattering intensity at 400 nm. The size of Pi-burst (●) was estimated by extrapolating the time course of TCA-Pi liberation in the steady state to time zero (see Fig. 1). The amount of S-1-ATP complex (△) was culculated as the amount of S-1 dissociated from F-actin minus the size of Pi-burst (see "RESULTS" for detail). 3 μM gizzard S-1, 0.45 mg/ml skeletal muscle F-actin, 1-15 μM ATP. Other cnditions were the same as for Fig.1.

on ATP concentration of the extent of dissociation of acto-S-1. When the concentration of ATP was less than that of S-1 (1, 1.5, and 3 μM), 0.62, 1.0, and 1.75 μM, respectively, of S-1 (about two third that of ATP) was dissociated from F-actin. When ATP concentration was increased to 6 and 15 μM, 2.6 and 2.9 μM, respectively of S-1 dissociated from F-actin. Observed dissociation constant of ATP, obtained as (acto-S-1)(Free ATP)/(free S-1) was 0.5 μM at 3-15 μM ATP but it was 0.8-1.0 μM at 1-2 μM ATP.

Amount of Myosin-ATP and Myosin-Pi-ADP Complexes Formed by Smooth muscle Subfragment-1—The amount of M_P^{ADP} formed by smooth muscle S-1 was estimated from the size of Pi-burst as described above (Fig. 2). The amount of M_P^{ADP} formed by S-1 was also measured in the presence of sufficient amount of ATP regenerating system (2mg/ml PK, 4 mM PEP) (3,13,31). Under the conditions used, the rate of regeneration of free ATP from free ADP was 40-fold faster than the steady state ATPase rate. Thus, the amount of ADP in the mixture is equal to that of M_P^{ADP} complex. The amount of M_P^{ADP} was 0.56 mol/mol myosin head at 1.0 mol of ATP added per mol of myosin head and was slightly higher than that of the Pi-burst size. The total amount of nucleotide bound to smooth muscle S-1 was estimated from the extent of ATP induced acto-S-1 dissociation which was measured from the decrease in light -scattering intensity (Fig. 2). The amount of bound ATP was estimated from the difference between the total bound nucleotide and the amount of M_P^{ADP}, and was shown in Fig. 2 by open triangles. When the concentration of ATP was less than that of

S-1 (1.5 and 3 μM), the amount of MATP was 0.47 and 0.86 μM, respectively, and they were almost the same as those of M_P^{ADP}. The amount of MATP reached to 1.15 μM (0.38 mol/mol S-1) at 6 μM ATP. MATP decreased slightly with further increase in ATP concentration.

Kinetic Properties of M-ADP-P Complex—When S-1 formes M_P^{ADP}, the tryptophan fluorescence of S-1 increases. The rate of M_P^{ADP} decomposition was measured from the decrease in fluorescence intensity after adding ATP to S-1. The rate was 0.02 s^{-1} and 0.018 s^{-1} for in the absence and presence of F-actin, respectively (Table I). The rate of Pi burst was estimated from the initial velocity of the Pi burst regarding as the amount of the Pi burst site was 0.5 mol/mol of S-1. The rate was proportional to the concentration of added ATP. The second order rate constant of M_P^{ADP} formation, k_f, was estimated to be 30 and 6.2 x 10^{-8} s^{-1} M^{-1} for the absence and presence of F-actin, respectively (Table II).

Kinetic Properties of MATP Complex—We studied whether MATP complex is in rapid equilibrium with M_P^{ADP}. In skeletal muscle myosin ATPase reaction M_P^{ADP} is in rapid equilibrium with small amount of MATP, and the reverse reaction from MATP in this site to M + ATP was slow compared to the decomposition of M_P^{ADP} into M + ADP + Pi. Then, MATP decomposed into M + ADP + Pi when the reaction was quenched with excess of unlabelled ATP (32,33). Figure 3 shows the effect of quenching of S-1 ATPase by addition of excess unlabelled ATP. (γ-^{32}P)ATP (7.5 μM) was mixed with 3

TABLE II. Rate constants for formation and decomposition of M_P^{ADP} and the dissociation constant of ATP for formation of M_P^{ADP}. The rate constant for formation of M_P^{ADP} (K_f) was estimated from the dependence on ATP concentration of the intial rate of Pi-burst. 0.2-0.4 μM (γ-^{32}P)ATP, 0.1 μM gizzard S-1, 0.5 M KCl, 10 mM $MgCl_2$, 0.1 mM EDTA, and 40 mM Tris-HCl at pH 7.8 and 20°C. The rate constant for decomposition of M_P^{ADP} (k_d) was determined from the time course of recovery in ATP-induced fluorescence enhancement. Excitation and emission wavelength were 296 and 340 nm, respectively. 3 μM gizzard S-1, 1.5-7.5 μM ATP, other conditions were the same as for measurement of k_f. The dissociation constant for formation of M_P^{ADP} was calculated as k_d/k_f.

	k_f[a] (S^{-1} M^{-1})	k_d (S^{-1})	K (uM)
- F-actin	30 x 10^{-8}	2.0 x 10^{-2}	0.067
+ 0.45 mg/ml F-actin	6.2 x 10^{-8}	1.8 x 10^{-2}	0.29

[a] k_f was calculated as the amount of M_P^{ADP} formation site is 0.5 mol per mol of S-1.

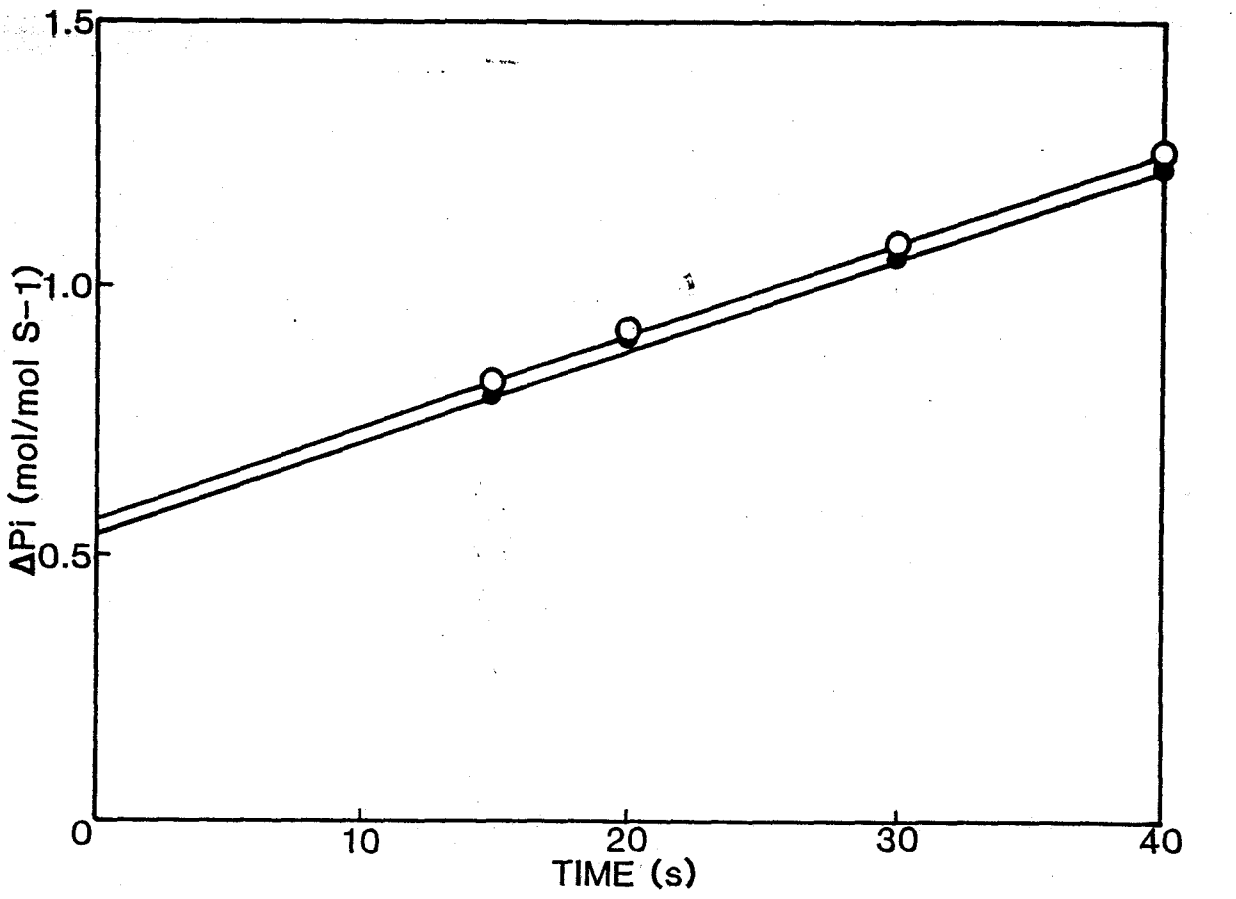

Fig. 3. Effect of quenching smooth muscle S-1 ATPase by addition of excess amount of unlabelled ATP. The reaction was started by adding 7.5 μM (γ-^{32}P)ATP to 3 μM S-1 and 0.45 mg/ml skeletal muscle F-actin. The reaction was quenched at each time with the excess (10 mM) of unlabelled ATP, and after 5 min the reaction was finally stopped with 5% TCA and 0.1 mM Pi(○). In the control experiment (●), ^{32}Pi formation was measured by quenching the reaction with 5% TCA and 0.1 mM Pi. Conditions were the same as for Fig. 1.

uM S-1 and 0.45 mg/ml F-actin in the reaction buffer and the reaction was quenched with TCA or excess of unlabelled ATP (2 mM). However, the amount of Pi measured by ATP quenching was almost equal to that of TCA-Pi, and treamount of M_P^{ADP} and bound nucleotide (MATP + M_P^{ADP}) estimated by extrapolating the steady-state rates of Pi measured by TCA and ATP quenching to zero time were 0.54 and 0.57 mol/mol S-1, respectively.

The rate of release of ATP from smooth muscle S-1-ATP complex was examined by adding excess of skeletal S-1 externally to remove free ATP (Fig. 4). The ATPase reaction was started by adding 4 μM (A) or 7.5 μM (B) (γ-^{32}P) ATP to 3 μM smooth muscle S-1 and 0.45 mg/ml F-actin in the raction buffer. At the initiation of the reaction 0.35 (A) or 0.53 (B) mol of ATP per mol S-1 was rapidly hydrolyzed. Then, after 20 s, equal volume of skeletal muscle S-1 (final 25 μM) was added to hydrolize free ATP. In the control experiment 1.71μM (A) or 4.62 μM (B) (γ-^{32}P)ATP was mixed with skeletal muscle S-1 in the presence of 0.45 mg/ml F-actin. Most of ATP remaining in this system was hydrolyzed within 4 sec.

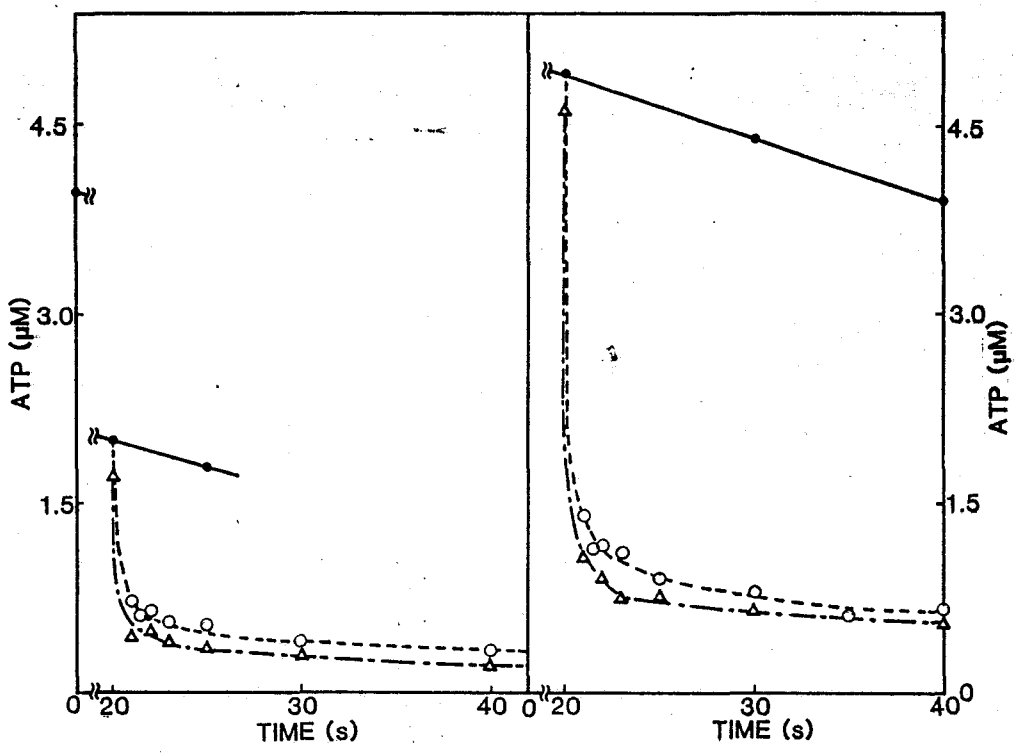

Fig. 4. Time course of nucleotide release from myosin-ATP complex by removal of free ATP with excess skeletal muscle S-1. The reaction was started by mixing of 4 (A) or 7.5 μM (γ-^{32}P)ATP (B) with 3 μM gizzard S-1 and 0.45 mg/ml skeletal muscle F-actin in the reaction buffer. At 20 s the reaction mixture was diluted with same volume of the mixture containing 50 μM skeletal muscle S-1, and the amount of ATP remaining in the mixture was measured (○). In the control experiments the mixture of 1.71 μM (A) or 4.62 μM (B) of(γ-^{32}P)ATP and 0.45 mg/ml skeletal muscle F-actin was diluted with same volume of 50 μM skeletal muscle S-1 (△). ● shows the time course of decrease in the amount of TCA-free (γ-^{32}P)ATP. The amount of (γ-^{32}P)ATP after the S-1 chase was expressed as the amount before the S-1 chase.

DISCUSSION

We studied the interaction of smooth muscle S-1 with ATP especially on the kinetic properties of M_P^{ADP} and MATP to know whether or not the two heads of smooth muscle myosin are identical.

We found that smooth muscle S-1 showed 0.5 mole of Pi-burst per mol of S-1 at low concentrations of ATP (see Fig. 2). This result agrees well with previous observations (8-12). Our S-1 preparation is not denatured because as shown in table II, S-1 bound tightly with F-actin in the absence of nucleotide, but dissociated almost completely in the presence of ATP. The affinity of S-1 for ATP estimated from the Pi-burst size at low ATP concentrations was found to be about 0.3 uM (Fig. 2). The affinity of ATP for M_P^{ADP} formation was also calculated based on the following mechanism:

$$M + ATP \xrightarrow{k_f} M_P^{ADP} \xrightarrow{k_d} M + ADP + Pi \quad (K = k_d/k_f)$$

The rates of M_P^{ADP} formation (k_f) and its decomposition (k_d) were estimated from the rate of Pi-burst and the rate of recovery in the ATP-induced fluorescent change. The dissociation constant, K, estimated as k_f/k_d was found to be 0.29 μM (TABLE II). This value was almost equal to that estimated from the Pi-burst size (0.33 μM). F-actin inhibited the formation of M_P^{ADP}, so in the absence of F-actin the value of K was about four fold lower than that in the presence of F-actin. The Pi-burst size increased to more than 0.5 mol/mol S-1 when ATP concentration incresed to several μM (see Fig. 2). The fluorescence enhancement and ATP induced dissociation of acto-S-1 did not change in such a

concentration range of ATP (see "RESULTS"). Then, we concluded that the increment in the Pi-burst size at high concentration range of ATP is not due to the formation of so called M_P^{ADP}, though the mechanism of increase in the Pi-burst size is unknown. At high ionic strength S-1 dissociates from F-actin by interaction with ATP, and the amount of ATP required for dissociation of acto-S-1 was one mole per mole of S-1 (29). Then, we estimated the amount of nucleotide bound to S-1 from the extent of dissociation of acto-S-1. Under the condition used (high ionic strength) the Pi-burst size and steady state rate of S-1 ATPase reaction were unaffected by the presence of 0.45 mg/ml F-actin (Fig. 1 and Table 1). Though the rate of Pi-burst (formation of M_P^{ADP}) was slightly inhibited by the presence of F-actin (see Table I).

The extent of ATP-induced dissociation of acto-S-1 was measured from the change in light-scattering intensity (Fig. 2). A linear relationship between the extent of dissociation and the change in light-scattering intensity was shown in the previous papers (28,31). The dissociation of gizzard S-1 from F-actin was followed by a simple saturation curve. The dissociation constant (0.8-1.0 and 0.5 μM at 1-2 and 3-15 μM ATP, respectively) was of the same order of magnitude as that for M_P^{ADP} formation. Assuming that amount of nucleotide bound to S-1 is equal to the amount of S-1 dissociated by ATP, we calculated the amount of MATP. At low concentrations of ATP, the amount of MATP was almost equal to that of M_P^{ADP} (see Fig. 2). The maximal amount of MATP was 0.35 mole per mol of S-1, but the Pi-burst size increased by an unknown mechanism, then it is likely that

the amount of MATP site is 0.5 mol per mole of S-1.

Since MATP and M_P^{ADP} were formed with the same affinity for ATP (Fig. 2), there remains two possibilities. One is that two heads of smooth muscle myosin are identical and both head form M_P^{ADP} in rapid equilibrium with MATP and the equilibrium constant of this step is about one. The other is that MATP and M_P^{ADP} are formed by the different head. These two ideas were tested by the following two experiments presented in this paper. When the ATPase reaction was quenched by adding excess of unlabelled ATP , no Pi was released from MATP (Fig. 3). Therefore, MATP decomposed mainly into M + ATP but not into M + ADP + Pi. This result can be explained also by the mechanism that MATP is in rapid equilibrium with M_P^{ADP} if we assume that the rate of the product release from M_P^{ADP} is equal to that of the ATP release from MATP complex. But this assumption is excluded by the result shown in Fig. 4. We measured the rate of the ATP release from MATP by adding excess of skeletal S-1 to remove free ATP. The rate of ATP release was more than ten fold faster than the rate of decomposition of M_P^{ADP} which was determined from the recovery of ATP-induced fluorescence enhancement. This result conflicts with the above assumption but can be explained easily by the nonidentical two head hypothesis i.e. one head forms MATP and the other M_P^{ADP} with the similar affinity for ATP but the ATP release from MATP is faster than M_P^{ADP} decomposition to M + ADP + Pi.

The result presented here agrees well with that of Shibata-Sekiya (34). She showed that myosins from mulluscan vertebrate and invertebrate (smooth) muscles have A-B non-idetical heads but the affinity of ATP for MATP was similar

to that for M_P^{ADP}. The non-identical two headed structure is also reported by Tanii et al. (35) for namatode myosin.

We previously considered that head A functions in the regulation of contraction. The ATPase reaction of skeletal muscle actomyosin is controled by the binding of Ca^{2+} to the Ca^{2+}-binding component (troponin C) of troponin-tropomyosin system, and the inhibition of actomyosin ATPase reaction by removal of Ca^{2+} requires high concentratins of ATP (7). The extent of inhibition of actomyosin-ATPase by removal of Ca^{2+} ions was related to the binding of ATP to head A. Then, we concluded that this head functions in the relaxation of muscle fiber. Smooth muscle actomyosin ATPase is controlled mainly by the Ca^{2+}-dependent phosphorylation and dephosphorylation of myosin light chain (36). Furthermore, the inhibition of smooth muscle actomyosin ATPase does not require high concentration of ATP. The report of Ikebe et al. (13) that smooth muscle myosin has two identical B-type heads agrees with the above idea. However, the results presented in this paper show that smooth muscle myosin also contains head A with head B. The absence of ATP requirement in the relaxation can be explained by the following two mechanism. (1) The affinity of ATP to head A is strong as that to head B, and (2) the binding of head A to the thin filament does not induce the structural change of thin filament.

Since head A does not actually function in the relaxation of smooth muscle, it is likely that head A functions in the contraction of muscle fiber. Head A has the following properties. It can bind with actin and interact with ATP but has no actomyosin-type ATPase activity. This head is in rapid

equilibrium with ATP and actin as: AM + ATP $\rightleftharpoons$ AMATP $\rightleftharpoons$ A + MATP. Therefore, it is possible that head A supports an effective contraction of muscle fiber by preventing the slippage of myosin heads when head B dissociates from one actin monomer and binds to the neighbor during contraction cycle.

REFERENCES

1. Inoue, A., Takenaka, H., Arata, T. & Tonomura, Y. (1979) Adv. Biophys. 13, 1-194
2. Inoue, A., & Tonomura, Y. (1974) Mol. Cel. Biochem. 5, 127-143
3. Inoue, A. & Tonomura, Y. (1974) J. Biochem. 76, 755-764
4. Taylor, E.W., Lymn, R.W., & Moll, G. (1970) Biochemistry 9, 2984-2991
5. Inoue, A., Shibata-Sekiya, K., & Tonomura, Y. (1972) J. Biochem. 71, 115-124
6. Inoue, A. & Tonomura, Y. (1976) J. Biochem. 80, 1359-1369
7. Inoue, A. & Tonomura,Y.(1975) J. Biochem. 78, 83-92
8. Takeuchi, K., & Tonomura, Y. (1977) J. Biochem. 82, 813-833
9. Takeuchi, K., & Tonomura, Y. (1978) J. Biochem. 84, 285-292
10. Takeuchi, K. (1980) J. Biochem. 88, 1693-1702
11. Srivastava, S.K., Tonomura, Y., & Inoue, A. (1979) J. Biochem. 86, 725-731
12. Ikebe, M., Tonomura, Y., Onishi, H., & Watanabe, S. (1981) J. Biochem. 90, 61-77
13. Ikebe, M., Onishi, H., & Tonomura, Y. (1982) J. Biochem. 91, 1855-1873
14. Ebashi, S. (1976) J. Biochem. 79, 229-231
15. Weeds, A.G. & Taylor, R.S. (1975) Nature 257, 229-231
16. Cooke, R. (1971) Biochem. Biophys. Res. Commun. 49, 1021-128
17. Sobieszek, A. & Bremel, R.D. (1975) Eur. J. Biochem. 15, 5813-5818
18. Marston, S.B. & Taylor, E.W. (1979) Eur. J. Biochem.

19. Perry, S.V. (1955) Methods in Enzymology (Colowick, S.T. & Kaplan, N.O., eds.) Vol.2, pp.582-588, Academic Press, New York

20. Spudich, J.A. & Watt, S (1971) J. Biol. Chem. 246, 4866-4871

21. Tietz, A. & Ochoa, S. (1962) in Methods in Enzymology (Colowick,S.P. and Kaplan,N.O.,eds.) Vol.5, pp.365-369, Academic Press, New York

22. Tonomura, Y. (1972) Muscle Proteins, Muscle Contraction and Cation Transpot Univ. Tokyo Press and Univ. Park Press, Tokyo and Baltimore

23. Johnson, R.A. & Walseth, T.F. (1979) Adv. Cyclic Nucleotide Res. 10, 137-167

24. Nakamura, H. & Tonomura, Y. (1968) J. Biochem. 88, 279-294

25. Martin, J.B. & Doty, D.M. (1949) Anal. Chem. 21, 964-967

26. Weber, K. & Osborn, M . (1969) J. Biol. Chem. 244, 4406-4412

27. Laemuli, U.K. (1970) Nature 227, 680-685

28. Inoue, A. & Tonomura, Y. (1980) J. Biochem. 88, 1643-1651

29. Takeuchi, K. & Tonomura, Y. (1969) J. Biochem.

30. Takemori, S., Nakamua, M., Suzuki, K., Katagiri, M., & Nakamura, T. (1972) Biochem. Biophys. Acta 284, 382-393

31. Furukawa, K., Inoue, A. and Tonomura, Y. (1981) J. Biochem. 89, 1283-1292

32. Bagshaw, C.R. & Trentham. D.R. (1973) Biochem. J. 133,

33. Inoue, A., Arata, T., & Tonomura, Y. (1974) J. Biochem. 76, 661-666

34. Shibata-Sekiya, K. (1982) J. Biochem. 92, 1151-1162

35. Tanii, I., Osafune, M., Arata, T., & Inoue, A. (1985) J. Biochem. 98, 1201-1209

36. Sobieszek, A. (1977) Eur. J. Biochem. 73, 477-483

III

Reaction Intermediates Formed by Myofibrils During ATPase Reaction under Relaxing Conditions

SUMMARY

We examined the species and the amounts of the intermediates formed by myosin in myofibrils during ATPase reaction under relaxing conditions. The amount of total nucleotides (ADP + ATP) bound to myofibrils were by a centrifugation method or a rapid filtration method, was 0.86 of nucleotides /mol myosin head bound to myofibrils. The amount of bound ADP was determined as ADP remaining in the mixture when ATP-regenerating system, which converts free ADP to ATP quickly, is added and was found to be 0.67 mol/mol myosin head. We measured the time courses of free Pi and total Pi formation (TCA-Pi). The amount of Pi bound to myofibrils was calculated by subtracting the burst size of free Pi (0.19 mol/mol myosin head) from that of TCA-Pi (0.60 mol/mol myosin head) and was found to be 0.41 mol/mol myosin head. The amount of tightly bound ATP estimated by an ATP-quenching method was 0.03 mol/mol myosin head. Thus, in the relaxed myofibrils, only half of myosin heads forms the myosin-phosphate-ADP complex, a fourth forms a myosin-ADP complex, and the remainder (a fourth) forms a myosin-ATP complex.

INTRODUCTION

Muscle contraction occurs as a result of interaction between myosin and actin coupled with the formation and the decomposition of reaction intermediates between myosin and ATP. Thus, it is important to know what kind of intermediates are formed in muscle.

The reaction intermediates have been studied by many investigators. Inoue and Tonomura (1), Furukawa et. al. (2) and Ikebe et. al. (3) studied the intermediates formed by isolated myosin and its proteolytic fragments by examining the amounts of nucleotides and Pi bound to myosin. They concluded that the two heads of myosin are different from each other and that one of the two heads (head A) forms a myosin-ATP complex (MATP) as while the other head (head B) forms a myosin-phosphate-ADP complex (M_P^{ADP}) as a stable intermediates.

On the other hand, several workers studied intermediates formed by myosin in a skinned fiber or myofibrils from a conformational change of myosin (4,5), Pi burst (6,7) or direct measurement of bound nucleotide and Pi (8-12). However, they measured only nucleotide binding or Pi burst and did not determined the species of intermediates. Thus, in this paper, we measured directly the amount of all the substrate and products (ATP, ADP and Pi) bound to myofibrils in the relaxed state. The reaction intermediates formed by myosin in myofibrils were discussed based on these results.

EXPERIMENTAL PROCEDURE

Materials— Myofibrils were prepared from rabbit white muscle by the method of Perry and Corsi(13). For myosin content in myofibrils the value of 51% was used according to Arata and Tonomura (14). Pyruvate kinase (PK) was prepared from rabbit skeletal muscle by the method of Tietz and Ochoa (15). The value of 4.8×10^5 was used as the molecular weight of myosin. The protrein concentrations were determined by means of the biuret reaction calibrated by nitrogen determination. SDS-PAGE was performed using buffer system of Laemmli (16).

[γ-^{32}P]ATP was synthesized enzymatically by the method of Johnson and Walseth (17). [α-^{32}P] ATP was purchased from the Radiochemical Center, Amersham, England. ATP and PEP were purchased from Kohjin Co. and Boehringer Manheim GmbH, respectively. ADP and AMP were purchased from Sigma Chemical Co., St. Louis, U.S.A..

Methods—The amount of total nucleotides bound to myofibrils was measured by a rapid filtration method. Myofibrils at 7 mg/ml were allowed to react with 7.5 - 50 μM (α-^{32}P)ATP for 5 min at 0°C in the presence of 1.6 mg/ml PK, 2 mM PEP, 0.1 M KCl, 50 mM $MgCl_2$, 0.1 mM EDTA. Under the above conditions free ADP produced was converted by pyruvate kinase system into ATP much faster than the ATPase reaction (98 % of free nucleotides exists as free ATP). Myofibrils in the reaction mixture were separated from a medium by a rapid filtration through a dry cotton filter (1 cm) in a syringe and the radioactivity of ^{32}P in the medium was measured. The filtration was completed within 2 sec. It was

examined by the SDS-PAGE of the filtrate revealed that more than 97% of myosin in myofibrils was trapped by the filter. No nonspecific binding of nucleotides or Pi to the cotton was observed.

The amount of total nucleotides (ATP + ADP) bound to myosin in myofibrils during the ATPase reaction was also measured by a centrifugation method. The reaction mixture was centrifuged at 2000 x g for 10 min. The free concentration of [α-^{32}P]ATP was determined from the radioactivity of ^{32}P in the supernatant. The amount of ADP bound to myosin in the myofibrils during the ATPase reaction was determined by measuring the amount of ADP remaining in the solution. After stopping the ATPase reaction which was carried under the above conditions with 5% TCA containing 10 mM ATP, ADP and AMP as carriers, the amounts of labeled ATP, ADP and AMP were determined by PEI-cellulose thin layer chromatography (18).

The time courses of free Pi and total Pi (TCA-Pi) nucleotides were determined as follows. The ATPase reaction was started by adding [γ-^{32}P]ATP (0.5 ml) to myosin or myofibrils (0.5 ml), and the reaction was stopped by adding 10% TCA (1 ml). The ^{32}Pi liberated from [γ-^{32}P]ATP was determined by the method of Nakamura and Tonomura (19). To determine the amount of bound Pi during the ATPase reaction, the time course of free Pi liberation was measured by the separation of myofibrils from the medium by the rapid filtration through the cotton filter as described above. The filtrate was mixed with TCA (5%) and the amount of ^{32}Pi was determined. To determine the amount of tightly bound ATP the reaction was quenched with the same volume of 10 mM cold

ATP, and 10 min later the reaction was finally stopped with 5% TCA and 0.1 mM Pi + 0.1 mM cold ATP as carriers, and then the amount of ^{32}Pi was determined.

RESULTS

Amounts of Nucleotides Bound to Myosin in Myofibrils during ATPase Reaction under Relaxing Conditions— Figure 1 shows the amount of nucleotides bound to myosin in myofibrils during ATPase reaction under relaxing conditions. The ATPase reaction was initiated by adding 7.5 - 50 μM [α-^{32}P] ATP and 2 mM PEP to 7 mg/ml myofibrils (7.4 μM myosin) in the presence of sufficient amount of ATP regenenating system (1.6 mg/ml PK) in 0.1 M KCl, 5 mM $MgCl_2$, 2 mM EGTA, 0.1 mM EDTA and 20 mM imidazole-HCl at pH 7.0 and 0°C. Five minutes later, we removed the myofibrils by a rapid filtration method and estimated the amount of total bound nucleotides from the radioactivity in the filtrate. The amount of total nucleotides bound to myofibrils increased with an increase in ATP concentration and reached 0.86 mol/mol myosin head at about 20 μM ATP added. The observed dissociation constant for ATP was estimated by replotting Scatchard plot to be about 2.0 μM.

We also measured the amount of total bound nucleotides by a centrifugation method under the same conditions as those for Fig. 1. At 5 min after the initiation of the ATPase reaction, we centrifuged the suspension at 2000 x g for 10 min to separate the myofibrils from the medium. The amount of bound nucleotides at 30 - 50 μM [α-^{32}P] ATP were 0.82 mol/mol myosin head and the amount of total bound nucleotides measured by the centrifugation method was exactly the same as those obtained by the rapid filtration method.

Next we estimated the amount of ADP bound to myofibrils from that of ADP remaining in the suspension, in which free ADP is

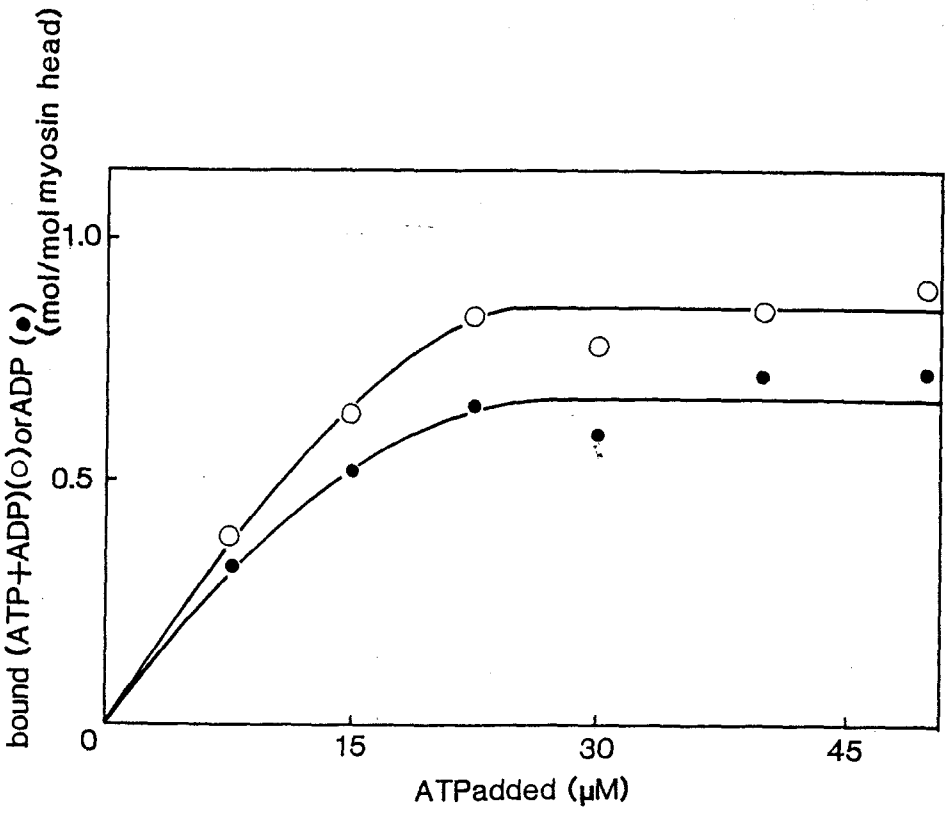

Fig. 1 Amounts of nucleotides (ADP + ATP) and ADP bound to myosin in myofibrils during the ATPase reaction as a function of concentration of ATP added. Myofibrils (7 mg/ml) was mixed with 7.5 - 50 μM [α-^{32}P]ATP in the presence of ATP regenerating system (1.6 mg/ml PK, 2 mM PEP). The amount of total bound nucleotides (ADP + ATP) (○) was measured by a rapid filtration method. The amount of bound ADP (●) was measured as the amount of ADP remaining in the suspension, using PEI-cellulose thin layer chromatography (see "EXPERIMENTAL PROCEDURE"). The concentration of myosin in the myofibrils was calculated to be 7.4 μM regarding that the myosin content in myofibrils is 51%. 0.1 M KCl, 5 mM $MgCl_2$, 2 mM EGTA, 0.1 mM EDTA, 20 mM imidazole-HCl at pH 7.0 and 0°C.

rapidly converted to ATP by PK system. The amount of ADP bound to myofibrils increased with an increase in ATP concentration and reached 0.67 mol/mol myosin at 20 μM ATP added. The dissociation constant for ATP was about 1.8 μM.

TCA-Pi and Free Pi-Burst in the Initial Phase of Myofibrillar ATPase Reaction— To examine the amount of Pi bound to myofibrils, we measured the liberation of both TCA-Pi (bound + free Pi) and free Pi. Figure 2 shows the time courses of TCA-Pi formation and free Pi formation by myofibrils. The reaction was started by adding 10 μM (A) or 30 μM (B) [γ-^{32}P]ATP to 7 mg/ml myofibrils (7.4 μM myosin), under the same conditions as those for Fig. 1 except that PK and PEP were absent. The TCA-Pi (▲) increased rapidly in the initial phase of the reaction and then the TCA-Pi increased at the steady-state rate of 9.7×10^{-3} s^{-1} (A) and 1.4×10^{-2} s^{-1} (B) respectively at 10 and 30 μM ATP. The sizes of TCA-Pi burst estimeted by extrapolating the steady-state rate of Pi liberation to zero time were 0.54 (A) and 0.6 (B). We measured also the time course of free Pi formation by the rapid filtration method. The free Pi (■) also showed initial burst whose sizes were 0.19 for both ATP concentrations. After the initial-burst phase the amounts of free Pi increased linearly with time at the rate of 1.8×10^{-2} s^{-1} (A) and 1.9×10^{-2} s^{-1} (B). The amounts of bound Pi estimated by subtracting the amount of free Pi from that of TCA-Pi were 0.34 (A) and 0.41 (B) mol/mol myosin head, at the initial phase. The amount of ATP added were 1.0 and 2.0 mol/mol myosin head, respectively. Therefore, the amounts of bound Pi decreased with time and reached 0 (A) and 0.26 mol/mol myosin head at 40 s.

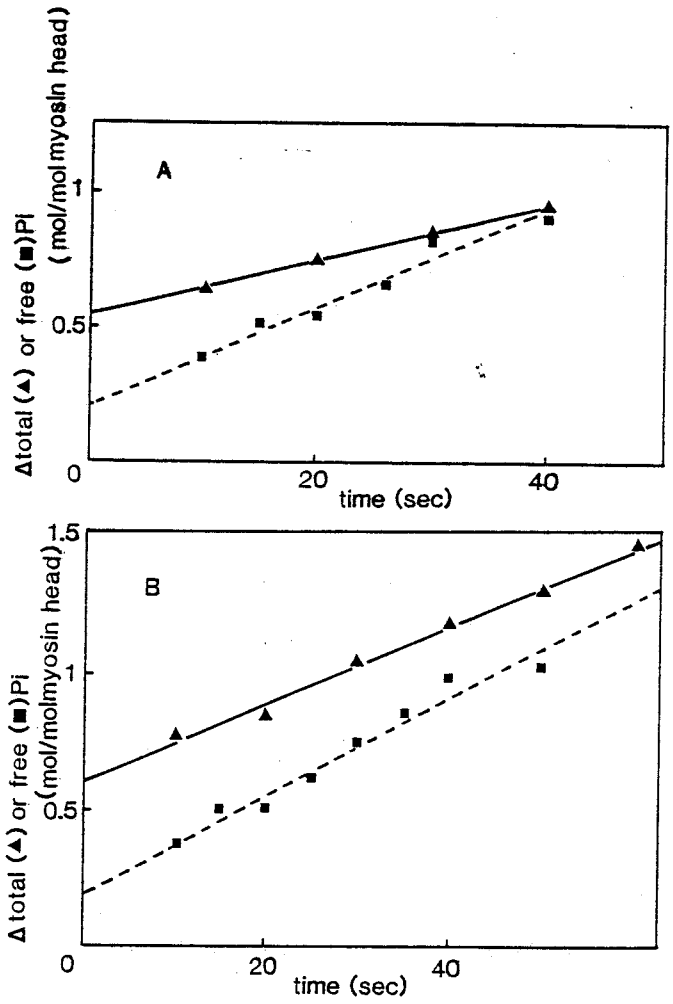

Fig. 2 Time courses of free-Pi and TCA-Pi formation by myofibrils. The ATPase reaction was started by adding 15 (upper) or 30 (lower) μM [γ-^{32}P]ATP to 7 mg/ml myofibrils (containing 7.4 μM myosin) in 0.1 M KCl, 5 mM $MgCl_2$, 2 mM EGTA and 20 mM imidazole-HCl at pH 7.0 and 0°C. Total amount of ^{32}Pi (TCA-Pi) was measured after stopping the reaction with 5% TCA (▲). The amount of free Pi liberated was measured by a rapid filtration method (see "EXPERIMENTAL PROCEDURES").

Amount of ATP Tightly Bound to Myofibrils— We measured the amount of tightly bound ATP in myofibrils during ATPase reaction by quenching the reaction with unlabeled ATP. We started the ATPase reaction by adding 20 μM [γ-^{32}P]ATP to 7 mg /ml myofibrils (7.4 μM myosin) under the same conditions as those for Fig. 2. The ATPase reaction was quenched at the time indicated by adding 5 mM unlabeled ATP which inhibited the further binding of labeled ATP. The reaction was allowed to proceed for 5 min to hydrolyze the tightly bound ATP completely. The reaction was finally stopped by adding 5% TCA (△). The amount of Pi showed an initial burst and following increase was observed at the steady-state rate of 1.1×10^{-2} s^{-1}. The burst size (tightly bound ATP + total Pi) was estimated as described for Fig. 2 to be 0.64 mol/mol myosin head. We also stopped the reaction simply by adding 5% TCA (▲) at the time indicated as shown in Fig. 2. The Pi-burst size was a little smaller (0.61 mol/mol myosin head) than that obtained by quenching with 5 mM unlabeled ATP, although the steady-state rates were almost the same. The amount of ATP bound tightly to myofibrils was estimated to be only 0.03 mol/mol myosin head, by subtracting the size of TCA-Pi burst from that obtained by ATP-quenching.

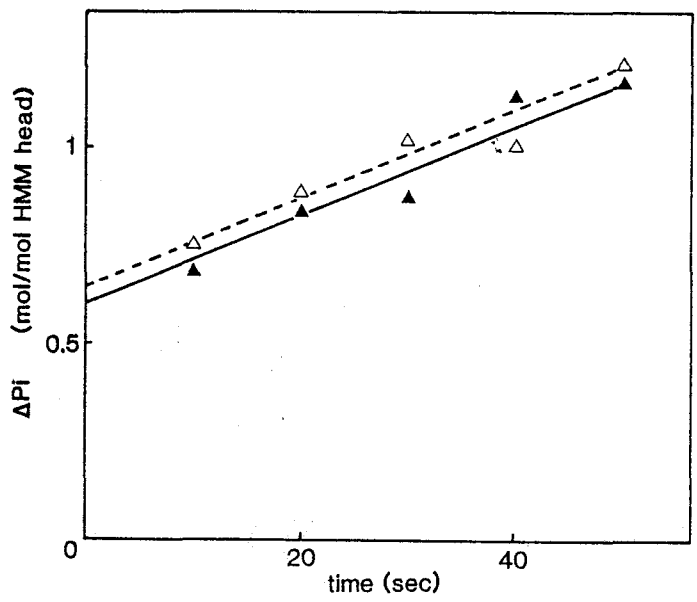

Fig. 3. Time course of Pi liberation when the reaction was terminated by cold ATP chase or by TCA. The ATPase reaction was started by addition of 20 μM [γ-^{32}P]ATP to 7 mg/ml myofibrils in 0.1 M KCl, 5 mM $MgCl_2$, 2 mM EGTA and 20 mM imidazole-HCl at pH 7.0 and 0°C. Total amount of ^{32}Pi was measured after stopping the reaction with 5% TCA (▲) at the time indicated. The amount of tightly bound ATP + total Pi (Δ) was measured as that of total ^{32}Pi measured by quenching the reaction by 2 mM unlabelled ATP at the time indicated and then terminated after 5 min with 5% TCA.

DISCUSSION

To know the species and the amounts of the reaction intermediates formed by myosin in myofibrils under relaxing conditions, we measured the amounts of ATP, ADP and Pi bound to myofibrils during ATPase reaction. In Table I, we summerized the results. We used a rapid filtration method to separate myofibrils from the medium. With this method, we can separate myofibrils within 2 sec. It is unlikely that the rapid filtration damaged to cause the amount of total bound nucleotides to decrease, because (1) the same result was obtained by a centrifugation method (2) only less than 3% myosin was found in the filtrate.

The amount of total nucleotides bound to myosin in myofibrils increased with ATP and reached 0.86 mol/mol myosin head at added ATP concentration of 20 μM (Fig. 1). This value did not increase even when the ATP concentration was increased further. Thus, 0.86 mol/mol myosin head must be available to react with ATP in myofibrils.

Myosin in myofibrils hydrolyzed 0.60 mol/mol myosin head (at 30 uM ATP) of ATP into ADP and Pi in the initial phase of the ATPase reaction (Fig. 2). There was a small amount (0.19 mol/mol myosin head) of free-Pi burst in the initial phase of ATPase reaction (Fig. 2). Therefore, the amount of bound Pi was smaller than that of TCA-Pi burst and was 0.41 mol/mol myosin head. Bound Pi decreased slowly (Fig. 2). This could be explained by the decrease in free ATP, using the affinity of the ATPase sites for ATP (K_d = 0.8 μM; Fig. 1).

The amount of ADP bound to myofibrils was 0.67 mol/mol myosin head. This value was higher than that of bound Pi. Therefore,

TABLE I. Amounts of nucleotides and Pi bound to myofibrils, and those of intermediates, during ATPase reaction. We regarded the amount of total bound nucleotides as that of available myosin head. See the text for details.

	mol/mol myosin head	(mol/mol available head)
total bound nucleotides	0.86	(1)
bound ADP	0.67	(0.78)
bound Pi	0.48	(0.56)
tightly bound ATP	0.03	(0.03)
loosely bound ATP	0.16	(0.19)
MATP (loose)[c]	0.16	(0.19)
MATP (tight)[a]	0.03	(0.03)
M_P^{ADPb}	0.48	(0.56)
MADP[d]	0.19	(0.22)

a = tightly bound ATP

b = bound Pi

c = total bound nucleotides - bound ADP - tightly bound ATP

d = bound ADP - M_P^{ADP}

not less than 0.26 mol/mol myosin head bound to myosin as MADP complex. The amount of initial free-Pi liberation (0.19 mol/mol myosin head) was almost the same as the amount of MADP bound to myofibrils during the steady-state ATPase reaction (0.67 mol/mol myosin head). Hence, it is likely that all of the ADP formed in the initial phase is bound to myosin.

From the difference between the amounts of total bound nucleotides and bound ADP, the amount of ATP bound to myofibrils during the steady-state ATPase reaction was estimated to be 0.19 mol/mol myosin head at ATP concentrations above 20 μM. Since the amount of tightly bound ATP was only 0.03 mol/mol myosin head, 0.16 mol of ATP /mol myosin head binds to myosin in myofibrils.

Several investigaters studied the intermediates formed by isolated myosin and its proteolytic subfragments. Inoue et. al. (20) proposed a nonidentical two-head theory in which one of the myosin heads (head A) forms loosely bound MATP with a low affinity for ATP and the other (head B) forms M_P^{ADP} with a high affinity for ATP. The other workers claimed that both of heads form M_P^{ADP}. In Table I. we attributed the value of total bound nucleotides as amount of available myosin heads. Our results suggest that half of myosin heads (head B) in myofibrils form M_P^{ADP} during ATPase reaction under relaxing conditions.

However, the intermediates formed by myosin in myofibrils had considerably different natures from those predicted by a nonidentical two head theory. First, we could explain the bindings of total nucleotides and ADP by one affinity of myosin head for ATP, although two heterogeneous affinities were needed to explain the extent of nucleotides to isolated myosin (20,21).

The K_d value which we adapted was about 2 μM. This value is almost the same as the larger one for isolated myosin. At low ATP concentrations, HMM interact with actin filament even in the absence of Ca^{2+}. Therefore, it is likely that the affinity of head B for ATP is lowered in myofibrils by the interaction of myosin heads with actin filament at low ATP concentration. Second, the amount of loosely bound MATP in myofibrils was considerably small (0.16 mol/mol head) and the amount of MADP was considerably large (0.19 mol/mol myosin head). This result is consistent with those of previous workers (6,7,10,15). ADP release from MADP may be rate-limiting in the ATPase reaction of a fruction of head A as suggested by Furukawa et. al. (23): M + ATP $\longrightarrow$ MATP $\longrightarrow$ MADP + Pi $\longrightarrow$ M + ADP + Pi . The rate of free Pi liberation after adding ATP was very rapid. Thus, it is difficult to explain these results by the mchanism in which ADP release from MADP may be partially rate-limiting in the ATPase reaction by head B as suggested by some workers (24,25):

$$M + ATP \longrightarrow MATP \longrightarrow M_P^{ADP} \longrightarrow MADP + Pi \longrightarrow M + ADP + Pi.$$

This report supports the nonidentical two head theory proporsed by Inoue et. al. (20). They suggested from the studies on acto-HMM ATPase system that the actomyosin type ATPase reaction which is coupled to muscle contraction is catalyzed by head B. However, the function of head A in muscle contraction has not yet been elucidated. It would be important to examine the formation of intermediates during contraction to elucidate this problem.

REFERENCES

1. Inoue, A. & Tnomura, Y. (1974) J. Biochem. 76, 755-764
2. Frukawa, K., Ikebe, M., Inoue, A., & Tonomura, Y. (1980) J. Biochem. 88, 1629-1641
3. Ikebe, M., Onishi, H., & Tonomura, Y. (1980) J. Biochem. 91, 1855-1873
4. Arata, T. & Shimizu, H. (1981) J. Mol. Biol. 151, 411-437
5. White, H. D. (1985) J. Biol. Chem. 260, 982-986
6. Ferenczi, M. A., Homsher, E., & Trentham, D. R. (1984) J. Physiol.
7. Frenczi, M. A. (1986) Biophys. J. 50, 471-477
8. Marston, S. (1973) Biochem. Biophys. Acta 305, 397-412
9. Marston, S. B. & Treger, R. T. (1974) Biochim. Biopys. Acta 333, 581-584
10. Maruyama, K. & Weber, A. (1978) Biochemistry 11, 2990-2998
11. Yanagida, T. (1981) J. Mol. Biol. 146, 539-560
12. Nagano, H. & Yanagida, T. (1984) J. Mol. Biol. 177, 769-785
13. Perry, S. V. & Corsi, A. (1958) Biochem. J. 68, 5-12
14. Arata, T. & Tonomura, Y. (1976) J. Biochem. 80, 1353-1358
15. Tietz, A. & Ochoa, A. (1962) in Methods in Enzymology (Colowick, S. P. & Kaplan, N. O., eds.) Vol. 5, pp. 365-369, Academic Press, New York
16. Laemmli, U.K. (1970) Nature 227, 680-685
17. Johnson, R. A. & Walseth, T. F. (1979) Adv. Cyclic Nucleotide Rec. 10, 137-167
18. Inoue, A. & Tonomura, Y. (1974) J. Biochem. 76, 755-764 20.
19. Nakamura, H. & Ynomura, Y. (1968) J. Biochem. 63, 279-294
20. Inoue, A., Takenaka, H., Arata, T., & Tonomura, Y. (1979)

Adv. Biophys. 13, 1-194

21. Inoue, A. & Tonomura, Y. (1974) J. Biochem. 76, 755-764

22. Inoue, A. & Tonomura, Y. (1975) J. Biochem. 78, 83-92

23. Furukawa, K-I, Inoue, A., & Tonomura Y. (1981) J. Biochem. 89, 1283-1292

24. Bagshow, C.R., & Trentham, D. R. (1974) Biochem. J. 141,331-349

25. Bechet, J. J., Colette, B., Guinand, S., Hill, M., & Albis, A. (1979) Biochemistry 18, 4080-4089

IV

Interaction of Two Heads of Myosin with F-actin

1. Binding of H-meromyosin with F-actin in the Absence of ATP

SUMMARY

The binding of two heads of HMM with pyrene-labeled F-actin was studied using the change in light-scattering intensity or fluorescence intensity of pyrenyl group. At low ionic strength (50 mM KCl), both S-1 and HMM bound tightly with F-actin (K_d < 0.1 μM) and both heads of HMM bound to F-actin. The affinities of S-1 and HMM for F-actin decreased by increasing KCl concentration. In 1 M KCl, the K_d values of S-1 and HMM for F-actin were 11 and 0.58 uM, respectively. Thus, HMM bound to F-actin 20 times more tightly as S-1. We compared the extent of binding of HMM to F-actin measured by centrifugation method with fluorescence change of pyrene F-actin, and found that even in 1 M KCl, HMM bound to F-actin with two headed attachment. We measured the time courses of the change in light-scattering intensity caused by the association and dissociation of acto-S-1 and acto-HMM. The time courses and the K_d values were explained by the following schemes and rate constants:

$$\text{S-1} + \text{F-actin} \underset{k_{-1}}{\overset{k_1}{\rightleftharpoons}} \text{S-1}\cdot\text{F-actin}$$

$$\text{HMM} + \text{F-actin} \underset{k_{-1}}{\overset{k_1}{\rightleftharpoons}} \underset{\text{(single headed)}}{\text{HMM}\cdot\text{F-actin}} \underset{k_{-2}}{\overset{k_2}{\rightleftharpoons}} \underset{\text{(double headed)}}{\text{HMM:F-actin}}$$

where the values for k_1 and k_{-1} for S-1 are 0.13 s^{-1}/ uM and 1.8 s^{-1}, respectively. The values for k_1, k_{-1}, k_2, k_{-2} of HMM are 0.45 s^{-1} / μM, 1.8 s^{-1}, 24 s^{-1}, 3.6 s^{-1}, respectively. The

scheme for HMM shows that the step from HMM F-actin to HMM F-actin does not depend on F-actin concentration and is fast ($24\ s^{-1}$). This association step causes the high affinity of HMM for F-actin and the double headed attachment of HMM with F-actin.

INTRODUCTION

Muscle contraction occurs through dissociation and recombination of actin and myosin coupled to ATP hydrolysis. Therefore, to elucidate the mechanism of muscle contraction, it is very important to know how myosin and its proteolytic fragments (HMM and S-1) associate with and dissociate from F-actin. Many investigators have been studied kinetics of the binding of S-1 to F-actin (1-5) and measured the rates of association and dissociation of acto-S-1. However, little is known about the association and dissociation of each HMM head and actin even in the absence of ATP. Several workers (5,6) showed negative cooperativity between two heads in the binding to F-actin, although strong interaction between two heads has not been detected (6,7). Furthermore, it is not yet clear whether HMM binds to F-actin with double-headed attachment (8-11) nor how HMM binds to F-actin more strongly than S-1 does (5,6,12). In this paper, we showed clearly that in the absence of ATP HMM binds to F-actin with double-headed attachment and binds about 20 times stronger than S-1 does. Moreover, we analyzed the elementary steps of HMM binding to F-actin precisely and showed that the shift in the equilibrium of bound HMM from single headed to double headed causes the strong binding of HMM to F-actin.

EXPERIMENTAL PROCEDURE

Materials—Myosin was prepared from rabbit white skeletal muscle by the method of Perry (13). S-1 and HMM were prepared by chymotryptic digestion of myosin as described by Weeds and Taylor (14). G-actin was prepared from an aceton powder of rabbit white skeletal muscle by the method of Spudich and Watt (15). F-actin was polymerized from G-actin by adding 50 mM KCl, 1 mM $MgCl_2$ and 10 mM imidazole-HCl at pH 7.8 and 0°C. Protein concentrations were determined by the biuret reaction calibrated by nitrogen determination. The molecular weights adopted for S-1, HMM and actin monomer were 12 , 35, 4.2×10^4, respectively. N-(1-pyrenyl) iodoacetamide and phalloidin were purchased from Molecular Probes, Inc., TX. and Boehringer Mannheim GmbH, respectivly. All other reagents were of analytical grade.

Preparation of pyrene-labeled F-actin—F-actin was labelled by the method of Kouyama et al. (16) with slight modifications. F-actin (1 mg/ml, 23.8 μM) was reacted with 1.2 times molar excess of N-(1-Pyrenyl) iodoacetamide in 50 mM KCl, 0.2 mM ATP, 0.1 mM $CaCl_2$, 1 mM $MgCl_2$, 10 mM imidazol-HCl at pH 7.0 and 20°C. After 20 h the reaction was stopped by adding 0.2 mM β-mercapt oethanol. Labeled F-actin was collected by centrifugation at 100,000 x g for 3h and was depolymelyzed by dialysis against 0.2 mM ATP, 0.1 mM $CaCl_2$, 0.2 mM β-mercaptoethanol for 36 h. After removing non-depolymerized actin by centrifugation at 100,000 x g for 3 h, we polymerized the Pyr-G-actin to Pyr-FA. Pyr-FA was collected by the ultracentrifugation and was dispersed in the reaction buffer (50 mM KCl, 2 mM $MgCl_2$, 0.1 mM EDTA and 20 mM

Tris-HCl at pH 7.8).

Methods—The binding of F-actin with S-1 or HMM was measured from the decrease in fluorescence intensity of pyrene group (excited at 366 nm and measured at 407 nm) attached to F-actin (16,17) or the increase in the light-scattering intensity at 407 nm (18,19). The light scattering of acto-S-1 or acto-HMM was measured by a Hitachi-Perkin Elmer MPF-4 fluorescence spectrometer. The time course in the change in the light-scattering intensity was measured using a stopped-flow apparatus combined with a Hitachi-Perkin Elmer MPF-2A fluorescence spectrophotometer (20). Binding extents of S-1 or HMM to F-actin were also measured using a centrifugation method. F-actin solutions (1 ml) containing various concentrations of S-1 or HMM with F-actin were centrifuged at 100,000 x g for 1.5 h. The protein concentrations of the supernatant were measured by the method of Bradford (21), and the amounts of proteins in the precipitate were measured by the Biuret method after dissolving the precipitate in the biuret reagent at 40°C, for 30 min. The rate constant for the association of S-1 or HMM with F-actin was calculated from the time course of the change in the light-scattering intensity. The time course of dissociation of acto-S-1 or acto-HMM was monitored from the light-scattering intensity after jumping the KCl concentration from 50 mM to 1 M. The time courses of change in light-scattering intensity were simulated using Runge-Kutta method by an NEC pc 9801 Vm computer.

RESULTS

Binding of S-1 or HMM to Pyr-FA— The fluorescence intensity of Pyr-FA excited at 366 nm and emitted at 407 nm was markedly reduced by the binding of S-1 or HMM (16). Therefore, the binding of S-1 or HMM to Pyr-FA was monitored both by the decrease in fluorescence intensity of pyrenyl group and by the increase in light-scattering intensity. Figure 1A shows the dependence on S-1 concentration of the change in fluorescence intensity at 407 nm with 366 nm excitation and of the change in light-scattering intensity at 407 nm. Various concentrations of S-1 were added to 20 μM Pyr-FA in 50 mM KCl, 2 mM $MgCl_2$, 0.1 mM EDTA, and 20 mM Tris-HCl at pH 7.8 and 20°C. The light-scattering intensity (▲) increased linearly with an increase in the S-1 / Pyr-FA molar ratio and was saturated at molar ratio of about 1. The fluorescence intensity (△) decreased linearly with an increase in the S-1 / Pyr-FA molar ratio and reached the saturated level (25% of free Pyr-FA) at a molar ratio of about 1. Both the fluorescence and light-scattering intensity recovered to the original level by adding 2 mM ATP (shown by an arrow). Figure 1B shows the dependences on HMM concentration of the change in fluorescence intensity (△) and the change in light-scattering intensity (▲). The light-scattering intensity also increased linearly with increase in HMM concentration and reached a saturated value at HMM / actin monomer molar ratio of 0.5. The fluorescence intensity decreased to 25% that of free Pyr-FA by the addition of 0.5 mole of HMM per mole of actin monomer. The amount of HMM or S-1 bound to Pyr-FA was also measured by a centrifugation method. Pyr-FA was mixed with 3 μM HMM or 6 μM S-1

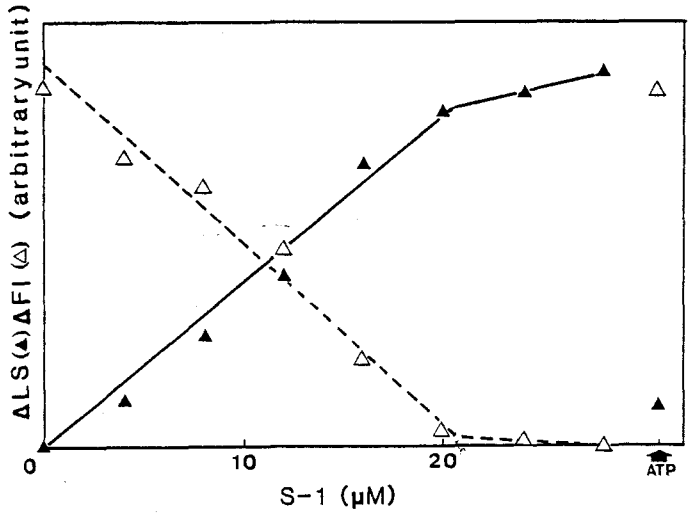

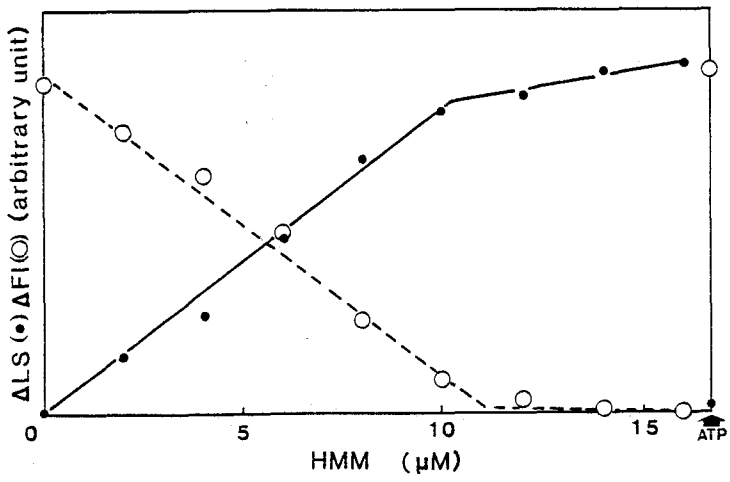

Fig. 1 Changes in the fluorescence intensity and light-scattering intensity as a function of the concentration of S-1 (A) or HMM (B) added to Pyr-FA. Pyr-FA (20 μM) was mixed with various concentrations of S-1 or HMM, and the fluorescence intensity at 407 nm emission with 366 nm excitation and the light-scattering intensity at 407 nm were measured. The arrow shows the extents of light-scattering intensity and fluorescence intensity which recovered to the original level by adding 2 mM ATP. 50 mM KCl, 2 mM $MgCl_2$, 0.1 mM EDTA and 20 mM Tris-HCl at pH 7.8 and 20°C. △ , ○ , fluorescence intensity , ▲ , ● , light-scattering intensity.

under the same conditions as those for Fig. 1. The amount of HMM and S-1 bound to Pyr-FA were 2.94 and 5.67 μM, respectively. The fluorescence change ($\Delta Fl/\Delta Fl_{max}$) of pyrenyl group caused by adding 3 μM HMM and 6 μM S-1 to Pyr-FA were 0.65 and 0.69, respectively. Hence, the fluorescence change induced by binding of one S-1 molecule to Pyr-FA (0.12) was about half that induced by binding of one HMM molecule (0.22).

Affinities of S-1 or HMM for Pyr-FA— We measured the affinity of S-1 or HMM with Pyr-FA under various ionic strengths from the changes in fluorescence intensity of pyrene group, and summarized them in Table I. Figure 2 shows the results obtained in 1 M KCl. Various concentrations of S-1 (upper) and HMM (lower) were mixed with 1 (upper) or 0.2 (lower) μM of Pyr-FA in 1 M KCl, 2 mM $MgCl_2$, 0.1 mM EDTA, 1.25 (upper) or 0.25 (lower) μM phalloidin, 20 mM Tris-HCl at pH 7.8 and 20°C. We added phalloidin to the solution to prevent the depolymerization of Pyr-FA. In the figures the extent of binding, α (= $\Delta Fl/\Delta Fl_{max}$) was plotted against α/(S-1). In the case of S-1, α is given by 1 - K_d α/(S-1). On the other hand, HMM binds with two actin monomers. Then α is given by 1 - K_d α/2 (HMM). Therefore, we estimated the K_d value of S-1 or HMM for Pyr-FA as the slope (S-1) or twice of the slope (HMM). The K_d values for S-1 and HMM under this condition were 11 μM and 0.58 μM, respectively. As shown in Table I, the affinities of S-1 and HMM for Pyr-FA were high at low ionic strength. However the value of K_d increased with an increase of ionic strength. In 0.05, 0.15, 0.5 and 1 M KCl, the K_d values for S-1 were 0.041, 0.3, 2.9 and 11 μM, respectively, while those for HMM were 0.014, 0.052, 0.19

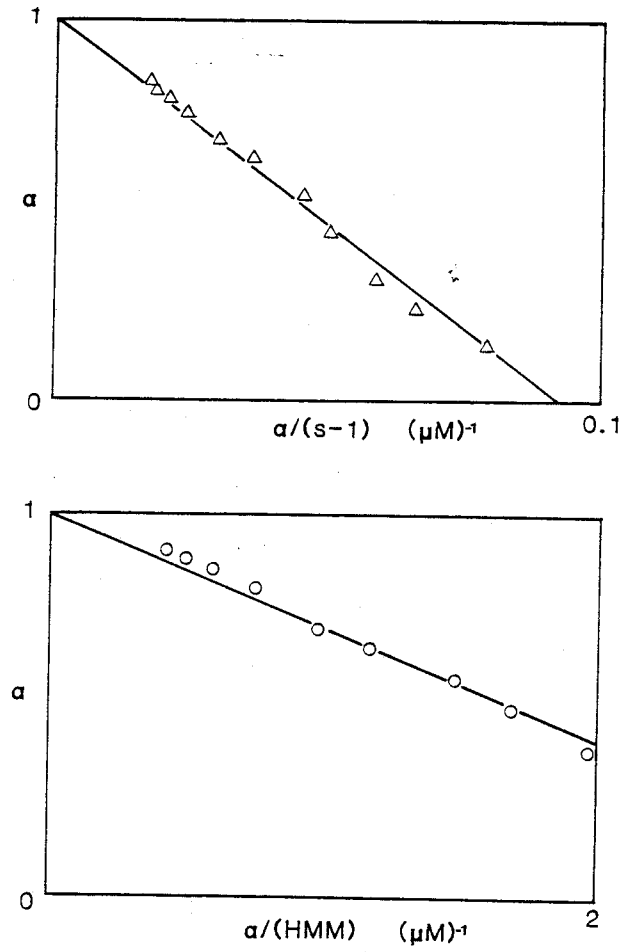

Fig. 2 Scatchard plot of the binding of S-1 or HMM with Pyr-FA. Extent of Pyr-FA bound with S-1 or HMM (Δ,o) was measured from the decrease in fluorescence intensity of the solution of Pyr-FA. 1 or 0.2 μM Pyr-FA, 1 - 49 μM S-1 or 0.125 - 2.2 μM HMM, 1.25 μM phalloidin, 1 M KCl, 2 mM $MgCl_2$, 0.1 mM EDTA, 20 mM Tris-HCl at pH 7.8, 20°C.

TABLE I. Dissociation constants of the binding of S-1 or HMM with Pyr-FA under various concentrations of KCl. The dissociation constants of S-1 or HMM binding were measured as described for Fig. 2 except that concentration of KCl was varied from 0.05 to 1 M. The amount of free F-actin was estimated by regarding that the amount of HMM bound to F-actin with single head little. 0.2 uM (both in 0.05 and 0.15 M KCl), 0.5 μM (HMM in 0.5 and 1 M KCl) or 1 μM (S-1 in 0.5 M and 1 M KCl) Pyr-FA, x 1.25 mol phalloidin per mol Pyr-FA, 0.05, 0.15, 0.5, or 1 M KCl, 2 mM $MgCl_2$, 0.1 mM EDTA, 20 mM Tris-HCl at pH 7.8 and 20°C.

KCl (M)		0.05	0.15	0.5	1
K_d (uM)	S-1	0.041	0.3	2.9	11.1
	HMM	0.014	0.052	0.19	0.58

and 0.58 μM, respectively. Thus, especially in 1 M KCl the affinity of S-1 for Pyr-FA was lower than that of HMM. The K_d value for S-1 (11 μM) was about 18 times larger than that for HMM (0.58 μM).

Binding of Two Heads of HMM with Pyr-FA— We examined whether HMM binds with Pyr-FA with double headed attachment or not. In Fig. 3 we compared the binding extents of S-1 to Pyr-FA measured by a centrifugation method with the changes in fluorescence intensity caused by the binding of S-1 to Pyr-FA. Pyr-FA (5 μM) was mixed with 2.5 - 50 μM S-1 in the same conditions as those for Fig. 2 except the concentration of phalloidin (6.25 μM). The binding extent of S-1 to Pyr-FA measured by the centrifugation method (■, ▲) and the change in fluorescence intensity increased as the concentration of S-1 added to Pyr-FA. The bound S-1 / Pyr-FA molar ratio was always equal to $\Delta Fl / \Delta Fl_{max}$ ratio. The smooth curve represents the calculated value regarding the K_d value as 11 μM. Figure 4 shows the result obtained using HMM under the same condition as Fig. 3. except that 1 - 18 μM HMM was mixed with 4.5 μM Pyr-FA. The maximal fluorescence change (ΔFl) was the same as for S-1 and the fluorescence change was fitted using the K_d value (0.58 μM). However, bound HMM / Pyr-FA molar ratio measured by the centrifugation method was always half of $\Delta Fl / \Delta Fl_{max}$. actin monomer (2.2 μM).

The Rates of Binding of S-1 and HMM to Pyr-FA— Geeves et. al. (22) claimed that the change in fluorescence intensity precedes the binding of S-1 to F-actin. Thus we estimated the rates of binding of S-1 and HMM with F-actin from the measurement of the change in light-scattering intensity. We measured the

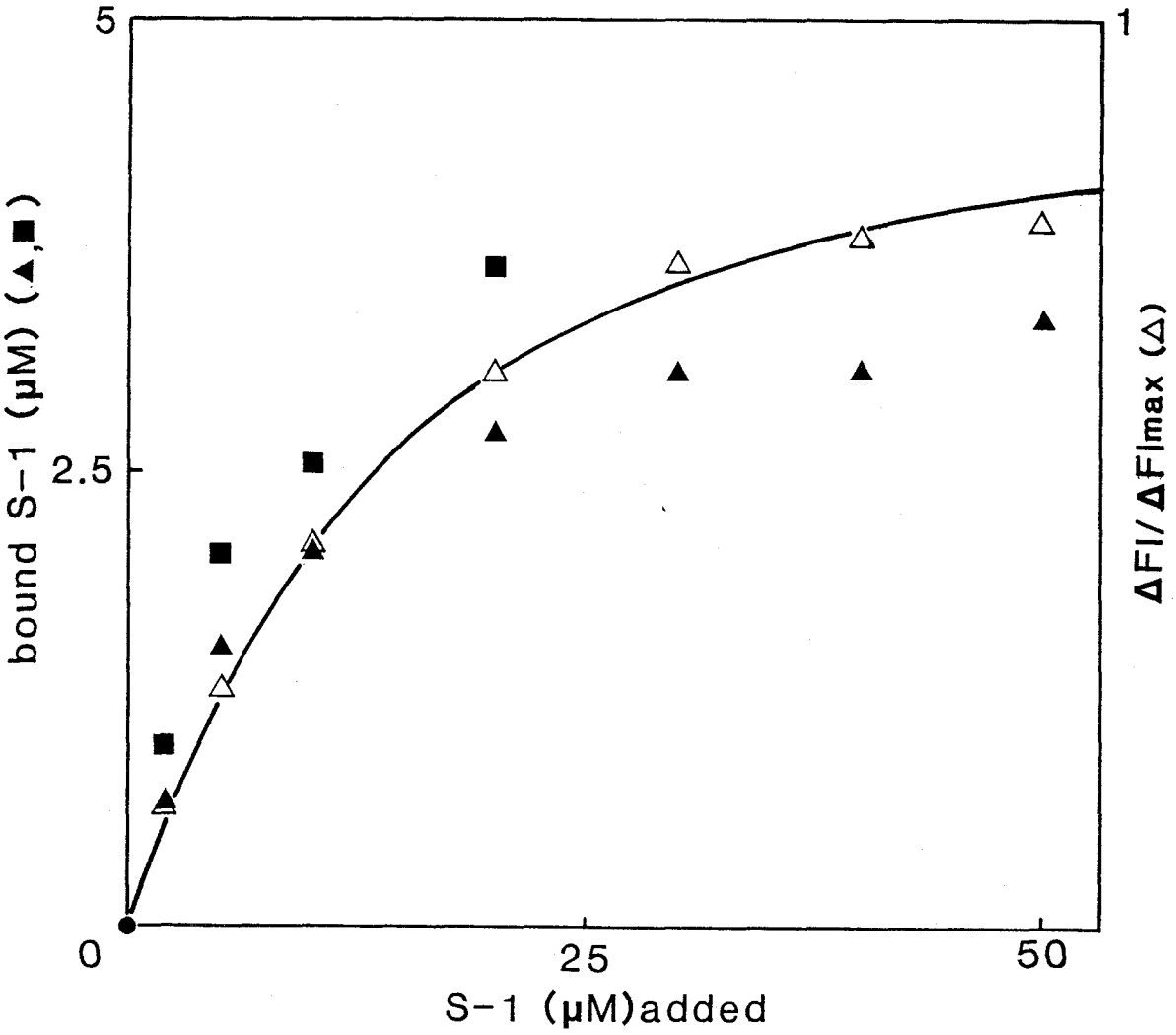

Fig. 3 The amount of S-1 bound to Pyr-FA measured by a centrifugation method and the change in fluorescence intensity of Pyr-FA by addition of S-1. The amount of S-1 bound to Pyr-FA (■, ▲) was measured by a centrifugation method (see EXPERIMENTAL). The fluorescence intensities (△) of Pyr-FA (5 μM) in the presence of various concentrations of S-1 were measured. The curve is drawn regarding that the dissociation constant of actoS-1 is 11 μM. 6.25 μM phalloidin, 5 μM Pyr-FA, 0-50 μM S-1, other conditions were the same as described for Fig. 2. ▲, ■, the amount of S-1 bound to Pyr-FA measured from the amount of S-1 in the precipitate (▲) or supernatant (■); △, fluorescence intensity

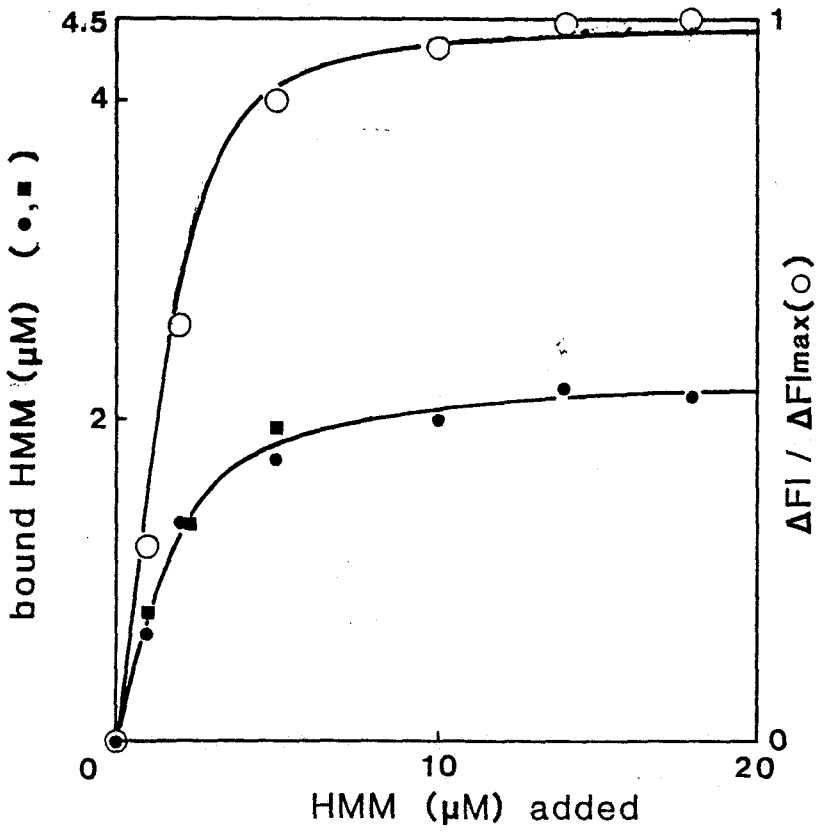

Fig. 4 Amount of HMM bound to Pyr-FA measured by a centrifugation method and change in fluorescence intensity of Pyr-FA caused by addition of HMM. The amount of HMM bound to Pyr-FA (●, ■) was measured by a centrifugation method (see EXPERIMENTAL). The fluorescence intensities (○) of Pyr-FA (4.5 μM) in the presence of various concentrations of HMM were measured. The curve is drawn regarding that the dissociation constant of actoHMM is 0.58 μM. 5.63 μM phalloidin, 4.5 μM Pyr-FA, 0 - 25 μM HMM, other conditions were the same as described for Fig. 2. ●, ■, the amount of HMM bound to Pyr-FA measured from the amount of HMM in the precipitate (●) or supernatant (■); ○, fluorescence intensity.

time course of change in light-scattering intensity after mixing 1.25 - 20 μM S-1 with 1.25 - 2.5 μM Pyr-FA using stopped-flow apparatus (Fig. 5). The concentration of S-1 was chosen to be much higher than that of S-1 bound to F-actin. Therefore, as shown in Fig 5A, the time courses of ln (Δ LS / Δ LS_{max}) gave straight lines and the rates of binding of S-1 with F-actin at 1.25, 5, 15 and 20 μM S-1 were estimated to be 1.5, 2.7, 3.9, 4.9 s^{-1}, respectively. Figure 5B (▲) shows the dependence on S-1 concentrations of the binding rate of S-1 to Pyr-FA. We also measured the binding rate of S-1 with Pyr-FA by mixing S-1 (3 - 6 μM) with excess amount of Pyr-FA (3.75 - 15 μM). The dependence on Pyr-FA concentration of binding rate of S-1 with Pyr-FA was shown by Fig. 5B (■). The dependence on Pyr-FA concentration did not differ from that on S-1 concentration. The dependence on S-1 or Pyr-FA gave a straight line. From the slope and the intercept of the line, we obtained the association (0.13 s^{-1} / μM) and dissociation (1.8 s^{-1}) rates. Figure 6A shows the time courses of the change in light-scattering intensity (ln Δ LS / Δ LS) after mixing 2.5 - 20 μM Pyr-FA with 0.5 - 2 μM HMM. The amount of HMM added was chosen to be much higher than that of HMM bound to Pyr-FA. The plot of ln(Δ LS / Δ LS_{max}) against time gave a straight line, and the association rates at 2.5, 5, 10, 20 μM Pyr-FA were 2.1, 3.0, 6.9, 11 s^{-1}, respectively. Figure 6B shows the dependence of the association rate of HMM with Pyr-FA on Pry-FA concentration. We fitted the plots with a straight line to get the slope and estimated the rate constant for association of HMM to Pyr-FA to be 0.45 s^{-1} / μM from the slope. The dissociation rate of acto-HMM estimated from the intercept

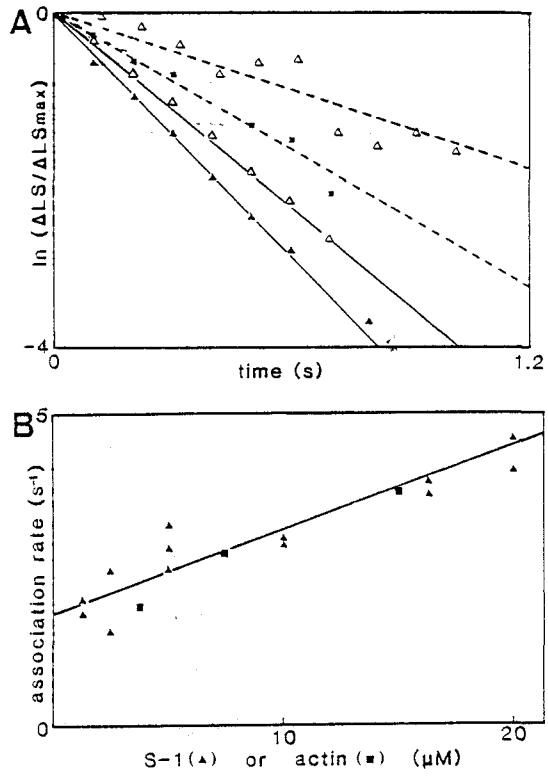

Fig. 5 Association rate of S-1 to Pyr-FA.

A) The time courses of the change in light-scattering intensity after mixing S-1 to Pyr-FA. Pyr-FA (1.25, 1.25, 2.5, 2.5, μM) was mixed with S-1 1.25 (-△-),5 (-×-),15 (—△—),20 (—▲—) μM, respectively.

B) Dependence of the association rate of Pyr-FA with S-1 on protein concentrations. Pyr-FA was mixed with excess amount (1 - 8 times as that of Pyr-FA) of S-1(▲) or S-1 was mixed with excess amount (1.25 - 2.5 times as that of S-1) of Pyr-FA (■). The association rate is plotted against the protein concentration of S-1 (▲) or Pyr-FA (■) which is much higher than the other. There was 1.25 mole / mole actin of phalloidin in the reaction mixture. Other conditions were the same as those described in Fig. 2.

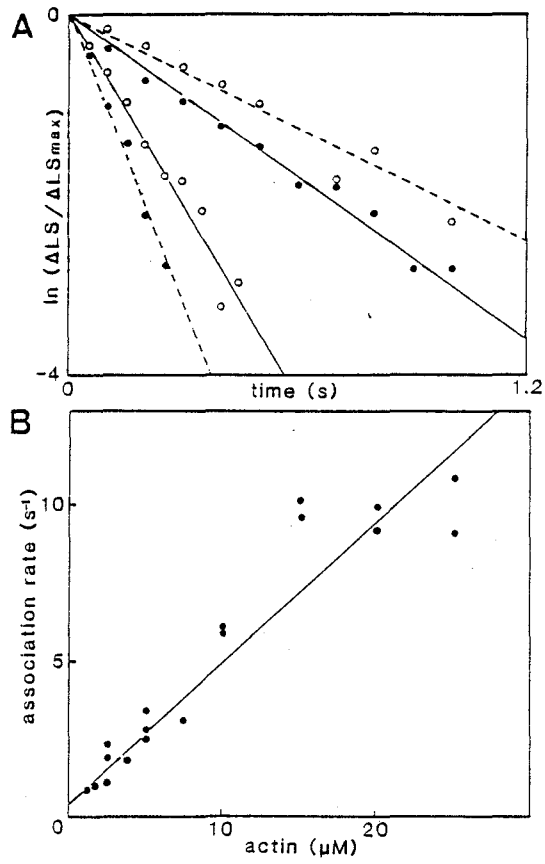

Fig. 6 Association rate of HMM to Pyr-FA.

A) The time courses of the change in light-scattering intensity after mixing HMM to Pyr-FA. HMM (0.5, 0.5, 1, 2 μM) was mixed with Pyr-FA 2.5 (-○-),5 (—●—),10 (—○—),20 (-●-) μM), respectively.

B) Dependence of the association rate of Pyr-FA with HMM on Pyr-FA concentration. HMM was mixed with excess amount (5-10 times as that of HMM) of Pyr-FA (●). The association rate is plotted against the protein concentration of Pyr-FA. Experimental conditions were the same as those of Fig. 5 except that HMM was used instead of S-1.

was smaller than 0.5 s^{-1}.

Dissociation of HMM or S-1 from Pyr-FA— At low ionic strength, HMM and S-1 bind tightly with Pyr-FA but the affinities were lowered by increasing KCl concentration to 1 M (Table I). Then we measured the time course of dissociation of acto-S-1 or acto-HMM after mixing acto-S-1 or acto-HMM at low ionic strength (50 mM KCl, 2 mM $MgCl_2$, 0.1 mM EDTA, 1.25 mol / mol actin monomer phalloidin, 20 mM Tris-HCl at pH 7.8 and 20°C) with the buffer cotaining 2 M KCl using the stopped-flow apparatus. Figure 7 shows the time courses of change in light-scattering intensity after mixing acto-S-1 with the buffer containing 2 M KCl. The light-scattering intensity decreased after the flow stop shown by arrow heads. We calculated the time courses of dissociation using a computer according to the following scheme: S-1 + Pyr-FA $\underset{k_{-1}}{\overset{k_1}{\rightleftharpoons}}$ S-1 Pyr-FA where k_1 = 0.13 s^{-1} / μM and k_{-1} = 1.8 s^{-1}. The concentrations of S-1, Pyr-FA and S-1 Pyr-FA complex before jumping KCl concentration were calculated with the K_d value (0.041 μM). The calculated time courses are represented by the dotted smooth curves (·····). These curves fitted very well to the change in light-scattering intensity under wide range of protein concentrations (A, 5 μM Pyr-FA, S-1 ;B, 2.5 μM Pyr-FA, S-1 ;C, 1.25 μM Pyr-FA, S-1). Figure 8 shows the time courses of the change in light-scattering intensity caused by the dissociation of HMM from Pyr-FA, which were examined by the same method as described for Fig. 7. The light-scattering intensity decreased after the flow stop as observed in the case of acto-S-1. We calculated the time courses of dissociation accoding to the following scheme:

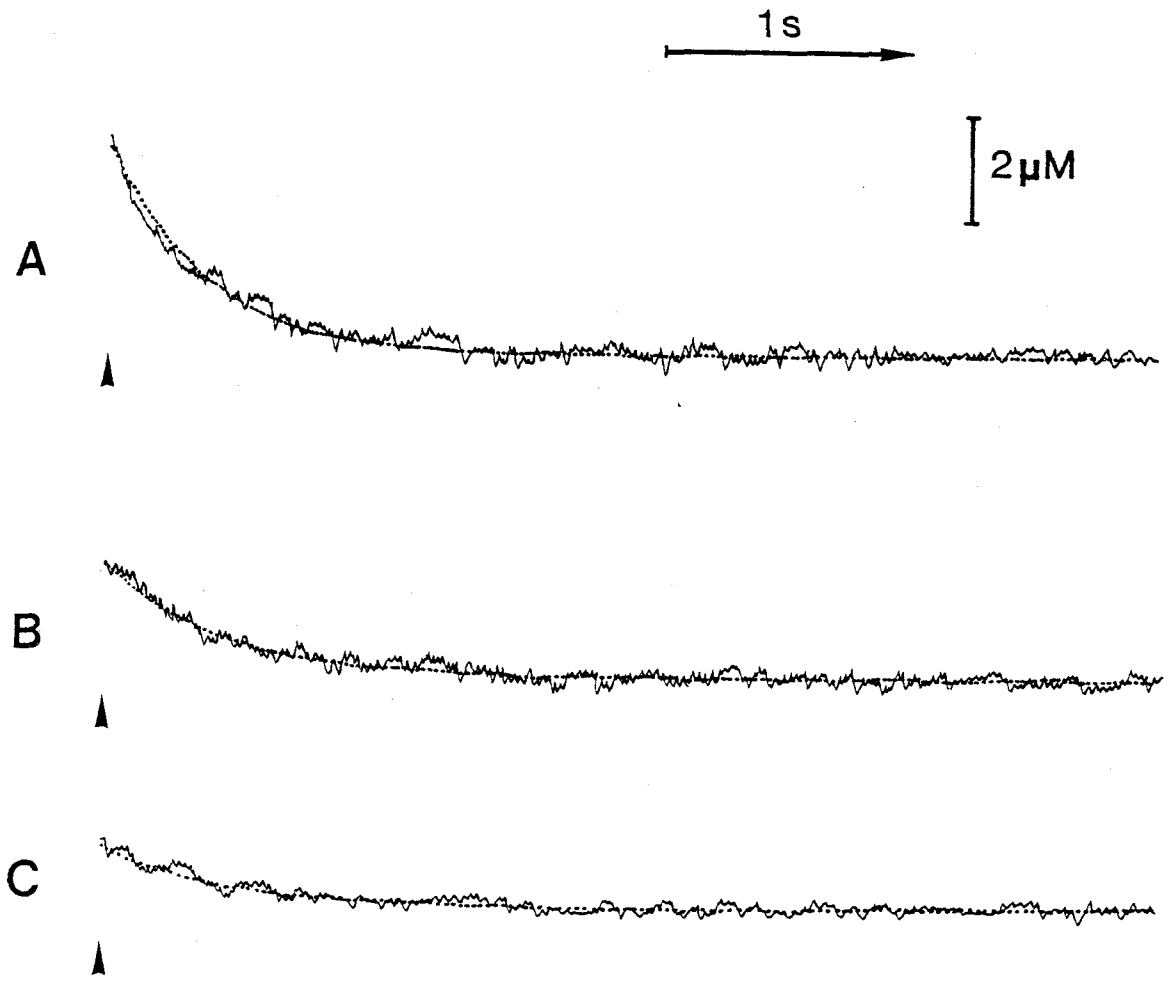

Fig. 7 Time courses of dissociation of S-1 from Pyr-FA. The dissociation of HMM from Pyr-FA was started by jumping the KCl concentration from 50 mM to 1 M and the time course of acto-S-1 dissociation was measured from the change in light-scattering intensity at 407 nm. The dotted smooth curves through the data is the computer fit simulating the time course of dissociation reaction using the rate constants obtained from Fig. 5 (k_1 = 0.13 s^{-1} / μM and k_{-1} = 1.8 s^{-1}). 5 (A), 2.5 (B), 1.25 (C) μM Pyr-FA and S-1, 6.25 (A), 3.13 (B), 1.56 (C) μM phalloidin, other conditions were the same as those of Fig. 2.

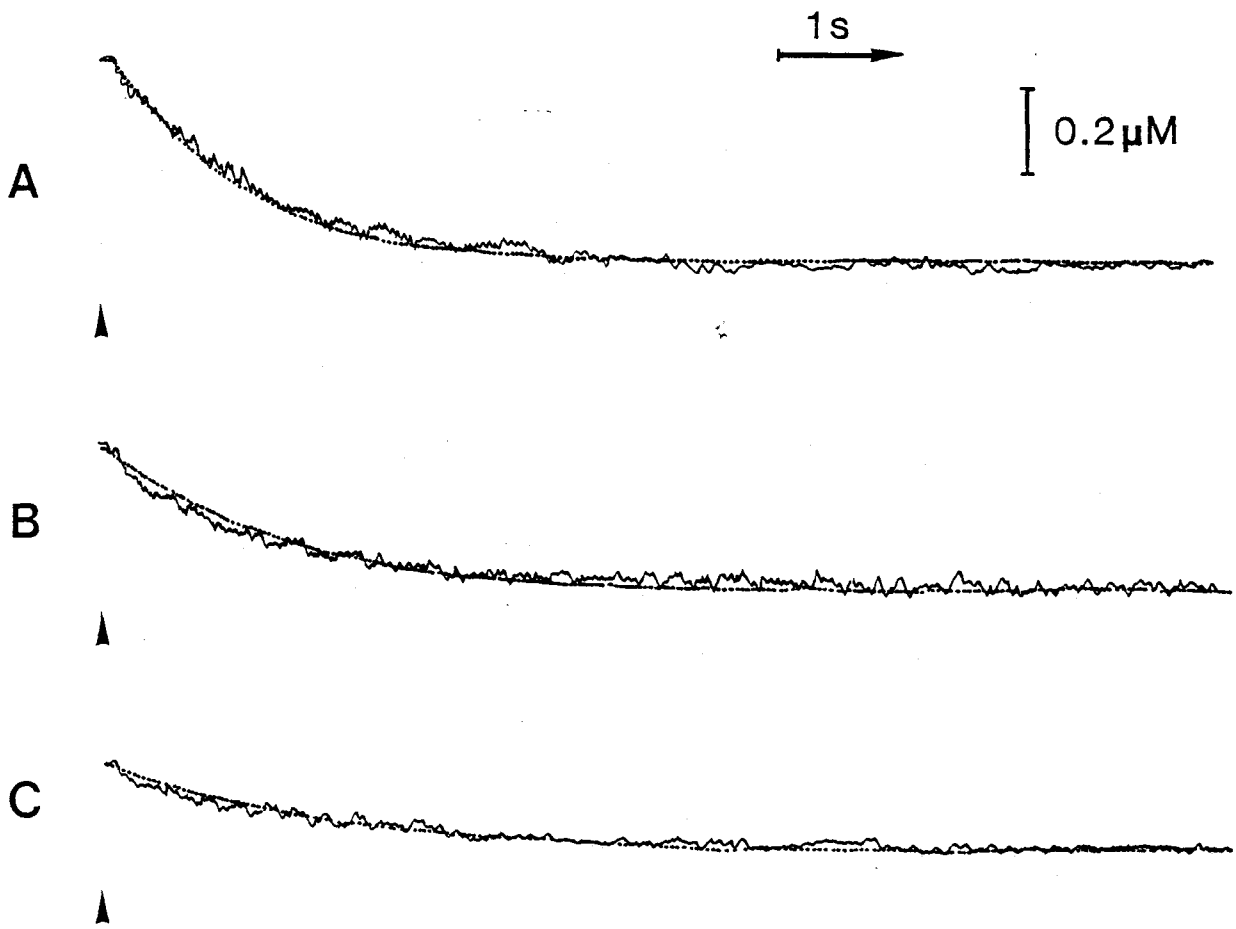

Fig. 8 Time courses of dissociation of HMM from Pyr-FA. The method for measurement is the same as that of Fig. 7 except using that HMM was used instead of S-1. The simulation was performed according to the scheme shown in Fig. 9, assuming that the light-scattering intensity does not change in the second step. 5 (A), 2.5 (B), 1.25 μM (C) Pyr-FA, 2.5 (A), 1.25 (B), 0.625 μM (C) HMM, 6.25 (A), 3.13 (B), 1.56 (C) μM phalloidin, other conditions were the same as for Fig. 2.

$$\text{HMM} + \text{F-actin} \underset{k_{-1}}{\overset{k_1}{\rightleftharpoons}} \text{HMM}\cdot\text{F-actin} \underset{k_{-2}}{\overset{k_2}{\rightleftharpoons}} \text{HMM:F-actin}$$

(single headed) (double headed)

where $k_1 = 0.45\ s^{-1}\ /\ \mu M$, $k_{-1} = k_{-2}\ /\ 2 = 1.8\ s^{-1}$ and $k_2 = k_{-1}\cdot k_{-2}\ /\ k_1\cdot K_d = 24\ s^{-1}$. The concentrations of HMM, HMM:F-actin (double headed) and F-actin before jumping the KCl concentration were calculated with the K_d value (0.014 μM). The curves calculatated by the computer according to this scheme (.....) fitted to the changes in light-scattering intensity in Fig. 8 so well under a wide range of protein concentrations (A, 5 μM Pyr-FA, 2.5 μM HMM ;B, 2.5 μM Pyr-FA, 1.25 μM HMM ;C, 1.25 μM Pyr-FA, 0.625 μM HMM).

DISCUSSION

Myosin has two separated heads, each of which can bind with F-actin and interact with ATP, and the function of two heads of myosin in muscle contraction is one of the most important problems in the elucidation of the molecular mechanism of muscle contraction.

In this paper, we studied whether myosin binds to F-actin with two heads and how the presence of two heads contributes the binding of myosin to actin in the absence of nucleotide. F-actin (Cys-374) was labelled with N-(1-pyrenyl) iodoacetamide (Pyr) (16). The fluorescence intensity of pyrenyl group bound to actin was decreased to 25% by the binding with myosin head (Fig. 1, ref. 16). Then, we mesured the binding of S-1 or HMM heads with Pyr-FA by the change in fluorescent intensity of pyrenyl group. The binding of S-1 or HMM was also measured from the increase in light-scattering intensity and by the ultracentrifugation method to study the mechanism of binding of myosin with F-actin. At low ionic strength the affinity of actin for S-1 decreased by less than a factor of 3 by incorporation of pyrenyl group into Cys-374 of actin (3,17).

At low ionic strength, S-1 and HMM bound tightly with F-actin. Under these conditions S-1 binds with one actin monomer (Fig. 1A), whereas HMM binds with two actin monomers(Fig. 1B). The decrease in fluorescence intensity of pyrenyl group induced by the binding of one mole of HMM was twice as that induced by one mole of S-1. Therefore, HMM binds to F-actin with two headed attachment and the binding of each head cause the same extent of

change in fluorescence intensity as S-1.

The difference between S-1 and HMM in their binding affinity for F-actin was studied by a centrifugation analysis (5,12) or a time-resolved fluorescence depolarization (6), but the results were controversial. Margossian and Lowey (5) and Highsmith (6) reported that the association constant for the binding of HMM to F-actin was about 3 - 10 times higher than that in the case of S-1. On the other hand, Greene and Eisenberg reported that HMM bound 10,000 fold more strongly to F-actin than S-1 did. It is difficult to study the affinities of HMM and S-1 for F-acin and the mechanism of HMM binding with F-actin at low ionic strength since both heads bind very tightly and rapidly with F-actin. As shown in Table 1 the affinity of S-1 or HMM with Pyr-FA decreased by increasing KCl concentration. The affinity of HMM for Pyr-FA was about 20 times higher than that of S-1 at high ionic strength. This result corresponds with those of Highsmith (6) and Margossian and Lowey (5).

We examined whether or not both heads of HMM binds to Pyr-FA at 1 M KCl. The change in fluorescence intensity of pyrenyl group induced by binding of one mole of HMM was also twice that of S-1 even under the conditions where there is large amount of free HMM (Figs 3 and 4). Thus under these conditions, HMM binds with F-actin by two headed attachment.

The mechanism of binding of S-1 and HMM with F-actin was also studied from the kinetics of association and dissociation of acto-S-1 and acto-HMM in 1 M KCl. In the case of S-1, the rate constants for the binding and dissociation were 0.13 s^{-1} / μM and 1.8 s^{-1}, respectively, and the Kd value calculated as k_{-1} /

k_1 was 13 μM, which was almost equal to that from the steady state level of fluorescence intensity (11 μM). Then, S-1 binds with F-actin by the following simple mechanism:

$$\text{S-1} + \text{F-actin} \underset{k_{-1}}{\overset{k_1}{\rightleftharpoons}} \text{acto-S-1}$$

This mechanism was further examined from the time course of dissociation of acto-S-1 induced by mixing acto-S-1 at low ionic strength with 2 M KCl (final 1 M KCl). The time courses of dissociation fit well to the curves calculated from the above mechanism (Fig. 5).

The results for the binding of HMM with F-actin were explained by the two step mechanism (Fig. 9). The amount of HMM bound to F-actin with single headed attachment was low, then the step 2 may shift to the right side. Since the extent of binding of HMM with F-actn was not the function of the square of F-actin concentration, k_2 might be independent on F-actin concentration. The rate of binding of HMM with F-actin was measured under the conditions where Pyr-FA concentration was much higher than that of HMM to exclude the effect of clowding of HMM on F-actin. The association of HMM to F-actin also showed a single exponential against time, and the association rate was proportional to the Pyr-FA concentration. This result suggests that the binding of the second head with F-actin (k_2) was much faster than that of the first head (k_1). The rate constant of binding of HMM with F-actin (0.45 s^{-1} / μM) was of the same order of magnitude as twice that of binding of S-1 with F-actin (0.13 x 10^6 $s^{-1}M^{-1}$). Therefore, the binding rate might be determined by k_1.

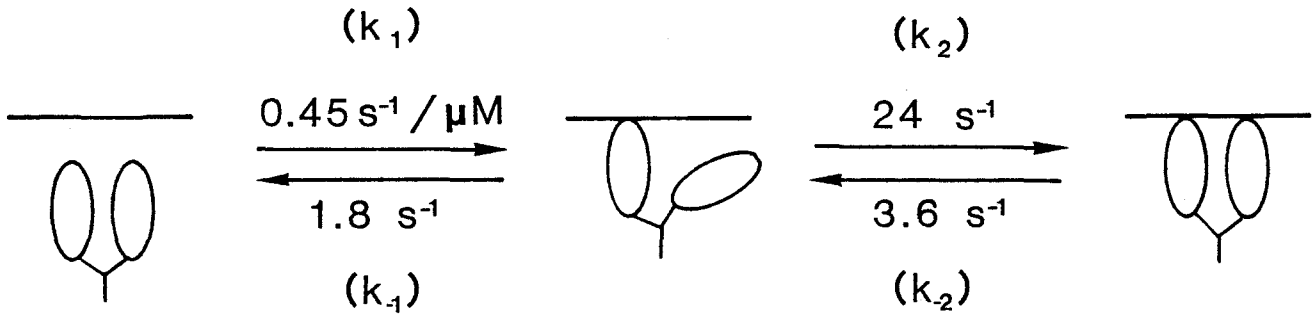

Fig. 9 Scheme for the binding reaction between HMM and F-actin. See text for details.

Since there was no co-operativity in F-actin-HMM binding and since the both heads induce the same structural change in actin monomer observed from the change in fluorescence intensity of pyrenyl group labeled to actin, we asumed that the rate of dissociation of each heads in HMM from F-actin was the same as that of acto-S-1, i. e. $k_{-1} = k_{-2} / 2 = 1.8\ s^{-1}$. The value of k_1 was assumed to be $0.45 \times 10^6\ s^{-1}M^{-1}$. Then, from the equation, $Kd = k_{-1} \cdot k_{-2} / k_1 \cdot k_2$, k_2 was calculated to be $24\ s^{-1}$ (see Fig .9). Therefore, the equilibrium of step (2) shifts to the double headed binding ($K_2 = k_{-2} / k_2 = 13.3\ \mu M$). This mechanism was examined from the time course of dissociation of acto-HMM after jumping the KCl concentration from 50 mM to 1 M. The observed time course was almost equal to that calculated using the above scheme and the rate constants.

In summary, when one of the two heads binds with actin, the binding of second head with F-actin is strong and independent of the actin concentration. Therefore, the affinity of HMM for F-actin is higher than S-1 and the binding of HMM with F-actin is not a function of square of F-actin concentration. Thus, we need not consider (actin-transmitted) negative cooperativity (6) nor nonidentical binding (5) to explain the binding affinity of HMM to F-actin. Inoue et. al. (23) reported that two heads of myosin are different from each other. We could not distinguish whether or not the binding property of HMM heads to F-actin is heterogeneous. In the following paper, we studied this probrem from the dissociation of acto-HMM by nucleotides.

There are issues about whether or not two headed structure of myosin is necessary for muscle contraction (24-29). Our results

do not answer this problem directly, but implicate that the existance of two heads plays an important role in the high affinity binding of crossbridges to actin filaments during muscle contraction.

REFERENCES

1. Millar, N. C. & Geeves, M. A. (1983) FEBS Lett. 160, 141-148
2. Yasui, M., Arata., & Inoue, A. (1984) J. Biochem. 96, 1673-1680
3. Criddle, A. H., Geeves, M. A., & Jeffries, T. E., (1985) Biochem. J. 232, 343-349
4. Coates, J. H., Criddle, A. H., & Geeves, M. A. (1985) Biochem. J. 232, 351-356
5. Margossian, S. S. & Lowey, S. (1978) Biochemistry 17, 5431-5439
6. Highsmith, S. (1978) Biochemistry 17, 22-26
7. Chantler, P. D. & Tao, T. (1986) J. Mol. Biol. 192, 87-99
8. Yamamoto, K. & Sekine, T. (1986) J. Biochem. 99, 199-206
9. Manuck, B. A., Seidel, J. C., & Gergely, J. (1986) Biophys. J. 50, 221-230
10. Duong, A. M. & Reisler, E. (1987) J. Biol.Chem. 262, 4129-4133
11. Pliszka, B. (1987) FEBS lett. 212, 254-258
12. Greene, L. E. & Eisenberg, E. (1980) J. Biol. Chem. 255, 549-554
13. Perry, S.V. (1955) in Methods in Enzymology (Colowick, S. P. & Kaplan, N. O., ads.) Vol. 2, pp. 582-588, Academic Press, Inc., New York
14. Weeds, A. G., & Taylor, R. S. (1975) Nature 257, 54-56
15. Spudich, J. A. & Watt, S. (1971) J. Biol. Chem. 246, 4866-4871
16. Kouyama, T. & Mihashi, K. (1981) Eur. J. Biochem. 114, 33-38

17. Inoue, A. & Tonomura, Y. (1980) J. Biodhem. 88, 1643-1651

18. Inoue, A., Ikebe. M., & Tonomura, Y. (1980) J. Biochem. 88, 1663-1677

19. Takemori, S., Nakamura, M., Suzuki, K., Katagiri, M., & Nakamura, T. (1972) Biochem. Biophys. Acta. 284, 382-393

20. Bradford, M. (1976) Anal. Biochem. 72, 248-254

21. Geeves, M. A., Jeffries, T. E., & Miller, N. C. (1986) Biochemistry 25, 8454-8458

22. Inoue, A., Takenaka, H., Arata, T., & Tonomura, Y (1979) Adv. Biophys. 13, 1-194

23. Tokiwa, T. & Morales, M. F. (1971) Biochemistry 10, 1722-1727

24. Chaen, S. & Shimada, M., & Sugi, H. (1986) J. Biol. Chem. 261, 13632-13636

25. Margossian , S. S. & Lowey, S. (1973) J. Mol. Biol. 74, 313-330

26. Cooke, R. & Frank, K. E. (1978) J. Mol. Biol. 120 361-373

27. Harada, Y., Noguchi, A., Kishino, A., & Yanagida, T. (1978) Nature 326, 805-808

28. Yano-Toyoshima, Y., Kron, S.J., McNally, E. M., Niebling, K. R., Toyoshima, C., & Spudich, J. A. (1987) Nature 328, 536-539

V

Interaction of Two Heads of Myosin with F-actin
2. Dissociation of Acto-HMM Induced by Nucleotides

SUMMARY

We studied how the two heads of HMM dissociate from Pyr-FA by ATP, using change in light-scattering intensity and decrease in fluorescence intensity of pyrenyl group bound to Cys_{374} of actin. In 0.05 M KCl and at 20°C, the extent of acto-HMM dissociation induced by ATP increased with an increase in ATP concentration and the amount of ATP required for the dissociation of acto-HMM was 1 mol of ATP added/mol HMM heads. At high ionic strength (1 M KCl), the extent of acto-HMM dissociaion was more than the stoichiometric amount of ATP per myosin head. At ATP concentrations less than 0.5 mol per mol myosin head, added ATP reacted with head B to show Pi burst. The results obtained here was compared with the binding of two heads of HMM with F-actin in the absence of ATP (Miyata et al. J. Biochem.). The above results cannot be explained by the mechanism in which two heads of myosin bind equivalently to F-actin. We can explain the result if we assume that one head (head B) binds more strongly with F-actin than the other head (head A) or that the reaction of one head (head B) with ATP weakens the binding of the other head (head A) to F-actin by factor of 6.

INTRODUCTION

Muscle contraction occurs as a result of cyclic interaction of myosin with actin filament coupled to ATP hydrolysis. The myosin molecule has two separated heads each of which can bind with F-actin. Then, it is very important to know how the two heads of myosin bind to F-actin. In the preceding paper (1), we analyzed the kinetics of elementary steps in the binding of HMM to F-actin in the absence of nucleotides, and showed that HMM binds to F-actin with double-headed attachment at wide range of ionic strength and that HMM binds to F-actin more strongly than S-1. This result suggests that both heads of myosin can bind to actin filament in a step of cross-bridge cycle in muscle contraction. If both heads attach to actin strongly and even during the force generation, the next problem is raised why one of two myosin heads does not hinder the movement of the other.

It has been proposed from the studies using isolated myosin and its proteolytic fragments that two heads of skeletal muscle myosin are not functionally and structurally identical (2). When ATP is added to myosin, one of two heads of myosin (head B) forms the myosin-phospate-ADP complex (M_P^{ADP}), while the other (head A) forms myosin-ATP complex (MATP) as reaction intermediates. Furthermore, Onishi et. al. (3) showed that all actomyosin dissociates by adding 0.5 mol of ATP/mol head. Takeuchi and Tonomura (4) and Inoue and Tonomura (5) reported that the extent of acto-HMM dissociation induced by ATP and AMPPNP were proportional to the nucleotide concentrations, not to the square of the concentrations, suggesting that the reaction of one head

with a nucluotide weakens the binding of the other head to F-actin. However, they could not examine the validity of the suggestion, because they did not analyze the binding of each head of myosin to F-actin.

In the present paper, we studied the dissociation of the each heads of HMM from F-actin by nucleotides from the changes in light -scattering intensity and in the fluorescence intensity of pyrenyl group labeled to F-actin. The result obtained here cannot be explained by the simple mechanism in which either head of myosin can bind equally to F-actin.

EXPERIMENTAL PROCEDURE

Materials—Myosin was prepared from rabbit white skeletal muscle by the method of Perry (6). S-1 and HMM were prepared by chymotryptic digestion of myosin as described by Weeds and Taylor (7). G-actin was prepared from an acetone powder of rabbit white skeletal muscle by the method of Spudich and Watt (8). F-actin was polymerized from G-actin by adding 50 mM KCl, 1 mM $MgCl_2$ and 10 mM imidazole-HCl at pH 7.8 and 0°C. ATP remaining in the F-actin solution was removed by dialysis against 40 μM ATP, 0.2 mM EDTA and 0.1 mM $CaCl_2$ for 8 h and by ultracentrifugation at 100,000 x g for 3 h. Protein concentrations were determined by the biuret reaction calibrated by nitrogen determination. The molecular weights adopted for S-1, HMM and actin monomer were 12 , 35, 4.2×10^4, respectively. N-(1-pyrenyl) iodoacetamide and phalloidin were purchased from Molecular Probes, Inc., TX. and Boehringer Mannheim GmbH, respectively. ATP and AMPPNP were purchased from Sigma chemical Co., St. Louis. [γ-^{32}P]ATP was synthesized enzymatically by the method of Johnson and Walseth (9). All other reagents were of analytical grade.

Preparation of pyrene-labeled F-actin—F-actin was labelled by the method of Kouyama et al. (10) with slight modifications. F-actin (1 mg/ml, 23.8 μM) was reacted with 1.2 times molar excess of N-(1-Pyrenyl) iodoacetamide in 50 mM KCl, 0.2 mM ATP, 0.1 mM $CaCl_2$, 1 mM $MgCl_2$, 10 mM imidazol-HCl at pH 7.0 and 20°C. After 20 h the reaction was stopped by adding 0.2 mM β-mercaptoethanol. Labeled F-actin was collected by centrifugation at 100,000 x g for 3h and was depolymelyzed by dialysis against 0.2

mM ATP, 0.1 mM $CaCl_2$, 0.2 mM β-mercaptoethanol for 36 h. After removing non-depolymerized actin by centrifugation at 100,000 x g for 3 h, we polymerized the Pyr-G-actin to bo Pyr-FA. Pyr-FA was collected by the ultracentrifugation, and was dispersed in the reaction buffer (50 mM KCl, 2 mM $MgCl_2$, 0.1 mM EDTA and 20 mM Tris-HCl at pH 7.8).

Methods— The fluorescence intensity of pyrenyl groupe labeled to F-actin excited at 366 nm and emitted at 407 nm is reduced linearly as the amount of S-1 bound to F-actin increase (10). The extent of ATP-induced dissociation of actomyosin was estimated from the change in light-scattering intensity (5,11) at 400 nm or the change in fluorescence intensity of pyrenyl group labeled to actin, using a stopped-flow apparatus combined with a Hitachi-Perkin Elmer MPF-2A fluorescent spectrophotometer (12). The time course of Pi-liberation in the HMM Mg^{2+}-ATPase reaction was measured using (γ-^{32}P)ATP as substrate. The reaction was started by adding ATP to acto-HMM solution. After stopping the ATPase reaction with 5% TCA with 0.1 mM ATP and 0.1 mM K-Pi as the carrier, the amount of ^{32}Pi was determined as described previously (13).

RESULTS

ATP-induced Dissociation of S-1 or HMM from Pyr-FA— The binding of S-1 to F-actin causes the change in light-scattering intensity (5,11) and that in fluorescence intensity of pyrenyl group labeled to Cys_{374} of actin excited at 366 nm and emitted at 407 nm (10,14). Thus, we estimated the extent of dissociation of acto-S-1 and acto-HMM with light-scattering intensity and also fluorescence intensity of Pyr-FA. We measured the time courses of change in light-scattering intensity and that in fluorescence intensity after mixing acto-S-1 or acto-HMM with buffer containing ATP (data not shown). Since the dissociation of acto-S-1 or acto-HMM is much faster than that of recombination (2), we could easily obtained the extent of dissociation induced by ATP from the amplitude of the change at the plateau.

In Fig. 1, the extents of dissociation of acto-S-1 estimated from light-scattering intensity (▲) and the fluorescence intensity (△) were plotted against the concentration of added ATP. The dissocition extents at low ionic strength (50 mM KCl) increased linearly upto about 0.6 and then reached unity (complete dissociation) when 1.5 mol of ATP/mol S-1 were added. A half of S-1 dssociated with high affinity for ATP while the other with low affinity. The two K_d values of S-1 for ATP were calculated to be about 0.04 μM and 0.4 μM.

Next, we examined the ATP concentration dependence of the extent of acto-HMM dissociation at low ionic strength as described in Fig. 1. The extent of dissociation increased linearly upto about 0.6 and then reached unity when 3 mol of

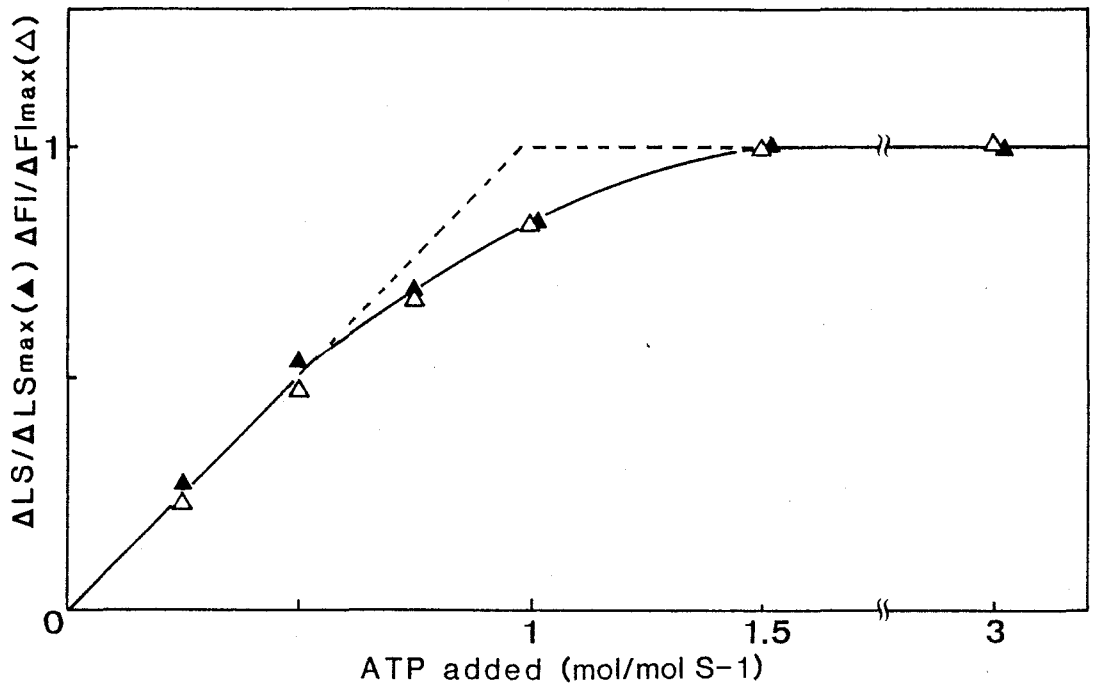

Fig. 1. Dependence on ATP concentration of the extent of dissociation of acto-S-1 at low ionic strength. The fluorescence intensity of acto-S-1 excited at 366 nm and emitted at 407 nm or the light-scattering intensity at 407 nm was monitored. The extent of dissociation of acto-S-1 is represented as Δ Fl / Δ Fl_{max} (Δ) and Δ LS / Δ LS_{max} (▲). Δ Fl_{max} and Δ LS_{max} were estimated from the change at ATP concentration 15 μM. Δ Fl / Δ Fl_{max} and Δ LS / Δ LS_{max} were obtained as the amplitudes at the plateau in the time course of change in fluorescence intensity and light-scattering intensity. 5 μM S-1, 10 μM Pyr-FA, 12.5 μM phalloidin, 1.25 - 15 μM ATP, 50 mM KCl, 2 mM $MgCl_2$, 0.1 mM EDTA, 20 mM Tris-HCl, at pH 7.8 and 20 °C.

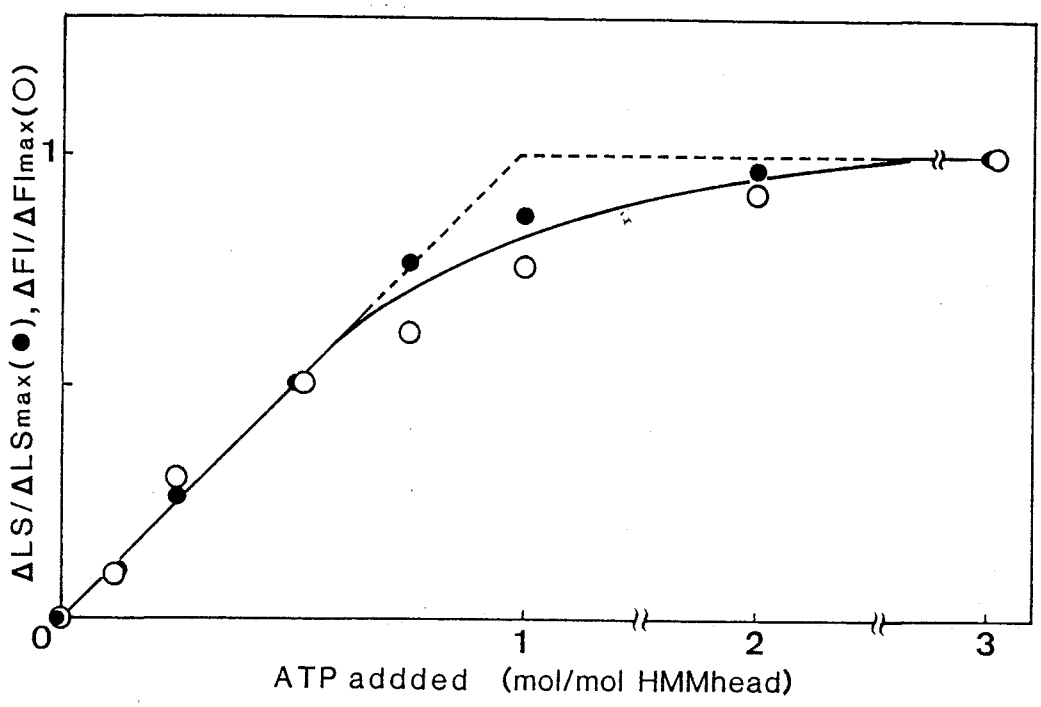

Fig. 2. Dependence on ATP concentration of the extent of dissociation of acto-HMM at low ionic strength. Δ Fl / Δ Fl_{max} (○) and Δ LS / Δ LS_{max} (●) were measured as described for Fig. 1. 2.5 μM HMM, 10 μM Pyr-FA, 12.5 μM phalloidin, 0.625 - 15 μM ATP, 50 mM KCl, 2 mM $MgCl_2$, 0.1 mM EDTA, 20 mM Tris-HCl, at pH 7.8 and 0°C.

calculated from the curve near the saturation was 0.3 μM, assuming that a half of HMM heads react with ATP with lower affinity for ATP than the other heads do.

We measured the dependence on ATP concentration of the extent of acto-HMM at high ionic strength at various concentrations of actin. The amount of heads dissociated from Pyr-FA was higher than that of added ATP. When the actin concentration was decreased from 20 μM to 5 μM, the extent of dissociation at 0.5 mol/mol HMM head increased from 0.5 to 0.8.

Reaction of Acto-HMM with ATP— We measured Pi liberation in the initial phase of HMM ATPase reaction in the presence of Pyr-FA at low (50 mM KCl; ●) and high (1 M KCl; ○) ionic strengths. We performed the ATPase reaction at 0.5 mol ATP / mol HMM head and 10 μM Pyr-FA. In 50 mM KCl, 87% of added ATP was hydrolyzed within 1 sec after the reaction was started, and the amount of ^{32}Pi increased gradually to 92% of added ATP at 13 sec (●). In 1 M KCl (○), most of added ATP was hydrolyzed in the initial phase, with a single exponential process. We also measured the Pi liberation in the initial phase of acto-HMM ATPase reaction at higher concentration of ATP (10 μM) in 50 mM and 1 M KCl. Both of the time courses of Pi liberation showed initial burst of ^{32}Pi, and the amount of Pi increased with steady -state rate constants (8.8×10^{-2} s^{-1} for 50 mM KCl and 1.9×10^{-2} s^{-1} for 1 M KCl). The sizes of initial Pi-burst estimated by extrapolating the time courses in steady states to zero time were 1.1 mol / mol HMM head for both KCl concentrations (data not shown).

Acto-HMM Dissociation Induced by Other Nucleotides— We

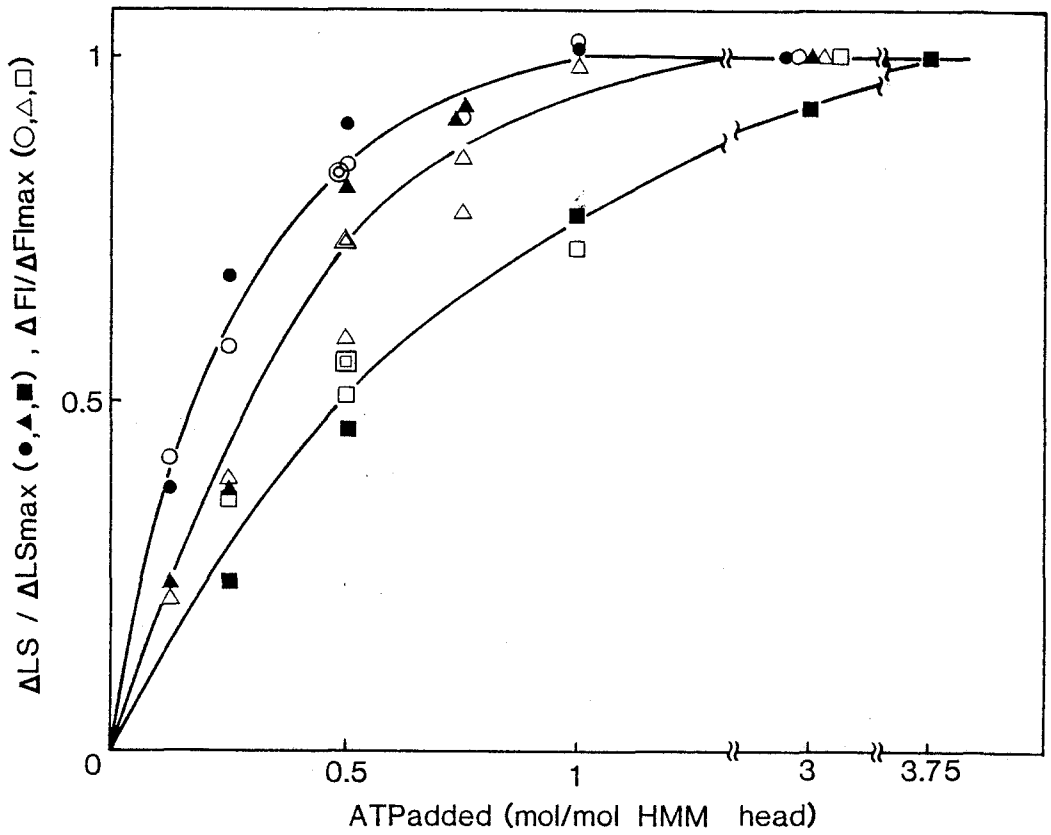

Fig. 3. Dependence on ATP concentration of the extent of dissociation of acto-HMM at high ionic strength. The extent of Δ Fl / Δ Fl_{max} (○ , △ , □) and Δ LS / Δ LS_{max} (● , ▲ , ■) were measured as described in Fig. 1. 2 μM HMM, 5 (○ , ●), 10 (△ , ▲), 20 (□ , ■) μM Pyr-FA, 1.25 mol phalloidin/mol Pyr-FA, 0.5 - 15 μM ATP, 1 M KCl, 2 mM $MgCl_2$, 0.1 mM EDTA, 20 mM Tris-HCl, at pH 7.8 and 0°C.

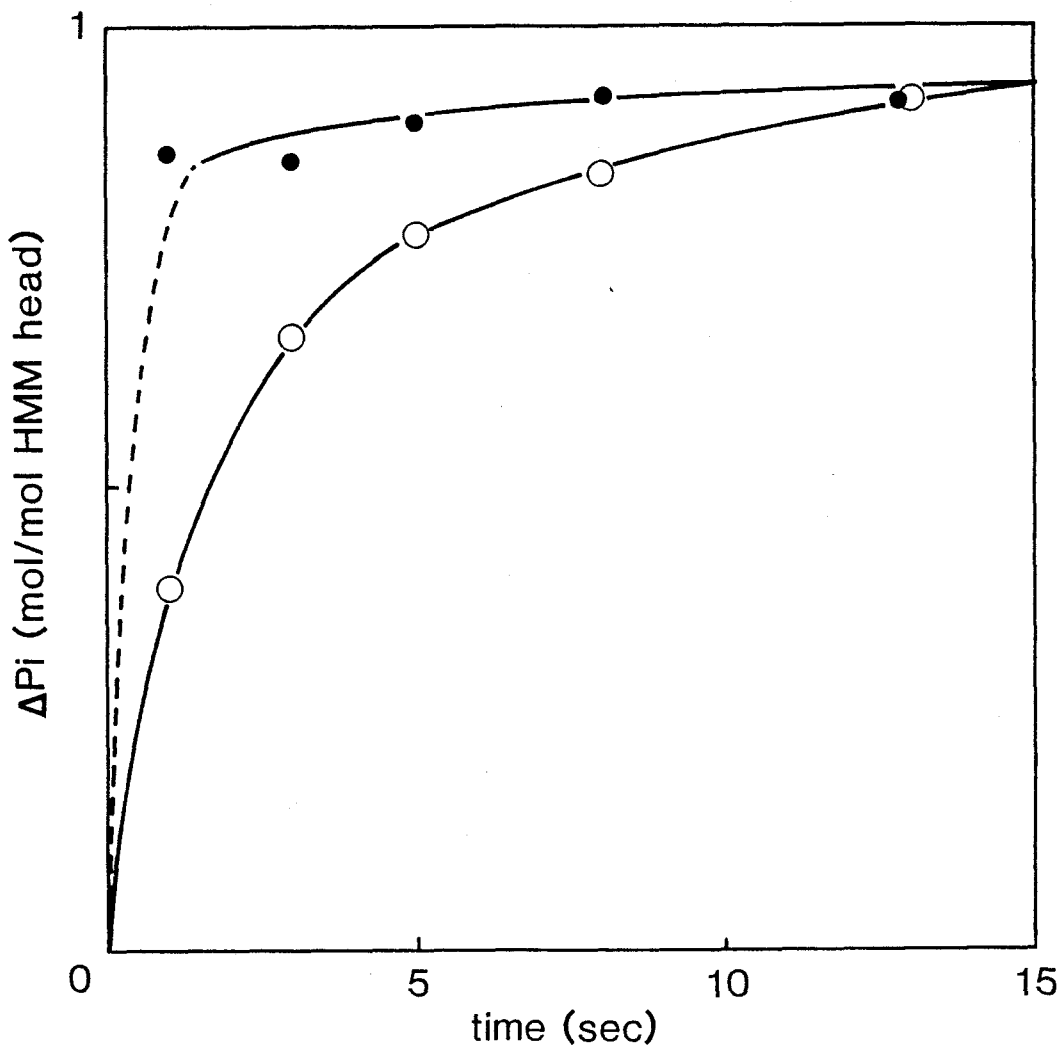

Fig. 4. Single turnover hydrolysis of ATP by HMM at low and high ionic strengths. The reaction was started by mixing [γ-^{32}P] ATP with acto-HMM and quenched the reaction with 5% TCA. 0.05 (●) or 1 (○) M KCl, 2 (○) or 2.5 (●) μM HMM, 2 or 2.5 μM [γ-^{32}P] ATP, 10 μM Pyr-FA, 12.5 μM phalloidin, 2 mM $MgCl_2$, 0.1 mM EDTA, 20 mM Tris-HCl at pH 7.8 and 20°C.

Acto-HMM Dissociation Induced by Other Nucleotides— We examined the dependences of the acto-HMM dissociation on AMPPNP and ADP concentrations at low ionic strength. The upper figure of Fig. 5 show the dependence on AMPPNP concentration. Δ LS / Δ LS_{max} increased with an increase in AMPPNP concentration, and reached 0.76 at 0.395 mM AMPPNP. Δ Fl / Δ Fl_{max} increased more than Δ LS / Δ LS_{max} did, and it reached the level of 0.93 at 0.395 mM AMPPNP. The lower figure of Fig. 5 shows the dependence of acto-HMM dissociation on ADP concentration. Δ LS / Δ LS_{max} increased with an increase in ADP concentration and reached 0.36 at 0.7 mM ADP. Δ Fl / Δ Fl_{max} increased slightly more than Δ LS / Δ LS_{max} did, and reached 0.36 at 0.7 mM ADP.

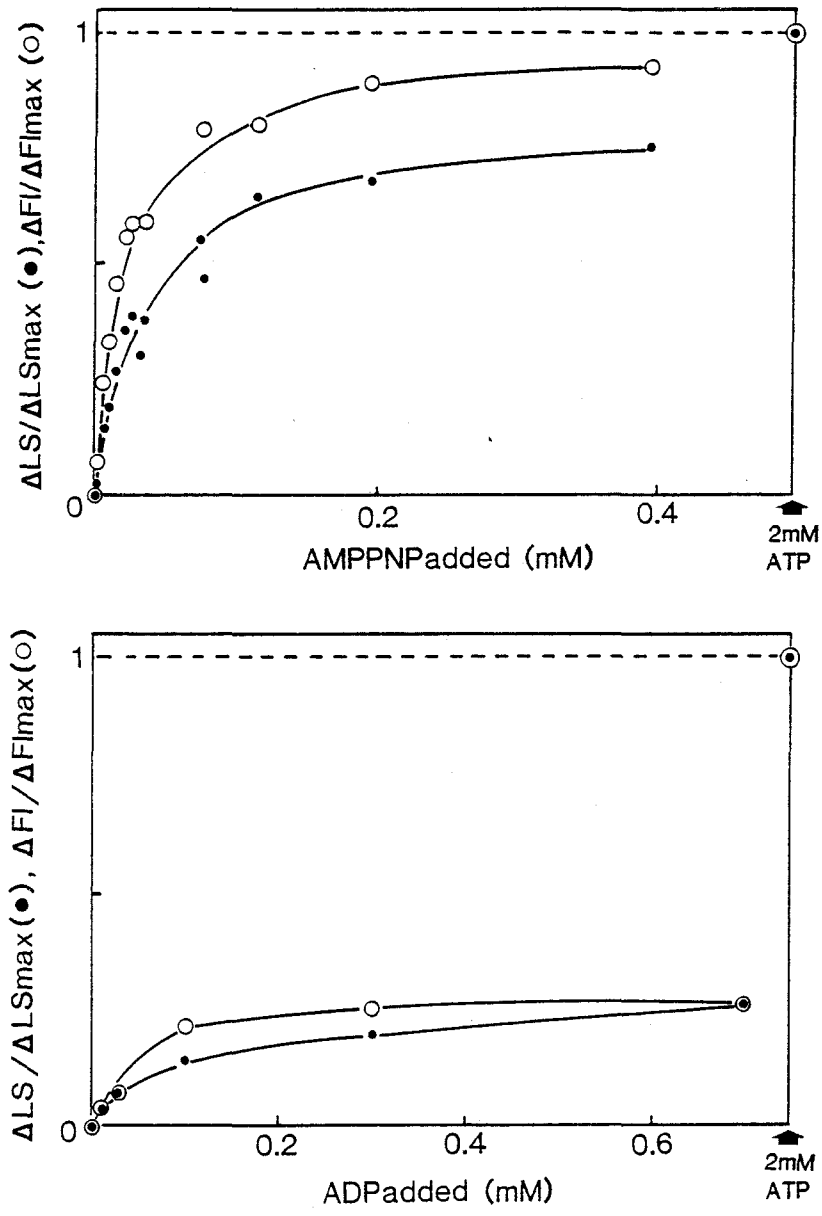

Fig. 5. Dependence of AMPPNP (top) or ADP (bottom) concentration of the extent of dissociation of acto-HMM at low ionic strength. The extent of dissociation of acto-HMM caused by AMPPNP and ADP were reprersented as Δ Fl / Δ Fl_{max} (○) and Δ LS / Δ LS_{max} (●) at given nucleotide concentrations. The value of Δ Fl_{max} and Δ LS_{max} were obtained by adding 2 mM ATP. 50 mM KCl, 8 μM HMM, 20 μM Pyr-FA, 2 mM $MgCl_2$, 0.1 mM EDTA, 20 mM Tris-HCl at pH 7.8 and 20°C.

DISCUSSION

It is an important to know whether or not two myosin heads interact with each other and work cooperatively. To answer this problem we studied the acto-HMM dissociation induced by ATP and other nucleotides. The change in light-scattering intensity (5,11) and that in fluorescence intensity of pyrenyl group labeled to actin (10,14) well reflect the binding extent of HMM or S-1 to F-actin.

Thus, we examined the dependence on ATP concentration of the extent of acto-S-1 dissociation induced by ATP (Fig. 1) in 50 mM KCl, at 20°C. Under these conditions most of S-1 binds tightly to F-actin and the K_d value of S-1 for F-actin is less than 0.1 μM (1). The extent of acto-S-1 dissociation increased with an increase in ATP concentration and reached unity at 7.5 μM ATP (Fig. 1). This result shows that the affinity of S-1 for F-actin is extremely weakened by reaction of S-1 with ATP, as described previously (3,4). Inoue et al. (2) has been proposed that two heads of myosin are not identical. One of two heads (head B) forms myosin-phosphate-ADP complex with high affinity for ATP during ATPase reaction and the other head (head A) forms myosin-ATP complex with low affinity for ATP. The K_d values of S-1 for ATP estimated from the extent of dissociation were less than 0.1 μM for head B and 0.4 μM for head A. These values do not conflict with the values described previously (2).

We examined the dissociation of HMM from Pyr-FA induced by ATP at low ionic strength (Fig. 2). The affinity of HMM for Pyr-FA is so high that most of HMM binds to Pyr-FA in the absence

of ATP (1). The fluorescence intensity increased linearly with increase in ATP concentration and reached a maximal level as observed for S-1. This result shows that the affinity of one HMM head is lowered when the head react with ATP. It was reported that light-scattering intensity reflect the binding of HMM and myosin molecules (not myosin head) to F-actin (5,11,15,16). The affinity of S-1 for F-actin under this condition is so high that the extent of dissociation should be proportional to the square of ATP concentration. However, in fact the extent of dissociation of acto-HMM estimated from light-scattering intensity was also apparently proportional to the ATP concentration, suggesting that there is little amount of single headed attachment speices in acto-HMM complex.

We do not know the details of the binding of HMM to F-actin at low ionic strength. Hence, we examined the dissociation of acto-HMM induced by ATP at high ionic strength (1 M KCl; Fig. 3). The amount of HMM heads dissociated from Pyr-FA by adding ATP was higher than that of ATP added.

It is important to know which head (A or B) reacted with ATP preferentially. Inoue et. al. (2) showed that only head B forms M_P^{ADP} complex and that the formation of this intermediate promotes the binding of head A with actin. The formation of M_P^{ADP} is very fast, while the decomposition is slow. Thus we can estimate the amount of M_P^{ADP} from the Pi-burst size (2). Most of added ATP was converted into ADP and Pi in the initial phase of Pi liberation at both low and high lionic strengths. Therefore, head B reacts with ATP more preferentially.

The observed dissociation constant of HMM which react with one

ATP for F-actin was about 25 μM. The duplicate symbols in Fig. 3 indicate the extent of acto-HMM dissociation predicted by using this K_d value. This value was higher than the dissociation constant (4 μM) of the step: A + HMM ⇌ A·HMM (single headed attachment). We could explain the result by assuming that the binding of head A to F-actin when head B forms M_P^{ADP}, is weaker than that predicted by the simple scheme.

There are two possibilities which cause the unexpectedly larger K_d value. One is that the two heads of HMM have different binding properties as shown in the following scheme:

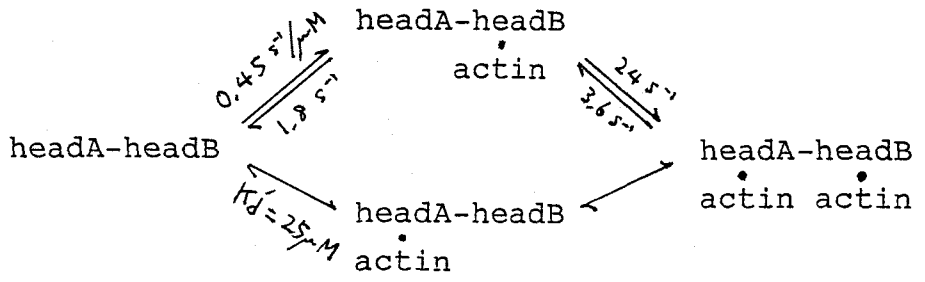

In the absence of ATP, HMM binds to F-actin through the upper pathway, while at 0.5 mol ATP / mol HMM head almost all the headB reacts with ATP and dissociates from F-actin. Therefore, HMM binds to F-actin only by head A which binds to F-actin more weakly than head B. The other possibility is that the reaction of ATP to head B weakens the binding of head A to F-actin by the conformational change transmitted through myosin head region.

Simple hyperbolic dependence of dissociation extent on AMPPNP and ADP concentrations (Fig. 4) also suggests that the reaction of head B with nucleotide cause acto-HMM to dissociate. Manuck et al. (17) and Duong and Reisler (18) suggested that HMM binds to F-actin with single-headed attachment in the presence of ADP. Hence, the difference between dissociation extents estimated from

the changes of light-scattering intensity and fluorescence intensity (Fig. 4) may indicate that some of HMM binds to F-actin with single-headed attachment.

REFERENCES

1. Miyata, M. Arata, T., & Inoue, A. (1988) J. Biochem. in preparation
2. Inoue, A., Takenaka, H., Arata, T., & Tonomura, Y (1979) Adv. Biophys. 13, 1-194
3. Onishi, H., Nakamura, H., & Tonomura, Y. (1968) J. Biochem. 64, 769-784
4. Takeuchi, K. & Tonomura, Y.(1971) J. Biochem. 70, 1011-1019
5. Inoue, A. & Tonomura, Y. (1980) J. Biochem. 88, 1643-1651
6. Perry, S.V. (1955) in Methods in Enzymology (Colowick, S. P. & Kaplan, N. O., ads.) Vol. 2, pp. 582-588, Academic Press, Inc., New York
7. Weeds, A. G., & Taylor, R. S. (1975) Nature 257, 54-56
8. Spudich, J. A. & Watt, S. (1971) J. Biol. Chem. 246, 4866-4871
9. Johnson, R.A. & Walseth, T.F. (1979) Adv. Cyclic Nucleotide Res. 10, 137-167
10. Kouyama, T. & Mihashi, K. (1981) Eur. J. Biochem. 114, 33-38
11. Inoue, A., Ikebe. M., & Tonomura, Y. (1980) J. Biochem. 88, 1663-1677
12. Takemori, S., Nakamura, M., Suzuki, K., Katagiri, M., & Nakamura, T. (1972) Biochem. Biophys. Acta. 284, 382-393
13. Nakamura, H. & Tonomura, Y. (1968) J. Biochem. 63, 279-294
14. Yasui, M., Arata., & Inoue, A. (1984) J. Biochem. 96, 1673-1680
15. Ikebe, M., Onishi, H., & Tonomura, Y. (1982) J. Biochem. 91, 1855-1873

16. Miyata, M., Arata, T., & Inoue, A. (1988) J. Biochem. 103, 111-116

17 Manuck, B. A., Seidel, J. C., & Gergely, J. (1986) Biophys. J. 50, 221-230

18. Duong, A. M. & Reisler, E. (1987) J. Biol.Chem. 262, 4129-4133

ACKNOWLEDGEMENTS

I would like to express to migrate appreciation to Professor T. Nakamura, Faculty of Science, Osaka University for his kind guidance and continuous encouragement during the course of this work.

I am greatly indebted to Doctors A. Inoue and T. Arata who gave me excellent guidances and many valuable suggestions.

I am also grateful to the members of Professor Nakamura's laboratory for their kind helps during this study.